



Trans. Nonferrous Met. Soc. China 32(2022) 1741-1780

Transactions of Nonferrous Metals Society of China

www.tnmsc.cn



## Recent advances in micro-alloyed wrought magnesium alloys: Theory and design

Bin JIANG<sup>1,2</sup>, Zhi-hua DONG<sup>2</sup>, Ang ZHANG<sup>2</sup>, Jiang-feng SONG<sup>1,2</sup>, Fu-sheng PAN<sup>1,2</sup>

National Engineering Research Center for Magnesium Alloys, Chongqing University, Chongqing 400044, China;
State Key Laboratory of Mechanical Transmissions, College of Materials Science and Engineering,
Chongqing University, Chongqing 400044, China

Received 7 October 2021; accepted 27 December 2021

**Abstract:** Micro-alloying design of wrought magnesium (Mg) alloys is an important strategy to achieve high mechanical properties at a low cost. In the last two decades, significant progress has been made from both theory and experiment. In the present review, we try to summarize recent advances in micro-alloying design of wrought Mg alloys from both theoretical and pragmatic perspectives, and provide fundamental data required for establishing the relationship between chemical composition and mechanical properties of Mg alloys. We start with theoretical attempts for understanding the mechanical properties of Mg alloys at different scales, by involving first principle calculations, molecular dynamics, cellular automata, and crystal plasticity. Then, the role of alloying elements is discussed for a series of promising Mg alloys such as Mg–Al, Mg–Zn, Mg–RE (rare-earth element), Mg–Sn, and Mg–Ca families. Potential challenges in the micro-alloying design of Mg alloys are highlighted at the end. The review is expected to provide helpful guidance for the intelligent design of novel wrought Mg alloys and inspire more innovative ideas in this field

**Key words:** magnesium alloys; alloying design; mechanical properties; theoretical calculations; experimental characterizations

#### 1 Introduction

Magnesium (Mg) alloys are widely known as the lightest metallic structural material with the density as low as  $\sim 1.8$  g/cm<sup>3</sup>. In combination with the merits such as high specific strength, satisfactory stiffness, good castability recyclability, and the abundant resources in earth's crust, Mg alloys are deemed to be very promising materials for structural components in automobile, aircraft, and aerospace industries [1-3]. The wide application of Mg alloys is expected to noticeably contribute to the global issue of energy conservation and emission reduction. Nevertheless, while many such potential applications are wrought products in the form of sheet, plate, extrusions and forgings, usage of Mg alloys is currently limited to cast applications [4].

A major barrier to wider application of wrought Mg alloys is the relatively low ductility and strength. It is closely correlated with the hexagonal crystal structure of Mg alloys, which leads to the absence of sufficient slip systems to coordinate the plastic deformation [5,6]. Moreover, owing to the relatively low critical shear stress, basal slip is readily activated during deformation, yielding low strength and noticeable anisotropy in Mg alloys [4]. In order to improve the comprehensive mechanical properties of wrought Mg alloys, successive efforts have been made during last two decades and significant progress has

been achieved [7–14]. The processing technologies such as pre-deformation, asymmetry extrusion, and thermo-mechanical treatment have been demonstrated to efficiently improve mechanical properties of Mg alloys via different mechanisms, such as weakened texture, grain refinement and work hardening [15–19]. However, realization of those technologies requires suited process and equipment conditions [20,21].

Addition of alloying elements is a very effective approach to improve mechanical properties of wrought Mg alloys. In the last two decades, a series of Mg alloy families, such as Mg-Al, Mg-Zn, Mg-RE (rare-earth element), Mg-Sn, and Mg-Ca, have been extensively investigated and new Mg alloys with improved mechanical properties have been developed [22–26]. Generally, addition of alloying element impacts on mechanical properties of Mg alloys via structural stability, intrinsic elastic and plastic properties, dislocation behaviors, microstructure evolution, and deformation mechanisms [27-35]. For instance, precipitation strengthening and dispersion strengthening can be adjusted by alloying design via controlling the type, content, size, and dispersion of precipitates. Solid solution strengthening can be achieved through choosing appropriate solute atoms and controlling their interactions with dislocations. In recent years, micro-alloying design of Mg alloys with relatively low alloying additions has attracted extensive research interest, which is deemed to be an efficient way to achieve the desired high mechanical properties at a low cost and facilitate significantly engineering applications of Mg alloys [36–38].

Despite numerous efforts made on the development of Mg alloys, current understanding of alloying influence on mechanical properties of Mg alloys is far away from expectation. In addition to advanced experimental methods, theoretical calculations performed at different scale levels are receiving increased attention. Considering the chemical and physical properties of crystalline materials, theoretical simulations including, for instance, first principle calculations, molecular dynamics simulation, cellular automata, and crystal plasticity, provide deep insight into the mechanism alloying influence, and facilitate of establishment of the composition-microstructureproperty relationship for Mg alloys [39-45]. With

the development of computational power, the integrated theoretical and experimental methodology is expected to significantly facilitate the design of Mg alloys with exceptional mechanical properties [46–53].

In the present work, the recent progress in micro-alloying design of wrought Mg alloys is summarized from theoretical and pragmatic perspectives. We start with theoretical attempts for understanding the mechanical properties of Mg alloys at different scales, by involving first principle calculations, molecular dynamics, cellular automata, and crystal plasticity. Then, the role of alloying elements is discussed for a series of promising Mg alloys such as Mg-Al, Mg-Zn, Mg-RE, Mg-Sn, and Mg-Ca families, for which binary and multicomponent systems are elucidated and mass fundamental data are summarized. At the end, potential challenges in the alloying design of Mg alloys are highlighted. The present review is expected to provide helpful guidance for the intelligent design of novel wrought Mg alloys and inspire more innovative ideas in the field.

# 2 Multi-scale simulations for wrought Mg alloys

## 2.1 First principle calculations

Intrinsic properties of materials such as Mg alloys are fundamentally interrelated to interactions of electrons and nuclei, which can be described by solving Schrödinger equation in the quantum mechanics theory [54]. Based on the Born-Oppenheime approximation [55], the total energy is described as a unique functional of the electronic density in the density functional theory [56]. The true electronic density minimizing the functional is determined by solving the effective one-electron Kohn-Sham equations [57], in which the motion of electrons within fully interacting system is mapped onto a fictitious state where electrons move within an effective single-particle potential. With the self-consistently determined electronic structure, a great variety of intrinsic properties can be derived from first principle calculations.

In the following part, we summarize the attempts applying first principle calculations in alloying design of Mg alloys, with the special emphasis on structural stability of intermetallic compounds, elastic properties, and stacking fault

energy correlating closely with the mechanical properties of Mg alloys.

## 2.1.1 Structural stability of intermetallic compounds

Precipitation strengthening of intermetallic compounds is one of the most important strengthening mechanisms in Mg alloys [58]. Understanding of their structural stability is thus of significance for prototyping novel Mg alloys with exceptional strength. The structural stability of intermetallic compounds can be evaluated by the formation enthalpy  $\Delta H$ , which can be calculated efficiently using ab initio methods. Generally, the formation enthalpy is expressed as

$$\Delta H = (E_{\text{tot}} - \sum n_i E_i) / \sum n_i \tag{1}$$

where  $E_i$  represents the total energy of atomic i in the equilibrium state and  $n_i$  is the corresponding number in the model of compounds.  $E_{\text{tot}}$  is the total energy of the compounds underlying with the certain crystal structure and the chemical order. Negative formation enthalpy indicates that the compound is thermodynamically stable. The lower the  $\Delta H$  is, the more stable the phase is.

Rare-earth elements are widely used in Mg alloys. Figure 1 shows some typical crystal structure of Mg intermetallic compounds. RAMESHKUMAR et al [59] recently compared the structural stability of the Mg–X (X=La, Nd, Sm) intermetallics in their respective ground state phase and metastable phases, as shown in Fig. 1. The computed  $\Delta H$  indicated that C15, D0<sub>3</sub>, and D2<sub>b</sub> phases are energetically stable compared to the

others, while C14, C11<sub>b</sub>, D0<sub>19</sub>, D0<sub>c</sub> and LI<sub>2</sub> phases are metastable. The relative stability of the main binary Mg–Ce compounds was investigated by YANG et al [60]. Accordingly, the cohesive energy of Mg–Ce intermetallic compounds declined with Ce content. MgCe compound exhibits a relatively high structural stability with respect to Mg<sub>2</sub>Ce and Mg<sub>3</sub>Ce. Similarly, the structural stability was investigated as a function of Y content in Mg–Y binary systems [61]. Among the studied compounds, MgY was found to exhibit the lowest formation energy and thus the highest structural stability.

Zn and Al are two important alloying elements in wrought Mg alloys. Their precipitates are attracting more and more attention. LIU et al [62] systematically investigated the structural stability of precipitates in Mg-Zn alloys. Among the considered phases including MgZn<sub>2</sub> cubic Laves phase, MgZn<sub>2</sub> hexagonal Laves phase, Mg<sub>4</sub>Zn<sub>7</sub>, Mg<sub>2</sub>Zn<sub>11</sub>, and Mg<sub>21</sub>Zn<sub>25</sub>, the formation energies of Mg<sub>4</sub>Zn<sub>7</sub> and MgZn<sub>2</sub> (cubic and hexagonal) were found to be very close to each other owing to the rather similar lattice structures. Nevertheless, the MgZn<sub>2</sub> hexagonal Laves phase becomes more stable at high temperature. A phase transition from the mixture of the compounds to the single hexagonal MgZn2 was predicted. Recently, ZHU et al [63] estimated the relative phase stability of a series of stable/metastable crystal structures in Mg-Al system. Mg<sub>15</sub>Al, Mg<sub>3</sub>Al and MgAl were determined to be the stable structures at the given chemical composition. Moreover, Al-RE phase

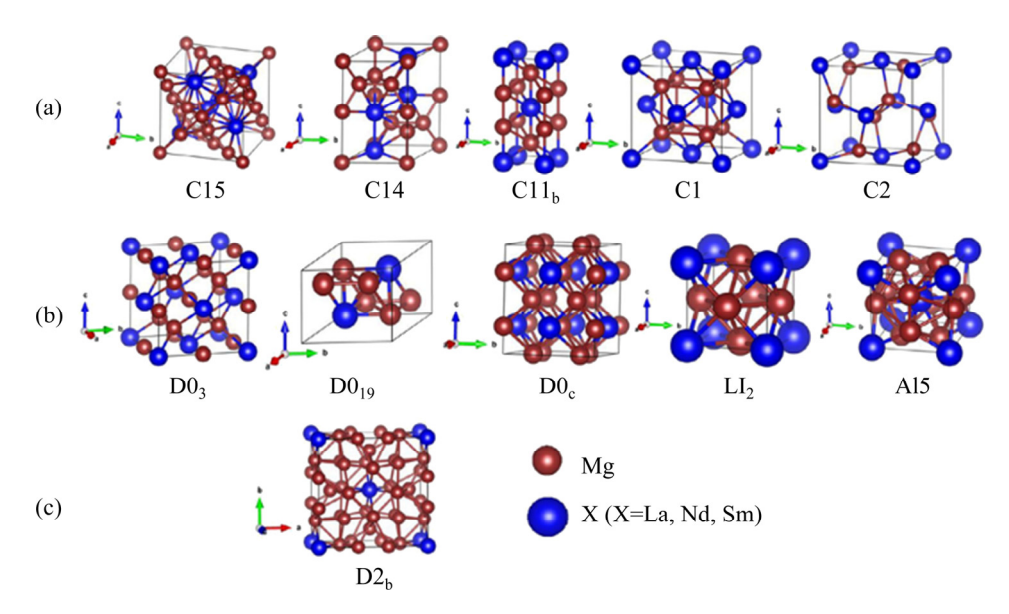
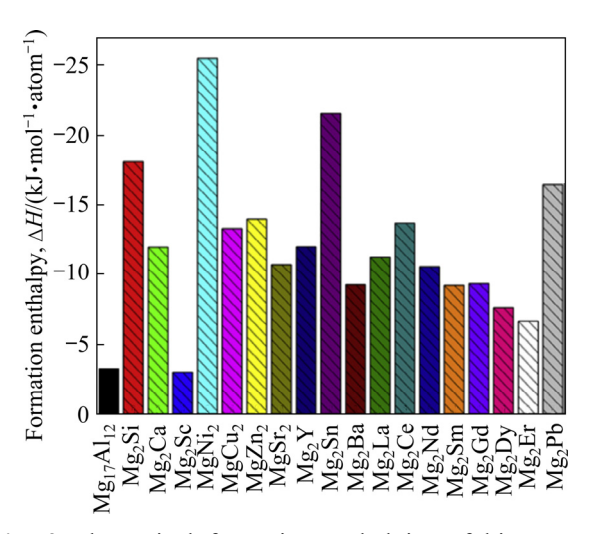


Fig. 1 Crystal structure of Mg–X (X=La, Nd, Sm) intermetallics [59]: (a) Mg<sub>2</sub>X in C15, C14, C11<sub>b</sub>, C1 and C2 phases; (b) Mg<sub>3</sub>X in D0<sub>3</sub>, D0<sub>19</sub>, D0<sub>c</sub>, LI<sub>2</sub> and A15 phases; (c) Mg<sub>12</sub>X in D2<sub>b</sub> phase

may precipitate in Mg–Al–RE system. According to the study by CHEN et al [64], the formation enthalpy of Al<sub>2</sub>RE (RE=Y, Gd) is lower than that of Al<sub>3</sub>RE, and Al–Y intermetallics show stronger structural stability than Al–Gd compounds.

Owing to the limited solubility, a series of alloying elements, such as Ni, Cu, Pb, and Sr, can form intermetallic compounds during the processing of Mg alloys. Their structural stability estimated from ab initio calculations was summarized by LIU et al [39]. As shown in Fig. 2, among the collected binary Mg compounds, MgNi<sub>2</sub>, Mg<sub>2</sub>Sn, Mg<sub>2</sub>Si and Mg<sub>2</sub>Pb exhibit relatively low formation enthalpy, whereas Mg<sub>2</sub>Sc and Mg<sub>17</sub>Al<sub>12</sub> indicate the high formation energy and the relatively low structural stability.



**Fig. 2** Theoretical formation enthalpies of binary Mg compounds [39]

More recently, the structural stability of different types of the long-period stacking ordered phase, which is one of the most important strengthening phases [65], was investigated by GUO et al [66] in Mg-Zn-Y and Mg-Ni-Y systems. Compared with 12R, 10H, and 18R structures, 14H-type phase was found to be energetically preferable. Nevertheless, the differences in the formation enthalpy among the phases are relatively small. Furthermore, beyond the binary intermetallic compounds discussed above, the influence of Zn doping on the AlLi compounds was recently investigated by GUO et al [67]. The formation enthalpy of (Al,Zn)Li phase was predicted to decrease with Zn concentration, indicating an increased structural stability. These advances in the structural stability of intermetallic

compounds provide fundamental understandings required for optimal controlling of the type, precipitating order, and amount of precipitates and ultimately the contribution from precipitation strengthening in Mg alloys.

# 2.1.2 Calculation of alloying influence on elastic properties

Fundamental knowledge of elastic properties contributes to the understanding of intrinsic properties of Mg alloys including interatomic potential, mechanical strength, and stiffness against deformation. In a hexagonal symmetry crystal structure, there are five independent elastic constants including  $C_{11}$ ,  $C_{12}$ ,  $C_{13}$ ,  $C_{33}$ , and  $C_{44}$ , which can be directly derived from ab initio calculations [68]. Based on the information, the polycrystalline elastic moduli, such as bulk modulus (B), shear modulus (G), and elastic modulus (E), can be evaluated using the average of single elastic constants in the schemes like Voigt, Reuss, and Voigt-Reuss-Hill method [68]. For pure Mg, elastic parameters  $C_{11}$ ,  $C_{12}$ ,  $C_{13}$ ,  $C_{33}$ ,  $C_{44}$ ,  $C_{66}$ =  $(C_{11}-C_{12})/2$ , B, G, and E have been determined to be ~60, 26, 22, 62, 16, 17, 36, 17, and 45 GPa, respectively [69]. Those data provide the benchmark for the design of Mg alloys.

Elastic properties of intermetallic compounds have been extensively investigated using ab initio calculations to understand the precipitation strengthening behaviors in Mg alloys [70-72]. Generally, elastic properties of intermetallics strongly depend on the crystal structure and the chemical composition. WANG et al [73] calculated the elastic moduli of MgRE (RE=Y, Dy, Pr, Sc, Tb) intermetallics with  $B_2$ -type structure. Among the considered intermetallics, MgSc was predicted to exhibit the largest elastic modulus (B>50 GPa at equilibrium). Similar conclusion was reached by TAO et al [74]. As shown in Fig. 3, while MgSc and MgLu compounds exhibit noticeably large bulk modulus compared with pure Mg, MgEu and MgYb show relatively low bulk modulus. For the intermetallic compounds with AB2 structure, CHEN et al [75] calculated the elastic properties of MgNi<sub>2</sub>, MgCu<sub>2</sub>, and MgZn<sub>2</sub>. Among them, MgNi<sub>2</sub> was predicted to have the largest elastic stiffness. Similarly, MgNi<sub>2</sub> and MgCu<sub>2</sub> were demonstrated to have high elastic moduli by GANESHAN et al [76] and MAO et al [77]. Regarding the intermetallics with anti-fluorite structure, FAN et al [78] found that the ideal tensile strength of Mg<sub>2</sub>X (X=Si, Ge, Sn and Pb) occurs in the [111] directions while the ideal shear strength appears in the (111)[11 $\overline{2}$ ] systems. With increasing atomic number of X, the two strengths decrease gradually. A comparison of single crystal elastic parameter of typical intermetallic compounds was made by LIU et al [39]. As shown in Fig. 4, MgNi<sub>2</sub> exhibits the largest elastic stiffness among the considered intermetallic compounds.

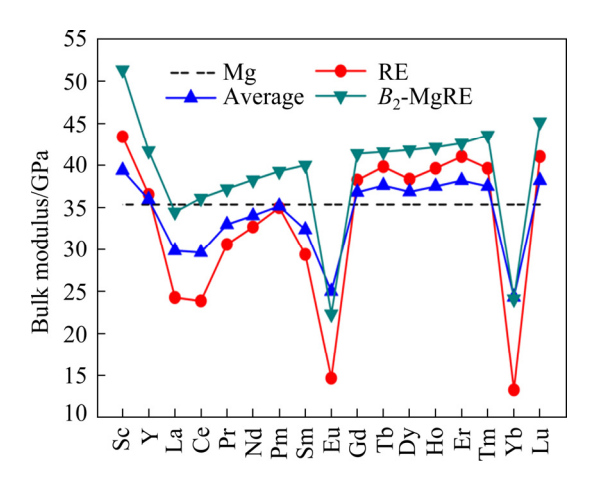


**Fig. 3** Calculated bulk moduli of Mg, RE and  $B_2$ -MgRE [74]

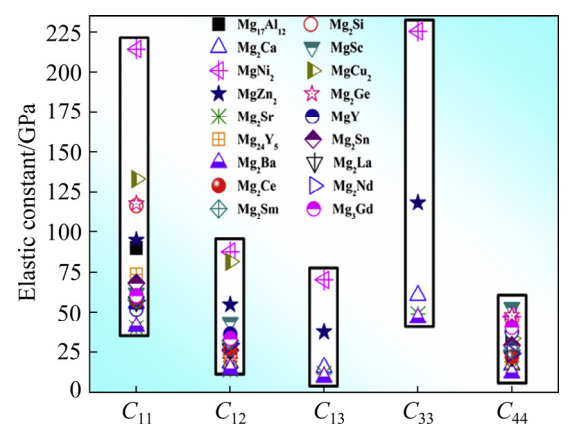


Fig. 4 Predicted elastic constants of Mg compounds [39]

Alloying elements in solid solution significantly influence the intrinsic properties of Mg matrix. By constructing different supercell models, increasing Y content in solid solution was found to improve the strength of Mg [79]. Similarly, the calculations for Y and Zn in solid solution showed that the bulk modulus of Mg increases slightly with adding Y or Zn, while shear modulus and elastic modulus decrease gradually [80]. In comparison, Y in solid solution leads to relatively large effect. The alloying influence of Sc becomes

even more noticeable compared to Y [81]. LIU et al [69] predicted that when Al and Er are doped into the Mg matrix, the bulk modulus, elastic modulus and shear modulus increase simultaneously, while Er yields relatively large alloying effect. Based on the calculations of elastic constants for 12 Mg-X solutions, GANESHAN et al [82] concluded that addition of solute atoms belonging to the s-block and p-block in the periodic table results in a lower bulk moduli than d-block elements. More recently, FANG et al [83] calculated the elastic constants for 17 Mg-X solutions. As shown in Fig. 5, Sc, Gd, Tm, and Y in solid solution noticeably increase elastic modulus along c axis, whereas Pb declines it significantly. Moreover, the alloying influence may change on the non-basal planes (i.e. xy plane in Fig. 5).

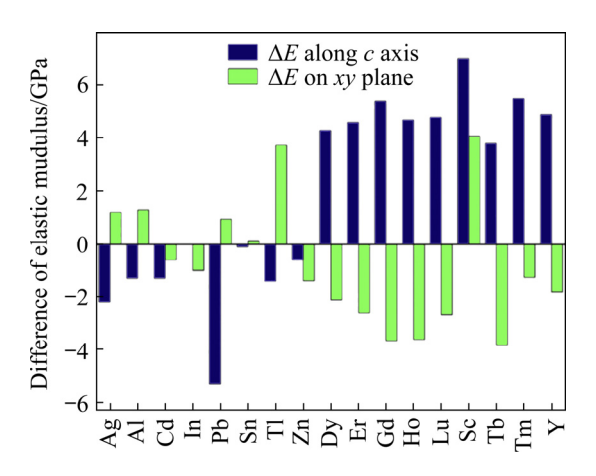


Fig. 5 Alloying influence on elastic modulus along c axis and on xy plane in contrast with pure Mg [83]

## 2.1.3 Calculation of stacking fault energy for Mg–X binary systems

The generalized stacking fault energy ( $\gamma$  curve) provides valuable information about plastic deformation of Mg alloys [84,85]. It represents the excess energy per unit area as a function of the atomic shear displacement along slip direction, and is fully accessible to ab initio calculations. Following the definition of the excess energy,  $\gamma$  is generally expressed as

$$\gamma(v) = [E(v) - E(0)]/A \tag{2}$$

where A is the interface area per atom, v represents the atomic shear displacement along slip direction, and E(v) and E(0) are the energies of faulted structure and lattice without fault, respectively. With the hcp crystal structure, several possible slip

modes can be activated during plastic deformation, which includes for instance basal  $\langle a \rangle$  dislocations, prismatic  $\langle a \rangle$  dislocations, and pyramidal  $\langle c+a \rangle$  dislocations.  $\gamma$  value on different slip planes differs significantly in Mg. I<sub>1</sub> and I<sub>2</sub> type stacking fault energies were predicted to be 8–20 mJ/m² and 30–50 mJ/m² for pure Mg, which are comparable with the available experiments [86]. They are however much lower than the intrinsic and unstable tacking fault energies on prismatic and pyramidal planes. This is the root cause for the low ductility of Mg and motivates extensive efforts on alloying design of Mg alloys.

Slip on the basal plane is preferentially activated in Mg alloys. The influence of alloying elements on  $\gamma$  value on basal plane has thus received extensive attention [87]. After the pioneer calculation of  $\gamma$  curve for pure Mg by WEN et al [88], HAN et al [89] found that addition of Li increases the  $\gamma$  values gradually, whereas Al reduces them noticeably. The alloying effect may change depending on slip planes. TSURU et al [90] reported an opposite/increased effect of Al on prismatic planes. Nevertheless, Y was predicted to yield the similar decreasing effect on  $\gamma$  values on both the basal and prismatic planes. Similar conclusion was reached by PEI et al [91]. Moreover, SANDLÖBES et al [92,93] investigated the effect of various rare-earth elements on I<sub>1</sub>-type stacking fault energy. Y was again demonstrated to noticeably decrease I<sub>1</sub> value. This was deemed to be the root cause for the increased density of I<sub>1</sub> stacking fault, which promotes the nucleation of  $\langle c+a \rangle$  dislocations on pyramidal plane and contributes to the improved ductility observed in experiment.

In order to provide fundamental data of  $\gamma$  required for the optimal design of Mg alloys, MUZYK et al [94] studied the influence of 13 alloying elements on basal and prismatic planes. Sn and Pb fully located on the faulted plane were found to reduce  $\gamma$  significantly, whereas Ni and Cu yielded an opposite effect. Based on the calculations for 21 alloying elements, WANG et al [95] found that except a few elements such as Ti and Zr, addition of alloying elements tend to reduce  $\gamma$  values, which is different from the aforementioned findings. Moreover, by constructing different supercell models, ZHANG et al [96] calculated the  $\gamma$  on basal plane as a function of

alloying concentration. Recently, DONG et al [97] systematically calculated the influence of 43 alloying elements on the  $\gamma$  curves on basal plane. Generally, the characteristic energies on  $\gamma$  curves (except I<sub>1</sub>-type fault energy) decrease with increasing the atomic radius of solutes. With these data, the authors proposed a model to correlate quantitatively the I<sub>2</sub> unstable stacking fault energy with intrinsic properties including bulk modulus, binding energy and atomic radius. The influence of alloying element on basal y value was recently summarized by NIE et al [98], which is shown in Fig. 6. It should be noted that the reported alloying contribution was evaluated for the segregated solutes in Mg-X binary systems. Namely, during the calculations, all the solutes substituting Mg atoms were placed on the slip plane.

Activation of non-basal slip systems is important to improve the ductility of Mg alloys. However, understanding of their energetics and dynamics is far from expectation [99,100]. WU et al [101-103] performed elaborated investigations on dissociation and motion of  $\langle c+a \rangle$  dislocations in Mg and Mg alloys. The cross-slip between the two pyramidal planes was deemed to be important to improve the ductility. Moreover, YIN et al [104] found that Al, Zn, and Y yield the similar decreasing effect on the stacking fault energy on basal plane. Namely, the effect of Y on the energy of I1 fault could not be the root cause for its noticeable improvement on ductility of Mg, in contrast with the theory proposed by SANDLÖBES et al [92,93]. Recently, DING et al [105] compared the  $\gamma$  curves on the two pyramidal planes. Addition of Y atoms in Mg was found to facilitate the dissociation of  $\langle c+a \rangle$  dislocations on pyramidal II, and increase the range of the flat potential-energy surface, which promotes different sliding pathways in the Mg-Y alloy and improves the ductility.

## 2.2 Molecular dynamics calculations

Molecular dynamics (MD) calculation is an effective method to understand physical properties of materials at atomic level. Basically, Newton's second law is applies in MD to numerically solve the motion equations of atoms or molecules in material systems, and obtain the coordinate and speed of each atom or molecule. Then, according to the statistical mechanic method, the relevant physical properties can be derived. The accuracy of

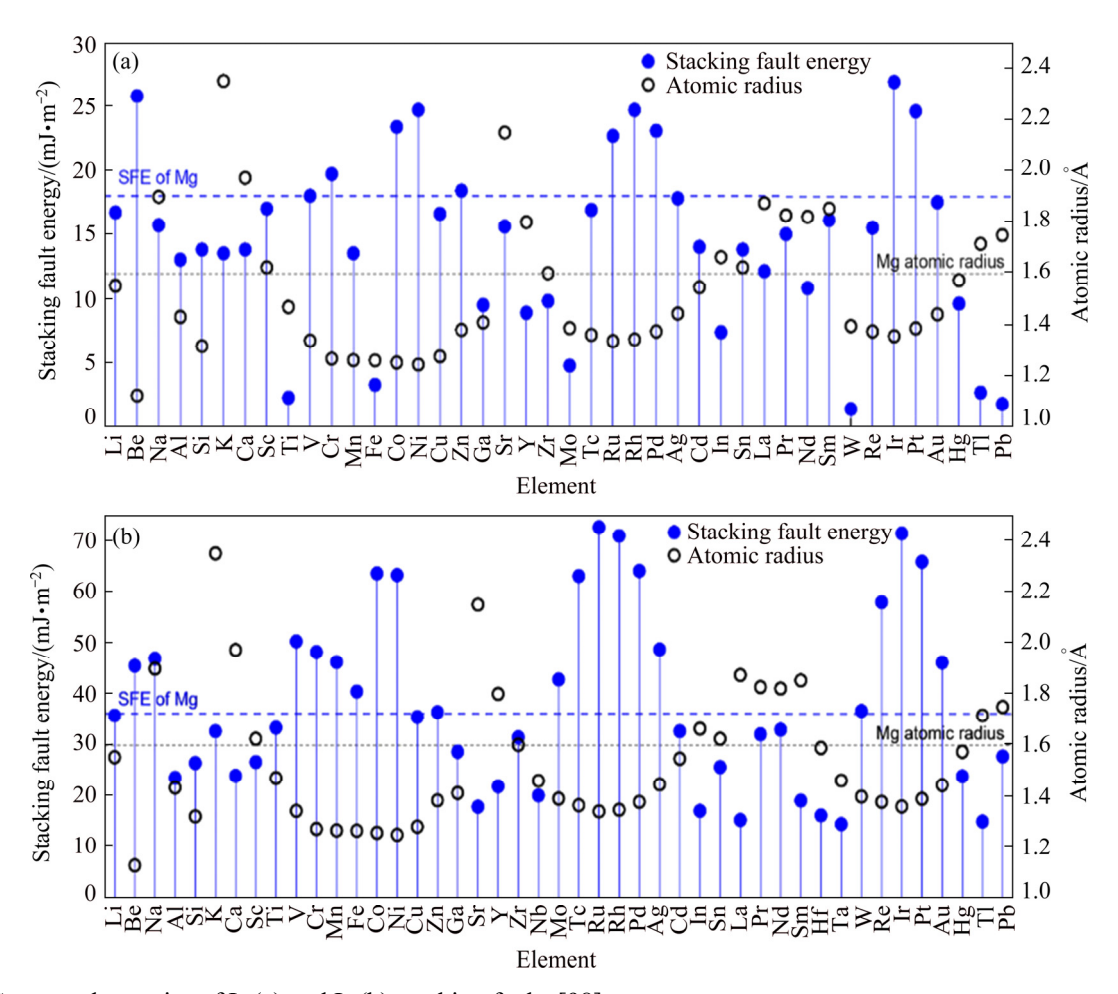


Fig. 6 Computed energies of I<sub>1</sub> (a) and I<sub>2</sub> (b) stacking faults [98]

MD calculations is dominated by the applied atomic potential [106]. MD method can not only directly simulate many intrinsic properties of materials, but also obtain the relationship among microstructure, particle motion and properties of materials.

Attempts have been made to apply MD simulations in Mg alloys. WU and HU [107] investigated thermodynamics, elastic constants and solid solution strength for Mg-xGd (x=0.5, 1, 2, 3, 4, wt.%) alloys by using MD simulations. Addition of Gd was found to enhance the strength of Mg, in good agreement with experimental observation and ab initio calculations. GROH et al [108] studied dislocation behavior in pure Mg. The MD calculations indicated that the dislocation velocity has a strong anisotropy depending on dislocation character (edge or screw) and the slip system (basal, prismatic and pyramidal). KIM et al [109] has attempted to probe the plastic behavior of a nano-crystalline hcp metal using MD simulations of [1120]-textured Mg. Most of the experimentally known slip and twin systems have been reproduced in the simulations. SOMEKAWA and MUKAI [110] simulated the influence of grain boundary structure on grain boundary deformation mechanism and the change of grain boundary energy. Figure 7 shows the internal energy distribution during the shearing test for the 78°-tilted boundary model. The migration at grain boundary was confirmed, and Al atoms were found to yield noticeable effect on the internal energy distribution. HUANG et al [111] calculated the segregation of atoms in Mg–9wt.%Al melt. Mg and Al were found to have a tendency to form bonds in Mg–9wt.%Al melt and the sizes of aggregated Al-centered clusters were within the characteristic scale of medium-range order.

Recently, YANG et al [112] simulated the uniaxial compression deformation at different temperatures and strain rates for AZ31 alloy, where the mechanical properties and microstructure evolution were elaborated. Moreover, the effects of different solute atoms on grain boundary behaviors were investigated in AZ31 alloy [113]. The results

indicated that the solute atoms can inhibit the grain refinement of Mg, improving the strength effectively. In addition, the solute atoms can change the lattice distortion during uniaxial compression of Mg alloys, which significantly increases dislocation density.

#### 2.3 Cellular automata simulations

Cellular automata (CA) is one of the powerful simulation methods for microstructure evolution of materials. In the CA simulations, the complex system is discretized in time and space based on the real physical evolution rule. The interaction among cells is limited to a certain range, i.e., each cell only interacts with its neighboring cells and the state at a certain moment is determined by that at the last moment according to the established rule. It has the characteristics of discreteness, synchronization and

homogeneity. To establish the relationship among meso-/micro-structures, properties and processing during wrought process, CA has been combined with principles of dynamic recrystallization (DRX) to simulate microstructure evolution, especially the growth direction and the shape of grains [114]. The variation of dislocation density can be determined in combination with physical principles.

With the development of numerical simulation, CA has been increasingly employed in the microstructure simulation of wrought Mg alloys. SHU et al [115] modeled the DRX of as-extruded AM50 alloy by CA simulation. The flow stress, DRX volume fraction and DRX grain size of the as-extruded AM50 alloy were predicted, which agrees well with the experimental results. Figure 8 shows the comparison between experimental and simulated microstructures at different temperatures.

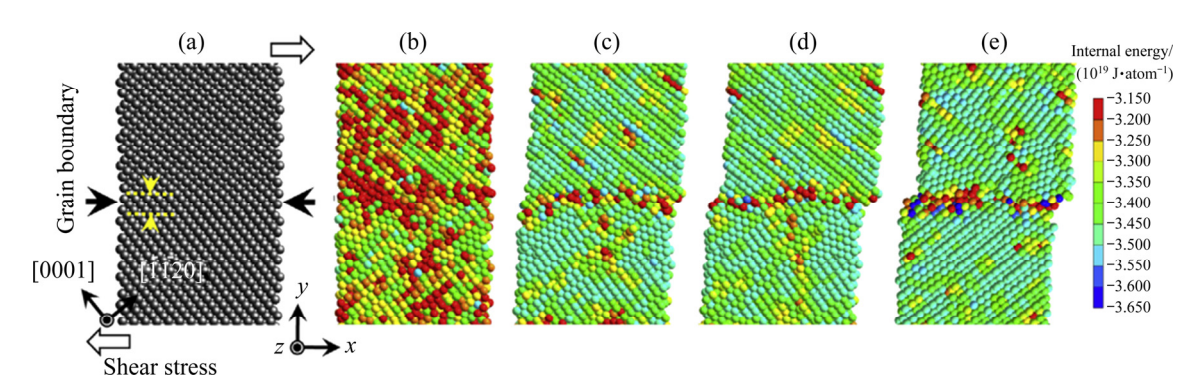


**Fig. 7** Typical snapshots of 78°-tilted boundary model showing internal energy distributions during shearing test at 0 ps (a), 1.0 ps (b), 5.0 ps (c), 10 ps (d) in Mg and 10 ps (e) in Mg-Al alloy [110]

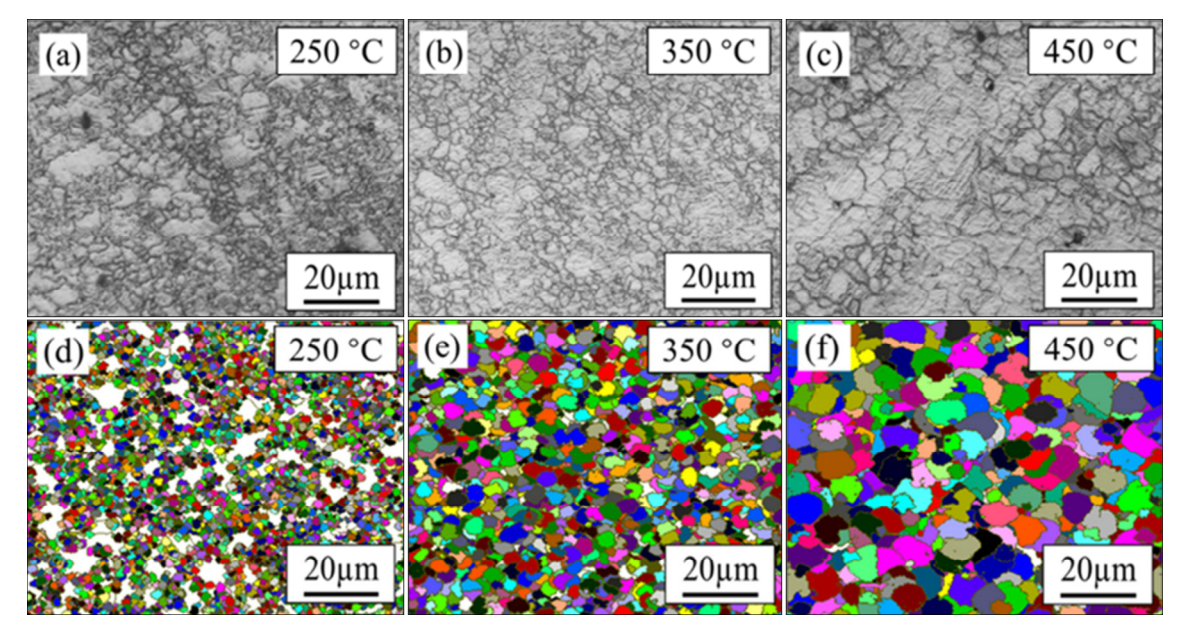


Fig. 8 Comparisons between experimental (a-c) and simulated (d-f) microstructures at different temperatures [115]

A high deformation temperature was found to benefit more dislocation energy, which promotes the DRX and increases the grain size. HATAMI SADR and JAFARZADEH [116] combined CA and finite element method to study the evolution of microstructure and mechanical properties of AZ91 alloy during cyclic shrinkage/expansion extrusion. The applied plastic strain and the change of dislocation density were found to induce discontinuous DRX, which refines grains of AZ91 samples. WU et al [117] combined hot compression experiment and cellular automata finite element model to study DRX behavior of AZ61 alloy during hot deformation. The stress-dislocation relationship and the strain rate were incorporated into the model. Both the experiments and CA simulations revealed the inhomogeneous microstructure during hot compression process. Recently, HE et al [118] combined CA and finite element method to study dynamic recrystallization behavior Mg-Al-Zn-RE alloy during hot extrusion. The effect of extrusion condition on microstructure evolution was discussed. More importantly, the relationship between the flow stress in compression and the dynamic recrystallization process was elucidated by the calculations.

## 2.4 Crystal plasticity simulations

Crystal plasticity (CP) describes the relationship between macroscopic deformation and microstructural evolution of materials, which can quantitatively reveal the plastic deformation mechanism of crystalline materials compared with the conventional macroscopic plasticity theory [119,120]. In the simulation of CP, the plastic deformation of crystals is attributed to the dislocation slip and twinning. The discrete dislocation slip and twinning are transformed into continuous plastic deformation by using the statistical method, thereby building the relationship between the mesoscopic scale deformation mechanisms and the macroscopic deformation [121-123]. With the improvement of computational power, CP simulations have been gradually applied to investigating the deformation mechanisms of Mg alloys, such as deformation twinning [124,125], texture evolution [126,127], grain boundary sliding [128,129] and fracture [130,131].

ABDOLVAND et al [124] investigated the

extension twinning in AZ31 with a strong basal rolling texture by tensile experiment and The results indicated that CP simulations. a small difference existed between the stress normal to the twin habit plane in the parent and twin. PARAMATMUNI and KANJARLA [125] developed a model including twinning pseudo-slip and accounted for the interaction between parent grains and the corresponding twin variants. The analysis of twinning-dominated deformation in AZ31 revealed that basal slip was the dominant active slip system during the twin nucleation and twin growth stages. MAYAMA et al [126] investigated the texture evolution during the extrusion of Mg alloy by experiment and CP simulations. The texture evolution during the equi-biaxial compression was reproduced through CP analysis. FEATHER et al [127] investigated the relationship mechanical among responses, twinning, and texture evolution during the deformation of WE43 by using a multi-level crystal plasticity model, which is shown in Fig. 9.

In the research of LI et al [128], a crystal plasticity modeling method integrating the slip, dynamic recrystallization and grain boundary sliding (GBS) was established to simulate the deformation behavior and texture evolution of Mg alloys at high temperatures. It was found that the grain boundary sliding played a more significant role in tension than in compression of Mg alloy. To identify if GBS can generate stress concentration and related defects at grain boundary, SON and HYUN [129] investigated the periodic defect formation along the serrated grain boundary during cold shear deformation. The results suggested that GBS at room temperature can nucleate twins and dislocation arrays periodically. In addition, the simulations validated that the serrated grain boundary generated the non-rotating region and split stress distribution with intensified value.

ARDELJAN and KNEZEVIC [130] used a three-dimensional crystal plasticity finite element (CPFE) framework to simulate the nucleation, formation, propagation, and growth of a discrete double twin lamella in AZ31. The results suggested that the contraction of twin-parent boundaries was weak link in the microstructure where voids can nucleate. HABIB et al [131] studied the fracture of an anisotropic rare-earth-containing Mg alloy (ZEK100) sheet at different stress states and strain

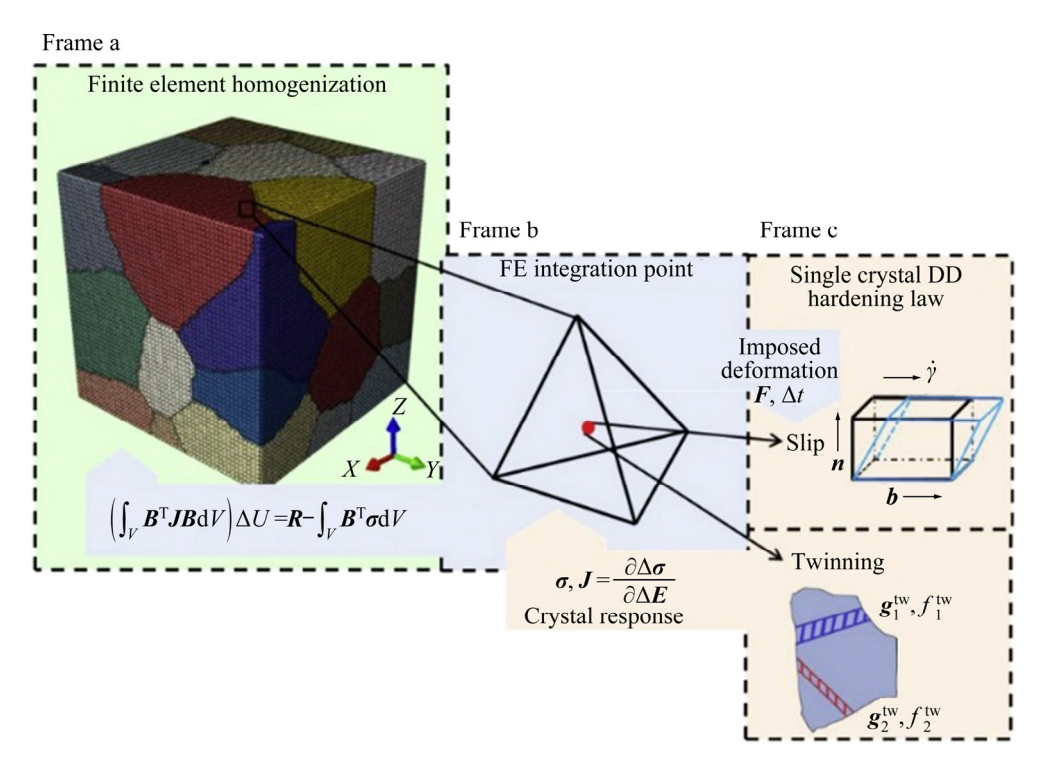
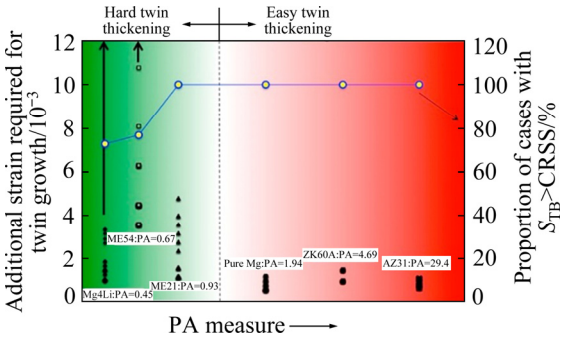


Fig. 9 Schematic of multi-level modeling framework [130]

rates. The crystal plasticity finite element model was used to simulate the local stress state and deformation mechanisms for each loading condition. The extension twinning was found to play an important role in the fracture response of ZEK100.

Alloying additions significantly influence the plastic deformation behavior of Mg alloys. In recent years, intensive efforts on CP simulations have been made to reveal the difference in deformation mechanisms for different Mg systems. For example, KUMAR et al [132] used a crystal plasticity model based on fast Fourier transform to characterize deformation twinning in different Mg alloys. In the model, the influence of alloying additions was represented by their effects on the critical resolved shear stress (CRSS) for slipping and twinning systems. It was found that the twin growth and twin transmission were relatively favorable in AZ31, ZK60 and pure Mg compared to WE54 and ME21. Similarly, the model was employed to study the effect of alloying addition on twin thickening in Mg alloys. The results suggested that the alloy with high plastic anisotropy favored twin thickening (see Fig. 10) [132]. HERRERA-SOLAZ et al [133] used an inverse optimization strategy based on CPFE simulations of polycrystalline alloys to obtain the CRSS values of two Nd-containing Mg-



**Fig. 10** Alloying effect represented by plastic anisotropic measure on twin growth in Mg alloys [132]

1%Mn alloys. It was found that, with respect to pure Mg, the presence of Nd increased the CRSS value of basal slip. RAEISINIA and AGNEW [134] simulated the tensile and compressive yielding of as-cast Mg–Zn alloys, with varying grain sizes and compositions ranging from 0 to 2.3 at.% Zn. The influence of grain size and composition on the CRSS of basal slip and tensile twinning was determined by the simulated results. The CRSS of basal slip was found to increase with decreasing the grain size and increasing the concentration of Zn. Nevertheless, the CRSS for twinning increased with Zn content within the interval of 0–0.8 at.%, whereas it decreased with Zn content when it was above 0.8 at.%.

## 3 Mg-Al system

#### 3.1 Binary system

Mg-Al family is one of the most commonly used wrought Mg alloys with moderate strength, high plasticity, good corrosion resistance, and low material cost [135,136]. Addition of Al reduces the anisotropy in the critical resolved shear stress among different slip systems, promotes the activation of the non-basal  $\langle c+a \rangle$  slip, and increases the ductility of Mg alloys [137,138]. Besides, Al can form precipitates with Mg and increase the strength of Mg alloys. During cooling process, non-equilibrium solidification may occur with the formation of  $\alpha$  (Mg) and  $\beta$  (Mg<sub>17</sub>Al<sub>12</sub>) phases [139]. With the addition of a small amount of alloying elements such as Zn, Ca, Sr, Si, Mn, and rare-earth elements, the morphology, size, amount, and distribution of  $\beta$  phase can be changed noticeably [1,58,139-146]. Moreover, new second precipitates can be formed and thus hinder the growth of  $\alpha$ -Mg and  $\beta$  phase.

The microstructure and mechanical properties of AZ (Mg-Al-Zn), AM (Mg-Al-Mn), AX (Mg-Al-Ca), and other wrought Mg alloys have been extensively studied [147-151].

## 3.2 Influence of micro-alloying Zn

When a small amount (<1 wt.%) of Zn is added into Mg-Al alloys, the solid solubility of Al in Mg matrix can be increased noticeably, which contributes to the improved mechanical properties. Mg alloys such as Mg-3Al-1Zn (AZ31), Mg-6Al-1Zn (AZ61), Mg-9Al-1Zn (AZ91), and Mg-8Al-0.5Zn (AZ80) are widely applied to

Mg-Al-Zn alloys [5,152-156].

ZHA et al [155] prepared the fine-grained AZ31, AZ61, and AZ91 alloys by the combined method of extrusion, homogenization, multi-pass rolling. The rolled AZ31, AZ61, and AZ91 sheets were found to show the similar average grain size of ~3.0 µm with cobblestone-like Mg<sub>17</sub>Al<sub>12</sub> particles. Nevertheless, the amount of Mg<sub>17</sub>Al<sub>12</sub> particles increased with increasing Al content. Compared to the fine-grained AZ91 prepared by other processes [152,154], AZ91 prepared by extrusion and multi-pass rolling was found to exhibit a reasonable comprehensive mechanical properties with the yield strength (YS), ultimate tensile strength (UTS), and elongation (EL) of ~244 MPa, 369 MPa, and 12.9%, respectively. Moreover, ZHANG et al [157] investigated the microstructure and mechanical properties of Mg-Al-Zn alloys prepared by large-reduction hard-plate rolling (HPR). The multimodal structure was observed in the HPRed AZ91, which yields relatively high strength but slightly low ductility with respect to the fine-grained AZ31 and AZ61. Recently, TRANG et al [158] designed Mg-3Al-1Zn-1Mn-0.5Ca (AZMX3110) alloy by taking advantage of the favorable effect of Zn/Ca co-segregation along grain boundaries. The AZMX3110 alloy was demonstrated to show the improved combination of formability (IE value of 8 mm) and yield strength (219 MPa). Table 1 lists the mechanical properties of several typical Mg-Al-Zn alloys at room temperature.

## 3.3 Influence of micro-alloying Mn

The addition of Mn can improve the corrosion resistance, creep behavior and damping

Table 1 Tensile mechanical properties of Mg-Al-Zn alloys at room temperature

Alloy	Processing condition	YS/MPa	UTS/MPa	EL/%	Ref.
AZ31	Extrusion + multi-pass rolling	201	289	22.2	[155]
AZ31	Large-reduction hard-plate rolling	182	260	17.0	[5]
AZ61	Extrusion + multi-pass rolling	205	327	18.0	[155]
AZ61	Large-reduction hard-plate rolling	221	312	13.5	[5]
AZ91	Powder metallurgy + extrusion	_	518	6	[152]
AZ91	Extrusion + multi-pass rolling	244	369	12.9	[155]
AZ91	Spray forming + extrusion	_	435	9	[5]
AZ91	Large-reduction hard-plate rolling	246	370	14.0	[5]
Mg-7.6wt.%Al-0.4wt.%Zn	Aging prior to extrusion	210	329	25.0	[153]

capacity of Mg alloys. Strengthening phases such as α-Mn and Al<sub>x</sub>Mn<sub>y</sub> can form in Mg-Al-Mn alloys [148,150,159-161]. HU et al [160] studied Mg-0.4Al-xMn (x=0, 0.3, 1.5, wt.%) alloys prepared by conventional one-step extrusion process. α-Mn and Al<sub>8</sub>Mn<sub>5</sub> precipitates were found to alter the behaviors of recrystallization nucleation and grain growth. Compared with the dynamically recrystallized Mg-0.4Al alloy, Mg-0.4Al-0.3Mn and Mg-0.4Al-1.5Mn alloy showed the bimodal microstructure (un-dynamically and dynamically recrystallized grains). Moreover, the dynamically recrystallized grains exhibit fine grain size of  $\sim$ 1 µm with random orientations. Interestingly, while Mg-0.4Al-0.3Mn shows a reasonable mechanical properties with the YS, UTS, and EL of 239 MPa, 262 MPa, and 30.1%, respectively, Mg-0.4Al-1.5Mn exhibits an extraordinary EL of 52.5% and a reasonable YS of 170 MPa.

## 3.4 Influence of micro-alloying Ca

With the addition of Ca into Mg–Al system, Al<sub>2</sub>Ca, Mg<sub>2</sub>Ca, and (Mg,Al)<sub>2</sub>Ca phases with high thermal stability can form during processing, which can increase the room- and high-temperature mechanical properties and creep resistance [162–166].

JIANG et al [166] studied the microstructure and mechanical properties of Mg-Al-Ca alloys with different Al and Ca contents. The extruded Mg-2.32Al-1.7Ca alloy was found to exhibit the best mechanical properties with the YS, UTS, and EL of 275 MPa, 324 MPa, and 10.2%, respectively. The improved mechanical properties were mainly ascribed to the combined effects of the fine dynamically-recrystallized grains, nano-scale platelike Al<sub>2</sub>Ca (30-50 nm) precipitates and the high density of submicron Al<sub>2</sub>Ca particles (0.5–1.0 μm) dispersed in the matrix. Recently, it was proposed that Mg-Al-Ca-Mn alloys possess great potential as one of promising high strength and low cost wrought Mg alloys. Addition of Mn can facilitate the formation of Al-Mn precipitates and monolayer Guinier Preston (G.P.) zones with Ca [167–171]. NAKATA et al [171] developed a new wrought Mg alloy, i.e. Mg-1.3Al-0.3Ca-0.4Mn (namely AXM10304), that can be extruded at a high die-exist speed of 24 m/min. The uniformly dispersed G.P. zones were found to facilitate the cross-slip. Moreover, the G.P. zones do not work as nuclei of micro-voids and propagation site during deformation, which helps to suppress the degradation of elongation after the age-hardening. After age-hardening treatment, AXM10304 was found to exhibit a good combination of strength and ductility with the YS of 287 MPa and EL of 20%. Considering the low processing cost associated with high-speed extrusion and the good workability, Mg-Al-Ca-Mn alloy could be a promising candidate for industrially viable low-cost wrought Mg alloy.

## 4 Mg-Zn system

Mg–Zn family serves as the strong wrought Mg alloy and attracts extensive attention [172]. As shown in Table 2, when the content of Zn increases from 1.5 to 6.0 wt.% [173–176], the yield strength and elongation increase noticeably. Nerveless, the YS and EL values of Mg–Zn binary systems are usually below 180 MPa and 20%, respectively. To improve the mechanical properties of Mg–Zn binary systems, a wide variety of researches have focused on the development of new-type Mg–Zn alloys through alloying additions. Table 2 gives the mechanical properties of Mg–Zn binary systems and multicomponent systems reported in literatures.

Addition of Ca was found to efficiently refine grain size and improve the mechanical properties of Mg-Zn alloys [172]. After hot extrusion at 300 °C, a YS of 220 MPa and an EL of 19.3% were achieved in Mg-5.3Zn-0.6Ca (wt.%) [190]. At the similar extrusion temperature, the EL was increased to 29% by adding 1 wt.% Ca into Mg-2Zn alloy [184]. In addition, HORKY et al [179] reported that the YS and EL of Mg-0.6Zn-0.5Ca (wt.%) reached up to 370 MPa and 7%, respectively, owing to the refined grain size and the high fraction of unrecrystallization during the process. Zr is another important alloying element used to efficiently improve the mechanical properties of Mg-Zn alloys. It was reported that the large elongation of 29% was reached in Mg-0.7Zn-0.2Zr-0.7Gd (wt.%) alloy by hot rolling at 400 °C and annealing at 440 °C for 1 h [180].

Addition of rare-earth elements, such as Gd [186], La [182,188], Ce [174,191], Y [183], Nd [183], can efficiently enhance mechanical properties of Mg–Zn alloys. LIU et al [173] studied the influence of Gd, Y, and Ce in Mg–2Zn alloy. A

**Table 2** Mechanical properties of Mg–Zn alloys

Alloy composition/wt.%	Processing condition	YS/ MPa	UTS/ MPa	EL/ %	Ref.
Mg-1.5Zn	Rolled at 450 °C + annealed at 350 °C for 1 h	110	190	12	[173]
Mg-4Zn	Extruded at 300 °C	118	223	15.4	[175]
Mg-3Zn	Extruded at 350 °C, 5 mm/s, 16:1	123	236	25.3	[174]
Mg-6Zn	Extruded at 300 °C, 5 mm/s, 16:1	168	287	16.7	[176]
Mg-0.21Zn-0.3Ca-0.14Mn	Extruded at 300 °C, 6 m/min, 20:1	100	200	30	[177]
Mg-0.4Zn-1.0Zr-1.5Ca-0.8Ti	Solution-treated at 500 °C for 7 h + aged at 200 °C for 20 h		145	3.2	[178]
Mg-0.53Zn-0.24Ca-0.27Mn	Extruded at 300 °C, 6 m/min, 20:1	103	205	33	[177]
Mg-0.6Zn-0.5Ca	Extruded at 350 °C + double equal channel angular pressed $(2 \times 300 \text{ °C} + 2 \times 280 \text{ °C})$	370	373	7	[179]
Mg-0.7Zn-0.2Zr-0.7Gd	Rolled at 400 °C + annealed 440 °C for 1 h	88	229	29	[180]
Mg-0.71Zn-0.36Ca-0.07Mn	Extruded at 300 °C, 6 m/min, 20:1	108	220	37	[177]
Mg-0.8Zn-0.3Gd-0.2Ca	Rolled at 320 °C + annealed at 350 °C + aged at 175 °C for 80 h	_	_	40	[22]
Mg-1.21Zn-0.18Zr	Rolled at 300 °C + annealed at 300 °C	206	244	22	[181]
Mg-1.21Zn-0.18Zr-0.39Ca	Rolled at 300 °C + annealed at 300 °C	197	253	28	[181]
Mg-1.5Zn-0.2Gd	Rolled at 450 $^{\circ}\text{C}$ + annealed at 350 $^{\circ}\text{C}$ for 1 h	97	210	27	[173]
Mg-1.5Zn-0.2Y	Rolled at 450 $^{\circ}\text{C}$ + annealed at 350 $^{\circ}\text{C}$ for 1 h	130	230	22	[173]
Mg-1.5Zn-0.2Ce	Rolled at 450 $^{\circ}\text{C}$ + annealed at 350 $^{\circ}\text{C}$ for 1 h	127	220	22	[173]
Mg-1.5Zn-0.4Mn-0.9LaMM	Extruded at 300 °C, 5 mm/s	349	353	19.4	[182]
Mg-2Zn-0.4Gd	Extruded at 310 °C	140	220	26	[183]
Mg-2Zn-0.4Ce	Extruded at 310 °C	190	260	18	[183]
Mg-2Zn-0.4Y	Extruded at 310 °C	160	240	30	[183]
Mg-2Zn-0.4Nd	Extruded at 310 °C	180	250	28	[183]
Mg-2Zn-1Ca	Extruded at 300 °C, 12:1		283	29	[184]
Mg-2Zn-0.7Ca-1Mn	Extruded at 300 °C	229	278	10	[185]
Mg-2.4Zn-0.8Gd	Extruded at 250 °C, 2 mm/s, 9:1	284	338	24.1	[186]
Mg-2.5Zn-0.7Y-0.4Zr	Extruded at 300 °C	329.3	347.1	12.8	[187]
Mg-3Zn-0.5La-0.2Ca	Extruded at 300 °C, 5 mm/s, 16:1	241	292	21.5	[188]
Mg-3Zn-0.05Ce	Extruded at 350 °C, 5 mm/s, 16:1	123	252	34.0	[174]
Mg-3Zn-0.9Y-0.6Nd-0.6Zr	Solution treated at 540 °C for 8 h + aged at 220 °C in an oil-bath	161	262	15.2	[189]
Mg-5.3Zn-0.6Ca	Extruded at 300 °C, 0.2 mm/s, 17:1	220.2	291.5	19.3	[190]
Mg-5.3Zn-0.6Ca-0.5Ce/La	Extruded at 300 °C, 0.2 mm/s, 17:1	270.2	311.1	14.8	[190]

relatively large elongation of 27% was achieved by adding 0.2 wt.% Gd, while a reasonable UTS of 230 MPa was realized by adding 0.2 wt.% Y. In contrast, Mg-2Zn-0.2Ce (wt.%) alloy exhibited a combination of moderate mechanical properties with UTS of 230 MPa and EL of 22%. Furthermore, co-addition of Ca with Mn, Zr, and RE [178,189] was shown as an effective approach to improve

mechanical properties. JIANG et al [177] investigated different Ca and Mn additions in Mg–Zn alloys. A relatively large EL of 37% and UTS of 200 MPa were achieved in Mg–0.71Zn–0.36Ca–0.07Mn alloy. BAZHENOV et al [185] also developed a new Mg–2Zn–0.7Ca–1Mn (wt.%) alloy with reasonable mechanical properties. Recently, XIA et al [181] showed that addition of

0.39 wt.% Ca increased EL and slightly decreased strength in Mg-1.21Zn-0.18Zr (wt.%) alloy. This was attributed to the basal poles tilted away from ND toward TD and the high activity of  $\langle c+a \rangle$  slip and tensile twins. For the co-addition of Ca and Gd, the modification of nano-precipitates and texture investigated in Mg-0.8Zn-0.3Gd-0.2Ca (wt.%). It was found that the microstructure was mainly characterized by the fine Mg<sub>2</sub>Zn<sub>3</sub>Gd<sub>2</sub> precipitates, monolayer ordered G.P. zone enriching in Ca and Zn atoms and a special circular non-basal texture [22]. Similarly, XU et al [187] reported that Mg-2.5Zn-0.7Y-0.4Zr was characterized by the fine DRXed grains and dense nanoscale precipitates (MgZn<sub>2</sub> and W phases) within the matrix, which increases the YS to 329.3 MPa with the reasonable EL of 12.8%.

## 5 Mg-RE systems

## 5.1 Mg-Gd based alloys

Gd exhibits a high solubility in Mg up to 23.5 wt.% at 819 K [192]. Addition of Gd is thus expected to yield noticeable solid solution strengthening effect [193]. It was reported that Mg alloys containing more than 10 wt.% Gd exhibit exceptional mechanical properties at room and elevated temperatures, mainly owing to the solid solution strengthening and the precipitation hardening. However, high Gd content increases the alloy density and cost, and decreases the ductility. Therefore, Mg-Gd alloys with low Gd content are aimed for the alloying design. STANFORD et al [194] reported that the addition of Gd weakens the recrystallization texture when the concentration is below 1%. Nevertheless, it remains unchanged with further addition of Gd. formation of RE textural component  $(\langle 11\overline{2}1\rangle || ED)$  was found to improve the EL, which is up to 30% along the extrusion direction [195]. Similarly, WU et al [196] reported an extruded Mg-1Gd (wt.%) binary alloy showing the elongation of ~30%. HU et al [197] investigated the microstructure and mechanical properties of the extruded Mg-xGd-0.6Zr (x=2, 4, 6, wt.%) alloys. The elongation of all the extruded alloys is over 30%, and the ultimate and yield tensile strengths of Mg-6Gd-0.6Zr alloy reach 237 and 168 MPa, respectively.

Recently, Mg-Gd alloys with micro-alloying of Mn, Ca, Zn, Ag, Ce and Nd have been extensively studied. WU et al [198] reported that the rolled Mg-Gd-Zn alloy sheet shows exceptional ductility and formability. ZHAO et al [199] investigated the effect of Mn (0, 0.5, 1.3, 1.5, 2.0, wt.%) on microstructure and mechanical properties of Mg-2Gd. It was found that addition of 0.5 wt.% Mn results the in complete recrystallization, yielding the relatively good ductility. The authors also found that adding Zn to Mg-2Gd-0.5Zr alloy can effectively improve the YS and UTS simultaneously [200]. Mg-2Gd-0.5Zr-3Zn was demonstrated to exhibit the well-balanced strength and ductility with the YS, UTS, and EL of 285 MPa, 314 MPa, and 24%, respectively. Moreover, ZHAO et al [201] reported that the co-addition of Zn and Ca into Mg-1Gd alloy resulted in noticeable grain refinement, yielding the relatively high strength. The authors also investigated the effect of Nd in the extruded Mg-4Gd-0.5Zr alloy [202]. It was found that addition of Nd can weaken the texture and increase the yield strength without reducing the elongation. SUN et al [203] developed a Mg-5.7Gd-1.9Ag (wt.%) alloy with high strength, of which the YS, UTS, and EL reach 300.1 MPa, 382.6 MPa and 7.2%, respectively. ZHAO et al [204] investigated the effect of Ce on microstructure and tensile properties of Mg-1Gd-0.5Zn alloys. It was found that grain refinement and massive Mg<sub>12</sub>Ce phases primarily contribute to the high strength of Mg-1Gd-0.5Zn-1.2Ce sheet. Moreover, the enhanced ductility of Mg-1Gd-0.5Zn with 0.3 wt.% Ce was mainly ascribed to the combined effects from the enhanced activities of basal slip and pyramidal slip. Table 3 lists the mechanical properties of different Mg-Gd alloys at room temperature.

## 5.2 Mg-Y based alloys

With the high solubility of 12.4 wt.% in Mg, Y is known to reduce the intensity of deformation texture of Mg alloys by altering the relative activity of deformation mechanisms and the interplay among recrystallization mechanisms [206–208]. The mechanical properties of typical Mg–Y alloys at room temperature are given in Table 4.

Table 3 Mechanical properties of Mg-Gd based alloys

Alloy composition/wt.%	Processing condition	YS/MPa	UTS/MPa	EL/%	Ref.
Mg-0.22Gd	Hot rolled at 400 $^{\circ}\text{C}$ +		190	6	Γ10 <i>4</i> 1
Mg-0.75Gd	annealed at 380 °C for 1 h	145	210	12	[194]
Mg-1Gd	Hot rolled at 400 °C + annealed at 350 °C for 1 h + water quenched	111	240	29.7	[205]
Mg-1Gd	Solution treated for 15 h at 500 °C + extruded at 450 °C	76	223	25.3	[201]
Mg-1.55Gd	Solution treated for 3 h at 530 °C + 5 h at 560 °C + extruded at 450 °C	102	214	23.9	[195]
Mg-2Gd	Extruded at 420 °C	115	189	49	[199]
Mg-2.75Gd	Hot rolled at 400 °C +	160	205	21	[10 <i>4</i> ]
Mg-4.65Gd	annealed at 380 °C for 1 h	165	210	26	[194]
Mg-1Gd-0.7Ca		92	201	13.2	
Mg-1Gd-0.7Zn	Solution treated for 15 h at 500 °C + extruded at 450 °C	97	291	30.2	[201]
Mg-1Gd-0.7Zn-0.7Ca	extruded at 450 °C	135	339	28.5	
Mg-1Gd-0.5Zn		103	288	28.5	
Mg-1Gd-0.5Zn-0.3Ce	Solution treated for 15 h at 500 °C +	107	323	33.6	[204]
Mg-1Gd-0.5Zn-0.7Ce	extruded at 430 °C	115	351	28.9	
Mg-1Gd-0.5Zn-1.2Ce		131	351	24.1	
Mg-2Gd-1Zn	Solution treated for 10 h at 500 °C + hot rolled at 430 °C + annealed at 400 °C for 1 h	129.9	233.4	40.3	[198]
Mg-2Gd-0.5Mn		84	172	51	
Mg-2Gd-1.3Mn	E 4 1 1 4 420 0G	132	206	45	F1007
Mg-2Gd-1.5Mn	Extruded at 420 °C	154	219	42	[199]
Mg-2Gd-2Mn		189	243	33	
Mg-2Gd-0.5Zr-3Zn	Extruded at 440 °C	285	314	24	[200]
Mg-3Gd-1Zn	Solution treated for 10 h at 500 °C + hot rolled at 430 °C + annealed at 400 °C for 1 h	130.6	220	40.3	[198]
Mg-4Gd-0.5Zr		87.9	185.7	44.6	
Mg-4Gd-0.5Zr-0.5Nd	Solution treated for 12 h at 510 °C +	96.5	195.9	42.3	[202]
Mg-4Gd-0.5Zr-1Nd	extruded at 450 °C	113.6	215.8	40.3	[202]
Mg-4Gd-0.5Zr-1.5Nd		160.2	223.9	39.3	
Mg-5.7Gd-1.9Ag	Solution treated for 24 h at 500 °C + hot rolled at 450 °C + aged at 200 °C for 30 h	300.1	382.6	7.2	[203]
Mg-6Gd-0.6Zr	Extruded at 450 °C	168	237	30	[197]

WU et al [210] reported that Y addition has noticeable effect on the microstructure evolution of Mg during hot extrusion and annealing. The elongation increases with Y addition, while the strength decreases. It was ascribed to the reduction of *c/a* ratio and the CRSS of pyramidal slip systems with Y. Activation of pyramidal slip systems was deemed to yield the high ductility of

Mg-Y alloys [213]. ZHOU et al [211] investigated mechanical properties and deformation behavior of as-extruded Mg-3Y alloy. It was shown that a high elongation of ~33% was achieved through common extrusion. Basal slip and extension twinning were revealed to be the dominant deformation modes. TEKUMALLA et al [209] reported that simultaneous increase in strength and ductility

**Table 4** Mechanical properties of Mg-Y based alloys

Alloy composition/wt.%	Processing condition		UTS/ MPa	EL/ %	Ref.
M= 0.4V		MPa	176	70	
Mg-0.4Y		120	1/0	/	
Mg-1Y	Extruded at 350 °C	111	166	10	[209]
Mg-1.8Y		109	167	31	
Mg-2Y	Solution treated for 12 h at 480 °C + extruded at 420 °C	92	189	21	[210]
Mg-3Y	Extruded at 350 °C	120	200	33	[211]
Mg-4Y	Solution treated for 12 h at 480 °C + extruded at 420 °C	87	177	30	[210]
Mg-2.4Y-0.3Ca	Solution treated for 12 h at 400 °C + extruded at 350 °C	117	184	36.6	[212]

was achieved by adding 1.8 wt.% Y into pure Mg. Moreover, ZHOU et al [211] investigated the recrystallization texture, microstructure and mechanical properties of Mg-2.4Y-0.3Ca alloy. A remarkable elongation of 37% was achieved. The enhanced ductility was attributed to grain refinement and activation of different deformation modes, resulting from the weakened texture by Ca and Y addition.

## 5.3 Mg-Nd based alloys

## 5.3.1 Binary system

Nd belongs to Y-group and has a maximum solid solubility of 3.63 wt.% (0.63 at.%) in Mg, which is an effective element for the improvement of mechanical properties [214-217]. According to the Mg-Nd phase diagram [218], Mg<sub>41</sub>Nd<sub>5</sub>, Mg<sub>3</sub>Nd, Mg2Nd and MgNd intermetallic phases can precipitate in Mg-Nd system. Recent discoveries reported that the Mg41Nd5 phase was the equilibrium intermetallic phase at the Mg-rich side [219-222]. The metastable Mg<sub>12</sub>Nd phase, which is not presented in the phase diagram, was also frequently found in Mg-Nd alloys. Moreover, HADORN and AGNEW [223] reported a new precipitate in a dilute hot-rolled Mg-0.15Nd (at.%) alloy, which does not belong to any of the well-documented Mg-Nd phases.

Mg–Nd alloy exhibits apparent precipitation hardening response during heat treatment. Its precipitation sequence was extensively studied from both theory and experiment [224,225]. NIE [219] concluded that the precipitation sequence of Mg–Nd is as follows: ssss (supersaturated solid solution)  $\rightarrow$  ordered G.P. zones  $\rightarrow \beta''(\text{Mg}_3\text{Nd}) \rightarrow \beta'(\text{Mg}_7\text{Nd}) \rightarrow \beta_1(\text{Mg}_3\text{Nd}) \rightarrow \beta(\text{Mg}_{12}\text{Nd}) \rightarrow \beta_e(\text{Mg}_{41}\text{Nd}_5)$ . The detailed characterization on the crystal structure of  $\beta'_f$  precipitate in Mg–3Nd

demonstrated that it has the similar structure with  $\beta_1$  precipitate (orthorhombic structure), which often attached with the end of  $\beta_1$  precipitate for the long aging time. Besides, a novel  $\beta_3$  phase was discovered at the endpoint of  $\beta_1$  precipitate in an aged Mg-3Nd alloy [226]. CHOUDHURI et al [227] proposed that the dislocations were prone to promote the formation of  $\beta'$  and  $\beta_1$  precipitates significantly even in the primary stage of annealing in Mg-Nd alloy.

When Mg-Nd alloys were subjected to different thermal-deformation and/or subsequent heat treatment processes, their microstructural features, including the dislocation-precipitate interactions, twinning behaviors, texture evolution and recrystallization can be different. HUANG et al [228] elucidated the dislocation-precipitate interactions in an aged Mg-2.4 wt.%Nd extruded bar using in-situ TEM characterization and MD simulation. It was found the basal dislocations can directly shear  $\beta'''$  precipitates during deformation, while it is more difficult to bypass  $\beta_1$  precipitates due to the creation of antiphase boundaries. Mg-2.4wt.%Nd with plentiful  $\beta_1$  precipitates was found to show higher ductility than that with  $\beta'''$ precipitates only, which was attributed to the promoted movement of dislocations on prismatic planes for the preservation of ductility [228]. LIU et al [229] investigated the effect of intermediate annealing on twin growth and nucleation in Mg-0.03Nd and Mg-0.18Nd (at.%). It was found the increase of Nd content reduces the fraction of twin nucleation in the alloys without annealing, whereas the twin nucleation was promoted with the increase of Nd in the annealed ones. HADORN et al [230] proposed that the dilute Mg-Nd alloys ( $\leq 0.01$  at.%) have a strong basal  $\langle a \rangle$  texture after hot rolling. Nevertheless, the Mg-Nd alloys with relatively high Nd show weak textures, which have predominately prismatic  $\langle a \rangle$  dislocations. Such different texture effect derives from the dynamic recrystallization mechanism.

### 5.3.2 Influence of micro-alloying Zn and Zr

Zn is commonly used in Mg-Nd alloy, which can reduce the eutectic temperature and make the precipitation hardening effect stronger. Unlike the precipitate sequence in Mg-Nd alloy, precipitation pathway of Mg-Nd-Zn is changed significantly: ssss  $\rightarrow$  ordered G.P. zones  $\rightarrow$  $\gamma''(Mg_5(Nd,Zn)) \rightarrow \gamma \text{ (possibly } Mg_3(Nd,Zn)) [219].$ Zr was often used as the effective grain refiner in Mg-Nd-Zn alloys [231]. WU et al [232] reported that the eutectic Mg<sub>12</sub>Nd is the dominant compound in as-cast Mg-2.7Nd-0.6Zn-0.5Zr (wt.%) alloy. Subsequent T6 treatment facilitates improvement of yield strength, ultimate tensile strength and ductility (191 MPa, 258 MPa and 4.2%, respectively). WANG et al [233] found that Zn<sub>2</sub>Zr<sub>3</sub> precipitates were additionally formed in Mg-2.7Nd-0.6Zn-0.5Zr (wt.%) alloy after solid solution and aging, which caused noticeable hardness improvement in the alloy. Meanwhile, the relatively low concentration of Zn in Mg matrix resulting from the formation of Zn<sub>2</sub>Zr<sub>3</sub> precipitates increased the density ratio of  $\beta_1$  to  $\gamma''$  precipitates.

HA et al [234] studied the mechanical properties and texture evolution during sheet rolling for Mg-0.5Nd (N05), Mg-1Nd (N10) and Mg-0.5Ca (X05) binary systems, and Mg-1Nd-1Zn (ZN10) and Mg-Ca-Zn (ZX10) ternary systems. Tensile properties along RD and TD are shown in Table 5 for the alloys. It is clear that N05 shows higher YS in both RD and TD than X05, ZN10 and ZX10, while ZN10 and ZX10 show relatively high UTS. The investigation of dislocation densities indicated that the individual addition of Nd and Ca yielded the increased activation of non-basal  $\langle a \rangle$  dislocations in N05 and

**Table 5** Tensile properties of Mg-Nd(Ca)-(Zn) alloys along RD and TD at room temperature [234]

A 11	RD		TD		
Alloy	YS/MPa	UTS/MPa	YS/MPa	UTS/MPa	
N05	118	171	109	170	
X05	105	177	108	160	
ZN10	113	188	83	181	
ZX10	109	200	94	197	

X05 alloys. Moreover, the addition of Zn further increased the activation of non-basal  $\langle a \rangle$  dislocations.

## 5.3.3 Influence of micro-alloying RE elements

The precipitation strengthening response of Mg alloy was reported to be enhanced by the co-addition of different types of REs [219]. REs from different groups, for instance, Ce-group (with relatively low solubility in Mg) and Y-group (with relatively high solubility in Mg), were often combined to prepare Mg-RE alloys with excellent mechanical properties. It was reported that the ratio of two REs in Mg alloys influences the mechanical properties and microstructure significantly. LIU et al [235] prepared various Mg-Gd-Y-Nd-Zr alloys with the Nd/Gd ratio ranging from 0.29 to 0.75. They found that the amount of fiber-like second phases increases as the Nd/Gd ratio increases. Although the mechanical properties of Mg-Gd-Y-Nd-Zr show alloys negligible difference with increasing Nd/Gd ratio, their aging hardening response decreases remarkably. LEI et al [202] found that the micro-alloying of Nd remarkably weakens the texture of Mg-4Gd-0.5Zr (VK41) and reduces the intensity of double peak texture. With addition of Nd from 0.5% to 1.5%, the yield strength of VK41 increased significantly without noticeable loss of ductility. Table 6 shows that VK41+1.5Nd alloy exhibited the best yield strength among the considered alloys. It was primarily ascribed to the solid solution strengthening.

LV et al [236] combined minor additions of Nd (0.6 wt.%) and Er (0.3 wt.%) in the extruded Mg-6Zn-0.5Mn (ZM60) to develop a novel wrought Mg alloy. It was found that the rod  $\beta'_1$  $(Mg_4Zn_7)$  and some thick  $\beta'_2$   $(MgZn_2)$  precipitates were largely formed due to the dislocation accumulation, which hindered the growth of DRX in ZM60-0.6Nd-0.3Er alloy. Accordingly, the compressive YS, ultimate compressive strength, and compressibility were increased from 210.9 MPa, 298.5 MPa, 11.8% (ZM60) to 245.8 MPa, 347.2 MPa and 16.3% (ZM60-0.6Nd-0.3Er),respectively. SHENG et al [237] investigated the static recrystallization process of extruded Mg-4Zn-0.6Y-0.5Nd alloy subjected to different annealing processes. It was found that the extruded Mg-4Zn-0.6Y-0.5Nd alloy contains primarily large elongated grains and some dynamic 

Table 6 Te	ensile properties	of as-extruded	VK41+xNd al	loys [202]

A 11	RD				TD			
Alloy composition/wt.%	YS/MPa	UTS/MPa	EL/%	YS/MPa	UTS/MPa	EL/%		
VK41	87.9±2.0	185.7±1.0	44.6±0.6	156.6±2.0	204.7±3.0	25.3±0.3		
VK41-0.5Nd	96.5±1.0	$195.9\pm2.0$	$42.3 \pm 0.4$	$152.7 \pm 1.0$	$227.9 \pm 2.0$	$24.5 \pm 0.5$		
VK41-1Nd	113.6±3.0	$245.8 \pm 1.0$	$40.3 \pm 0.5$	$158.3 \pm 1.0$	$238.1 \pm 2.0$	$24.3 \pm 0.4$		
VK41-1.5Nd	$160.2 \pm 2.0$	223.9±2.0	$39.3 \pm 0.5$	$169.2 \pm 2.0$	$250.0 \pm 1.0$	23.6±0.5		

recrystallized grains. The extruded Mg-4Zn-0.6Y-0.5Nd alloy annealed at 250 °C indicated the relatively high mechanical properties (see Table 7).

## 5.4 Mg-Ce based alloys

#### 5.4.1 Binary system

The solid solubility of Ce is around 1.6 wt.% at 590 °C and reduces as the temperature is decreased [238]. Accordingly, various intermetallic phases, such as Mg<sub>12</sub>Ce, Mg<sub>3</sub>Ce, Mg<sub>41</sub>Ce<sub>5</sub>, Mg<sub>2</sub>Ce, Mg<sub>39</sub>Ce<sub>5</sub>, and Mg<sub>3.6</sub>Ce can form in binary Mg-Ce system [239,240]. It was reported that Mg-Ce alloys show the similar precipitation sequence with Mg-Nd binary, i.e., ssss  $\rightarrow$  GP zone  $\rightarrow \beta'' \rightarrow \beta' \rightarrow$  $\beta$ , in which  $\beta''$  and  $\beta'$  are the metastable phases and  $\beta$  is the equilibrium phase [219]. Similar conclusion was reached by SAITO and KANEKI [241] via the detailed identifications of precipitation behavior for the aged-hardened Mg-0.5Ce (at.%) alloy. Because Ce has a lower equilibrium solid solubility in Mg than Nd, its age-hardening response is expected to be weaker than that of Nd.

HADORN et al [242] studied the influence of Ce (0.0056-0.49 at.%) on the texture evolution in the hot-rolled Mg. They found that a strong texture with typical basal  $\langle a \rangle$  dislocations was formed in dilute Mg-Ce alloy (<0.043 at.%), while the concentrated Mg-Ce alloys show weaker textures with accumulations of  $\langle c+a \rangle$  and non-basal  $\langle a \rangle$ dislocations. Twinning behaviors in the extruded Mg and Mg-0.5Ce alloy were studied using in-situ EBSD under compressive loading [243]. It was found that most of the twins in Mg did not match the Schmidt's law, as opposed to the crystal plasticity simulation findings. A modified threshold energy criterion was then proposed to predict the formation of twins in Mg and Mg-Ce alloys. Recently, JIANG et al [244] studied the dynamic strain aging behaviors of Mg-0.5Ce alloy within wide temperature and strain rate ranges.

**Table 7** Tensile properties of extruded Mg-4Zn-0.6Y-0.5Nd alloy [237]

Processing condition	YS/MPa	UTS/MPa	EL/%
Extruded	153	246	20
Extruded + annealed at 200 °C for 12 h	166	255	19
Extruded + annealed at 225 °C for 12 h	162	252	15
Extruded + annealed at 250 °C for 12 h	174	258	14.5

## 5.4.2 Influence of micro-alloying elements

PAN et al [245] developed a novel lightweight and micro-alloyed Mg-Ce-Al alloy with the high extruded strength of 365 MPa. As shown in Figs. 11(a, d, g), the planar co-segregation of Ce and Al can be found at grain boundaries in both AE300 and AE300H (denoted by different extrusion processes). Several linear defects were also observed within the grain interiors (Figs. 11(b, e, h), implying the possible solute segregation in the adjacent of dislocations. The Ce-Al segregations at both the grain boundaries and dislocations were thus deemed to facilitate the micro-sized grain refinement in the matrix, thereby enhancing the yield strength of AE300. Furthermore, addition of Zn and Zr was found to noticeably influence the mechanical properties of Mg-Ce alloys. HU et al [246] reported that Mg-0.8Ce-0.69Zn-0.03Zr (wt.%) alloy extruded at 300 °C shows UTS and EL of ~325 MPa and 7%, respectively. Similarly, Mg-2.8Ce-0.7Zn-0.7Zr alloy extruded at 350 °C showed improved ductility with relatively low strength. The YS, UTS and EL are 222.4 MPa, 257.8 MPa and 12.0%, respectively [247].

In addition, Ce is widely used as microalloying element in other Mg alloys. ZHAO et al [204] investigated the effect of minor contents of Ce (0, 0.3, 0.7, 1.2, wt.%) on the microstructures and tensile properties of the extruded Mg-1Gd0.5Zn sheets. They revealed that Mg<sub>12</sub>Ce phase was additionally formed in Mg-1Gd-0.5Zn-xCe sheets, the amount of which increases with Ce content. Table 8 shows that the YS and UTS are gradually improved with addition of Ce in the extruded Mg-1Gd-0.5Zn sheets. This was ascribed to the grain refinement and the increased amount of Mg<sub>12</sub>Ce precipitates. LV at al [248] compared the

micro-alloying effects of Ce and Nd on the mechanical properties of Mg-2.0Zn-1.0Mn (ZM21) alloys. Table 9 shows that the minor addition of 0.4 wt.% Ce improves the mechanical properties of ZM21, while the addition of Nd decreases the mechanical properties. Ce was found to yield relatively large effect on the microstructure evolution.

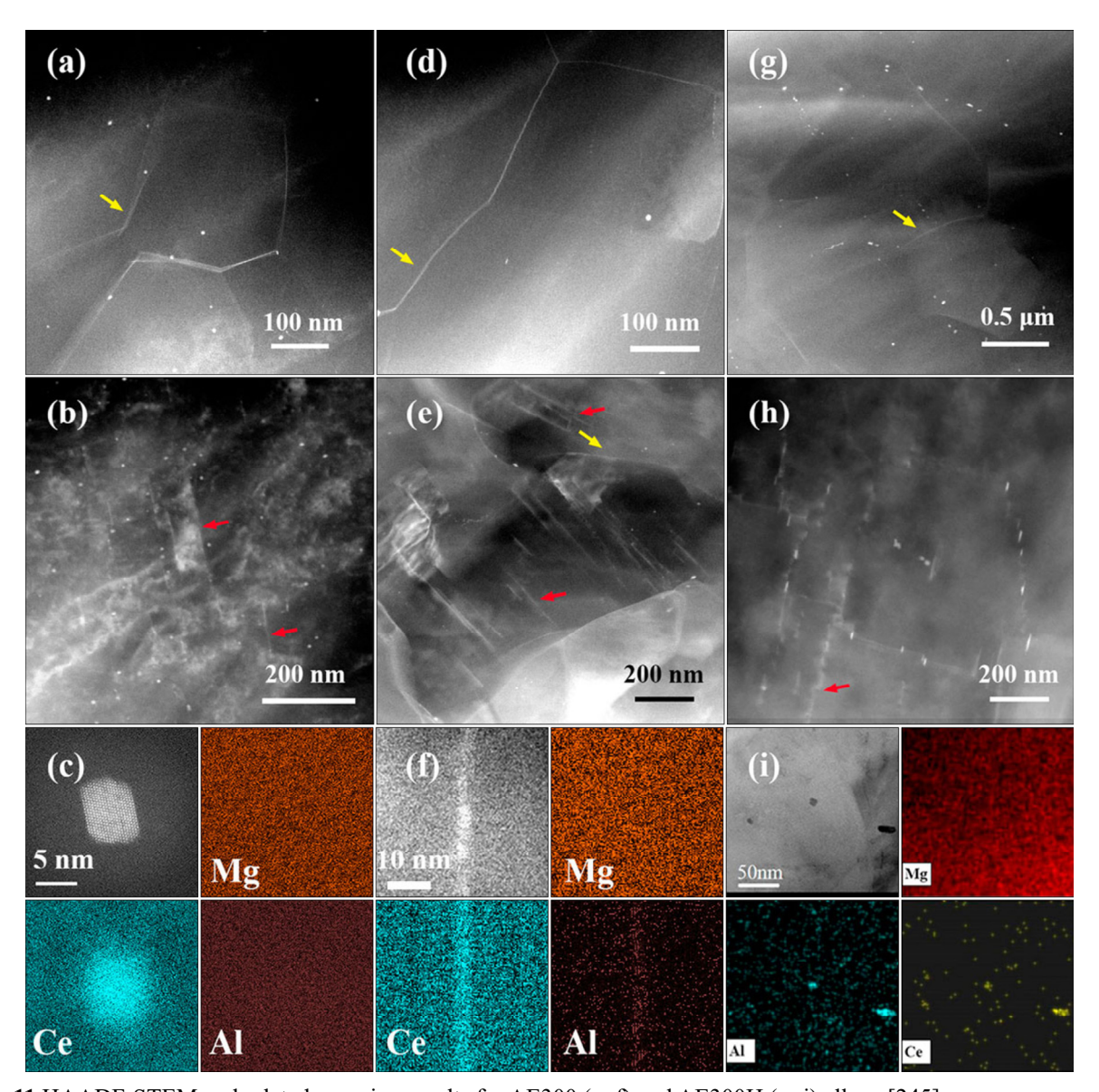


Fig. 11 HAADF-STEM and related mapping results for AE300 (a-f) and AE300H (g-i) alloys [245]

**Table 8** Tensile properties of extruded Mg-1Gd-0.5Zn-xCe sheets along ED and TD [204]

A 11	ED			TD			
Alloys composition/wt.%	YS/MPa	UTS/MPa	EL/%	YS/MPa	UTS/MPa	EL/%	
Mg-1Gd-0.5Zn	103±3.7	288±3.2	28.5±2.1	154±3.3	285±4.5	22.6±1.6	
Mg-1Gd-0.5Zn-0.3Ce	$107 \pm 2.8$	$323 \pm 3.8$	$33.6 \pm 1.2$	158±2.9	$288 \pm 2.7$	21.5±1.5	
Mg-1Gd-0.5Zn-0.7Ce	115±2.4	351±3.6	$28.9 \pm 1.7$	175±3.1	$305 \pm 3.1$	$18.7 \pm 2.3$	
Mg-1Gd-0.5Zn-1.2Ce	131±2.1	$351\pm2.5$	24.1±1.1	185±2.3	320±3.2	$16.8 \pm 2.4$	

**Table 9** Mechanical properties of extruded ZM21– xNd/Ce alloy [248]

Alloys composition/wt.%	YS/MPa	UTS/MPa	EL/%
ZM21	171±0.9	251±1.2	13.7±0.1
ZM21-0.4Nd	148±1.1	235±0.7	28.8±2.0
ZM21-0.4Ce	185±0.6	261±0.8	19.2±0.4

## 5.5 La-containing Mg alloys

La is a cheap rare-earth element [249]. However, the solid solubility of La in Mg is very limited [250]. The eutectic microstructure consisting of α-Mg and Mg<sub>12</sub>La generally occur in Mg–La binary systems. During hot extrusion process, the precipitation of Mg<sub>12</sub>La impacts on the mechanical properties of Mg–La alloys. A relatively high EL of 19.4% was reported for extruded Mg–0.22La (wt.%) alloy by STANFORD and BARNETT [195], in contrast with ~8.1% for pure Mg.

With the limited solubility, La is usually taken as the micro-alloying element in Mg alloys. DU et al [251] reported that the yield strength, ultimate tensile strength, and elongation of the extruded Mg-2.5Zn-0.3Ca-0.4La reach 325 MPa, 341 MPa, and 15%, respectively. The improvement of strength was mainly ascribed to grain refinement and precipitation strengthening. Similarly, DU et al [176] systematically studied the microstructure and mechanical properties of Mg-6Zn-xLa alloys (x=0, 0.2, 0.5, 0.9, wt.%). It was found that the Mg alloy with 0.2% La shows an outstanding ductility with large elongation of 35%. Nevertheless, the ductility and strength decrease with La within the high concentration regime. For Mg-6Zn-0.5Zr (ZK60) alloy, addition of 1% La was reported to lead to exceptional properties with high YS and UTS of 311 MPa and 360 MPa, respectively, owing to the good combination of grain refinement and dispersion strengthening [252]. Interestingly, HU et al [182] reported a new low Zn-containing Mg-1.5Zn-0.4Mn-0.9LaMM(La-rich metal) alloy, which indicates high strength (UTS ~353 MPa) and good ductility (EL ~19.4%) with relatively low alloying concentrations. The high strength was primarily correlated with the grain refinement, precipitation strengthening, and the elongated unDRXed grains. Moreover, addition of 0.3% La in Mg-Li alloy was reported to yield a large elongation of 34% owing to the refined

microstructure and the weakened texture emerging from rod-like Al<sub>2</sub>La phase [253].

Addition of La in rare-earth contained Mg alloys improves mechanical properties significantly. The influence of La and Gd was systematically investigated for as-extruded AZ80 alloy (denoted by AZ80LG) by BU et al [254]. The extruded AZ80LG was found to exhibit much higher strength than AZ80. Recently, MA et al [255] reported that adding 0.5% La can significantly improve the mechanical properties of Mg-9Gd-3Y-0.5Zr, which shows high tensile yield strength of 480 MPa. It was mainly correlated with significant improvement of recrystallization with La addition. ZHANG et al [256] investigated the influence of co-addition of Ca and Ce/La. It was shown that the co-addition yields an enhanced strengthening effect in the extruded Mg-Zn alloy, owing to the grain refinement during the extrusion process. Table 10 shows the mechanical properties for typical La-containing Mg alloys.

## 6 Other promising Mg alloy systems

## 6.1 Mg-Ca based alloys

Mg-Ca based alloys, possessing obvious advantages of high formability and low cost, have recently received much attention [257]. Extensive efforts have been made on developing extrusion alloys based on Mg-Ca system, as given in Table 11. JEONG and KIM [258] studied the effect of Ca microstructure mechanical content and properties of the extruded Mg alloys. The results indicated that with increasing Ca to 2 wt.%, the average grain size was refined to ~3.35 μm. Accordingly, the yield strength was improved to be 252.8 MPa, while the elongation gradually decreased to 14.6%.

Micro-alloying elements noticeably impact on mechanical properties of Mg–Ca system, as shown in Table 11. SHE et al [259] found that the YS and EL of Mg–1.0Ca (wt.%) are increased to 305 MPa and 18.2%, respectively, by adding 1 wt.% Mn. This was attributed to the ultrafine-DRXed grains and the formation of ring fiber texture. In comparison, with adding 1 wt.% Al to Mg–1.0Ca alloy, the YS increased further to 373 MPa, whereas the EL decreased to 6.1%, owing to the formation of high-density G.P. zone and nano-disk Al<sub>2</sub>Ca phase [260]. Moreover, the addition of 0.5% Sr was

**Table 10** Mechanical properties of La-containing Mg alloys [176,195,251–256]

Alloy composition/wt.%	Processing condition	YS/MPa	UTS/MPa	EL/%
Mg-0.22La	Extruded at 450 °C, 30:1	115	232	19.4
Mg-2.5Zn-0.3Ca-0.4La	Extruded at 350 °C, 16:1	325	341	15
Mg-6Zn-0.2La	Extruded at 300 °C, 16:1	146	275	35
Mg-6Zn-0.5La	Extruded at 300 °C, 16:1	150	273	30
Mg-6Zn-0.9La	Extruded at 300 °C, 16:1	135	265	26
Mg-6Zn-0.5Zr-0.5La	Extruded at 300 °C, 16:1	283	348	14
Mg-6Zn-0.5Zr-0.5La	Extruded at 400 °C, 16:1	274	341	16
Mg-6Zn-0.5Zr-1La	Extruded at 300 °C, 16:1	311	360	13
Mg-6Zn-0.5Zr-1La	Extruded at 400 °C, 16:1	287	346	15
Mg-0.5Zn-0.2Mn-0.2Sm-0.3La	Extruded at 350 °C, 17.4:1	190	239	23.9
Mg-1.5Zn-0.4Mn-0.9LaMM	Extruded at 300 °C, 17:1	349	353	19.4
Mg-1.5Zn-0.4Mn-0.9LaMM	Extruded at 350 °C, 17:1	287	303	25.6
Mg-1.5Zn-0.4Mn-0.9LaMM	Extruded at 400 °C, 17:1	200	253	33.3
Mg-8Al-0.5Zn-0.3Mn-0.5Gd-1La	Extruded at 230 °C, 22:1	341	397	10.6
Mg-9Gd-3Y-0.5Zr-0.5La	Extruded at 360 °C, 7:1	364	407	10.3
Mg-6.0Zn-0.5Ca-0.5RE (Ce/La)	Extruded at 300 °C, 17:1	203	297	20.8
Mg-6.0Zn-1.0RE (Ce/La)	Extruded at 300 °C, 17:1	140	273	25.7
Mg-14Li-1Al-0.3La (0°)	Extruded at 250 °C, 89:1	_	146	29
Mg-14Li-1Al-0.3La (45°)	Extruded at 250 °C, 89:1	_	137	34
Mg-14Li-1Al-0.3La (90°)	Extruded at 250 °C, 89:1	_	154	20

Table 11 Mechanical properties of typical Mg-Ca based alloys

Alloy composition/wt.%	Processing condition	YS/MPa	UTS/MPa	EL/%	Ref.
Mg-0.4Ca	Extruded at 350 °C, 16.9:1	165.6	243.1	34	[258]
Mg-1Ca	Extruded at 350 °C, 16.9:1	185.1	239.3	19.5	[258]
Mg-1Ca	Extruded at 280 °C, 2.5 m/min, 25:1	181	209	11.0	[259]
Mg-1.2 Ca	Extruded at 350 °C, 0.4 mm/s, 20:1	360	370	3.9	[257]
Mg-1.2 Ca	Extruded at 350 °C, 1 mm/s, 20:1	258	266	12.2	[257]
Mg-1.2 Ca	Extruded at 350 °C, 2.4 mm/s, 20:1	326	319	8.3	[257]
Mg-2Ca	Extruded at 350 °C, 16.9:1	204.7	252.8	14.6	[258]
Mg-3Ca	Extruded at 350 °C, 16.9:1	248.9	273.8	7.3	[258]
Mg-0.84Ca-0.4Al-0.02Mn	Extruded at 350 °C, 19.6:1	185	239	19.5	[258]
Mg-1Ca-0.6Al	Extruded at 250 °C, 0.4 mm/s, 20:1	398	406	1.3	[260]
Mg-1Ca-1Al	Extruded at 250 °C, 0.3 mm/s, 20:1	373	378	6.1	[260]
Mg-1Ca-0.5Sr	Extruded at 275 °C, 25:1	304.3	307.4	0.104	[261]
Mg-1Ca-0.5Sr	Extruded at 340 °C, 25:1	202.7	234.9	0.183	[261]
Mg-1Ca-0.5Sr	Extruded at 400 °C, 25:1	157.2	215.1	0.187	[261]
Mg-1Ca-0.3Mn	Extruded at 280 °C, 2.5 m/min, 25:1	210	241	15.5	[259]
Mg-1Ca-1Mn	Extruded at 280 °C, 2.5 m/min, 25:1	305	322	18.2	[259]
Mg-1Ca-1Zn-0.6Zr	Extruded at 350 °C, 0.1 mm/s, 30:1	314	306	11	[262]
Mg-1Ca-1Zn-0.6Zr	Extruded at 400 °C, 0.1 mm/s, 30:1	262	291	11.7	[262]
Mg-1Bi-1Zn-0.6Ca	Extruded at 300 °C, 16:1	215	272	27.1	[263]
Mg-1Al-1Ca-0.4Mn	Extruded at 200 °C, 1.0 mm/s, 25:1	445	453	5	[264]
Mg-1Al-1Ca-0.4Mn	Extruded at 200 °C, 1.5 mm/s, 25:1	412	419	12	[264]
Mg-1Al-1Ca-0.4Mn	Extruded at 200 °C, 2.0 mm/s, 25:1	386	396	13.2	[264]
Mg-1Al-1Ca-0.4Mn	Extruded at 200 °C, 4.0 mm/s, 25:1	342	349	14.4	[264]
Mg-1Al-1Ca-0.4Mn	Extruded at 200 °C, 7.0 mm/s, 25:1	249	301	17.6	[264]

reported to reduce the YS and slightly influence the EL [261]. More recently, the co-addition of alloying elements was conducted to improve the comprehensive mechanical properties of Mg-Ca alloy, such as Zn, Bi, Al, and Mn [262,263]. The addition of 0.4 wt.% Al and 0.02 wt.% Mn was found to enhance the YS and EL of Mg-0.84Ca alloy to 185 MPa and 19.5%, respectively. When the content of Al and Mn were increased to 1.0 wt.% and 0.4 wt.%, respectively, the YS of Mg-1Ca alloy was improved to a high value of 445 MPa with a relatively low EL of 5% [264]. Also, GENG and NIE [262] found that Mg-1.0Ca alloy with addition of 1 wt.% Zn and 0.6 wt.% Zr exhibited the YS of 314 MPa with an EL of 11% through extrusion at 350 °C.

## 6.2 Mg-Sn based alloys

Mg–Sn based alloys have attracted a lot of attention in recent years. For Mg–Sn binary alloys, ZHAO et al [265] reported that with increasing Sn content, the yield strength and ultimate tensile strength of as-extruded Mg–Sn binary alloys increased, which was mainly attributed to the grain refinement and the increased volume fraction of Mg<sub>2</sub>Sn phase. In contrast, the elongation to fracture of as-extruded Mg–Sn binary alloys decreased with increasing Sn, since the Mg<sub>2</sub>Sn precipitates become the crack sources during deformation. The mechanical properties of Mg–Sn binary alloys are summarized in Table 12 [265–269].

However, Mg-Sn binary alloys exhibit

relatively low mechanical properties, which limits their wide applications. In order to improve the comprehensive mechanical properties of Mg-Sn alloys, the addition of micro-alloying elements is considered to be an economical and effective method.

Addition of Y noticeably influences the mechanical properties of Mg-Sn alloys. QIAN et al [270] reported that addition of Y into Mg-0.5Sn decreased the grain size, modified the texture and increased the activity of non-basal slip. Accordingly, Mg-0.5Sn-0.3Y alloy exhibited good mechanical properties with YS of 141 MPa and EL of 30.3% along the extrusion direction. Similarly, WANG et al [269] reported that when 0.7 wt.% Y was added into Mg-0.4Sn, EL was significantly enhanced along the ED, 45° and TD tensile directions. In particular, it significantly increased to 32.7% from 7.8% along the ED direction. The outstanding EL of Mg-0.4Sn-0.7Y alloy was attributed to the high grain boundary cohesion, modification, refinement, texture grain existence of prismatic  $\langle a \rangle$  slip.

Zn and Ca are generally considered to be effective alloying elements for improving the ductility of Mg alloys. Based on Mg-0.4Sn-0.7Y alloy showing high ductility but low strength, WANG et al [271] developed a new Mg-0.4Sn-0.7Y-0.7Zn alloy, which has a YS of 188.4 MPa along the ED direction. CHAI et al [266,272] studied the effect of Ca and Zn addition in Mg-1Sn alloy by considering both individual addition and

Table 12 Mechanical properties of Mg-Sn binary alloys

Alloy composition/wt.%	Extrusion condition	Tensile direction	YS/MPa	UTS/MPa	EL/%	Ref.	
Mg-0.4Sn	400 °C, 51:1	ED	97.4	198.7	7.8		
		45°	104.6	206.6	8.6	[269]	
		TD	121.8	229.5	8.7		
Mg-1Sn	400 °C, 32:1	ED	103.9	218.7	12.9	[266]	
		TD	136.3	253.2	8.9	[266]	
Mg-1Sn	300 °C, 25:1	_	157.7	238.8	19.8	[265]	
Mg-2Sn	260 °C, 20:1	_	157.0	230.0	16.0	[267]	
Mg-3Sn		_	177.1	253.9	17.8		
Mg-5Sn	300 °C, 25:1	_	218.4	268.3	11.2	[265]	
Mg-7Sn		-	234.8	279.3	11.7		
Mg-6Sn	300 °C, 25:1	_	191.0	252.0	20.5	[268]	

co-addition. It was found that addition of Zn improved the strength, while the addition of Ca improved the strength and ductility simultaneously. This was attributed to the refined grains and weakened ED-tilted texture. Furthermore, co-addition of Ca and Zn was demonstrated to significantly improve the EL of Mg-1Sn alloy because of the activation of prismatic slip and the enhancement of intergranular strain propagation capacity. Similarly, PAN et al [267] reported that when 1% Ca and 2% Zn were added into Mg-2Sn alloy, MgSnCa, MgZnCa and MgZn2 phases were revealed with refined grain size, which contributes to the improved YS and EL. When Ca content was increased to 2 wt.%, Mg-2Sn-2Ca exhibited the YS as high as 358-443 MPa [273]. On the basis of Mg-2Sn-2Ca, ZHANG et al [274] developed a new Mg-2Sn-2Ca-0.5Mn alloy with a high YS of 450 MPa and an improved EL of ~5%. In addition, Ce addition to ternary Mg-Sn-Ca alloy was found to refine grain size and change the structural stability from CaMgSn to (Ca,Ce)MgSn and Mg<sub>12</sub>Ce. The EL of Mg-1Sn-0.6Ca-0.2Ce reached 27.6%, which is larger than that of Mg-1Sn-0.6Ca (21.9%) [275].

Regarding the influence of Al, SHE et al [268] investigated the mechanical properties for a series of hot extruded Mg-xAl-5Sn-0.3Mn alloys (x=1, 3, 6, 9, wt.%). The UTS was found to increase with Al content increasing, reaching 370 MPa at 9 wt.% Al. However, the increase of Al content was found to yield negligible role in Mg-9.8Sn-1.2Znbased alloys [276]. At relatively low Sn content in Mg-2.5Sn-1.5Ca-xAl alloys (x=2, 4, 9, wt.%), increasing Al content was reported to decrease the grain size, promote  $\langle a \rangle$  and  $\langle c+a \rangle$  dislocations, and increase fraction the of  $Mg_{17}Al_{12}$ precipitate [277]. The mechanical properties of Mg-Sn based alloys mentioned above are listed in Table 13 [266-277].

## 6.3 Mg-Li based alloys

Li is the lightest metal with the density of 0.533 g/cm<sup>3</sup>. The advantage of Mg–Li-based alloys is their ultra-lightweight [278]. With the increase of Li content, the phase constitution of Mg alloys changes gradually. When Li content is between  $\sim$ 5.5 and 11 wt.%, the alloy is composed of  $\alpha$ -Mg (hcp) and  $\beta$ -Li (bcc) phases. The single  $\beta$ -Li phase survives when Li content is over  $\sim$ 11 wt.%. Li was

reported to promote the non-basal slips and ultimately the ductility of Mg–Li alloys. The mechanical properties of Mg–Li based alloys are listed in Table 14 [279–288]. It can be seen that the YS of Mg–Li binary alloys ranges between 60 and 100 MPa. With the increase of Li content, the YS decreases and the EL increases. The EL of Mg–11Li–3Zn extruded alloy that predominantly consists of  $\beta$ -Li phase was reported to be as high as 55% [286].

Addition of Li improves the ductility of Mg alloys, but the relatively low strength of Mg-Li binary alloys limits their application. Addition of micro-alloying elements into Mg-Li binary alloys is considered to be an effective method to improve the mechanical properties.

Addition of Al was found to promote the formation of MgAlLi<sub>2</sub> phase in Mg-Li alloys, which effectively improves the strength through the precipitation strengthening and the solid solution strengthening [283]. Similar conclusion reached by GUO et al [282]. Nevertheless, when the content of Al was higher than 6 wt.%, the strength remained unchanged and the EL noticeably decreased with Al content. Zn addition enhances the strength of Mg-Li alloys owing to the effective solid solution strengthening effect. HAO et al [283] developed a new Mg-3.5Li-2Zn alloy, which exhibited noticeably improved the mechanical properties compared with ternary Mg-Li-X (X=Al, Ca, Y, Ce, Sc, Mn and Ag) alloys. Similarly, ZHAO et al [288] reported that addition of 1 wt.% Zn increased the EL from 5.6% to 10.1%.

Addition of rare-earth elements in Mg-Li alloys can noticeably increase the strength mainly owing to the formation of dispersive RE-rich precipitates. DONG et al [281] studied the influence of Y content on microstructure and mechanical properties of Mg-7Li alloy. They found that the addition of Y refined the microstructure of α-Mg. OHUCHI et al [280] reported that Mg<sub>3</sub>Nd precipitate would be formed when Nd was added into Mg-8Li alloy, which increased the strength of the alloy. For other elements, addition of 0.5 wt.% Sr was found to increase the EL of Mg-8Li-based alloy from 15.6% to 22.4%, and Mg-8Li-3Al-0.5Mn-0.75Sr alloy showed an optimal tensile strength of 265.46 MPa [187]. The mechanical properties of Mg-Li based alloys discussed above are compared in Table 14.

Table 13 Mechanical properties of Mg-Sn based alloys

Alloy composition/wt.%	Extrusion condition	Tensile direction	YS/MPa	UTS/MPa	EL/%	Ref	
Mg-0.4Sn-0.7Y		ED	99.1	264.2	32.7		
	400 °C, 51:1	45°	115.3	226.8	25.8	[269	
		TD	124.9	236.7	24.7		
		ED	188.4	252.1	33.1		
Mg-0.4Sn-0.7Y-0.7Zn	400 °C, 51:1	45°	130.3	221.8	47.2	[27	
		TD	124.3	231.4	39.1		
		ED	141.0	288.0	30.3	[270]	
Mg-0.5Sn-0.3Y	400 °C, 41:1	45°	170.0	286.0	28.1		
		TD	188.0	302.0	28.0	_	
M 10 0.57		ED	129.4	260.9	17.6		
Mg-1Sn-0.5Zn		TD	153.1	262.1	14.3		
M 10 070	400.00 20.1	ED	137.8	264.8	17.3	F2.6	
Mg-1Sn-0.7Ca	400 °C, 32:1	TD	209.3	293.7	10.3	[26	
10 057 050		ED	104.2	311.9	30.5		
Mg-1Sn-0.5Zn-0.5Ca		TD	188.9	295.6	12.9		
Mg-1Sn-0.5Zn-0.5Ca		-	158.7	302.2	21.3		
Mg-1Sn-0.5Zn-1Ca	360 °C, 32:1	_	137.3	310.9	23.6	[27	
Mg-1Sn-0.5Zn-2Ca		_	180.7	300.0	17.9		
Mg-1Sn-0.6Ca		_	93.3	244.6	21.9		
Mg-1Sn-0.6Ca-0.2Ce	430 °C, 32:1	_	96.8	263.6	27.6		
Mg-1Sn-0.6Ca-0.5Ce		_	109.4	266.3	25.2	[27	
Mg-1Sn-0.6Ca-1Ce		_	104.2	261.9	22.2		
Mg-2Sn-1Ca	260 °C, 20:1	_	269.0	305.0	6.0		
Mg-2Sn-1Ca	300 °C, 20:1	_	207.0	230.0	12.0	[26	
Mg-2Sn-1Ca-2Zn	260 °C, 20:1	_	218.0	285.0	23		
	220 °C, 20:1	_	443.0	460.0	1.2		
	240 °C, 20:1	_	420.0	435.0	3.0		
Mg-2Sn-2Ca	280 °C, 20:1	_	386.0	414.0	5.8	[27	
	320 °C, 20:1	_	358.0	365.0	8.9		
Mg-2Sn-2Ca-0.5Mn	260 °C, 20:1	_	450.0	462.0	5.0	[27	
Mg-2.5Sn-1.5Ca-2Al	, .	_	130.0	248.0	12.5		
Mg-2.5Sn-1.5Ca-4Al	350 °C, 20:1	_	136.0	252.0	11.4	[27	
Mg-2.5Sn-1.5Ca-9Al	,	_	157.0	269.0	9.8	L= / /	
Mg-5Sn-1Al-0.3Mn		_	248.0	294.0	20.6		
Mg-5Sn-3Al-0.3Mn		_	240.0	315.0	15.18	[268]	
Mg-5Sn-6Al-0.3Mn	300 °C, 25:1	_	232.0	346.0	15.66		
Mg-5Sn-9Al-0.3Mn		_	298.0	370.0	8.2		
	250°C, 20:1	_	319.0	358.0	6.1		
Mg-9.8Sn-3Al-1.2Zn	300°C, 20:1	_	289.0	353.0	9.1	[27	
6	400°C, 20:1	_	214.0	315.0	11.0	L '	

Table 14 Mechanical properties of Mg-Sn based alloys

Alloy composition/wt.%	Extrusion condition	Tensile direction	YS/MPa	UTS/MPa	EL/%	Ref.
		ED	104.1	184.6	11.8	
Mg-1Li	300 °C, 30:1	45°	89.1	190.8	16.7	[288]
		TD	90.7	176.5	14.4	
Mg-1Li	300 °C, 6.5:1	ED	93.0	162.0	15.0	[2041
	300 C, 0.3.1	TD	97.0	163.0	14.0	[284]
		ED	93.4	182.3	14.9	[288]
Mg-2Li	300 °C, 30:1	45°	77.3	180.7	24.6	
		TD	78.6	164.4	19.3	
Ma-21 ;	300 °C, 6.5:1	ED	65.0	154.0	16.0	F20.41
Mg-3Li	300 C, 0.3:1	TD	61.0	144.0	19.0	[284]
		ED	85.4	173.4	17.5	[288]
Mg-3Li	300 °C, 30:1	45°	68.6	148.6	28.6	
		TD	70.3	178.5	24.8	
		ED	72.7	175.6	22.4	
Mg-5Li	300 °C, 30:1	45°	58.5	151.3	33.6	[288]
		TD	60.3	180.4	27.3	
	300 °C, 6.5:1	ED	77.0	159.0	17.0	[284]
Mg-5Li		TD	66.0	144.0	19.0	
Mg-3.5Li-0.5Zn		_	132.3	202.0	20.8	[285]
Mg-3.5Li-2Zn		_	163.7	246.0	21.2	
Mg-3.5Li-4Zn	200.00.16.1	_	160.2	250.0	21.8	
Mg-6.5Li-0.5Zn	280 °C, 16:1	_	150.8	222.5	23.5	
Mg-6.5Li-2Zn		_	142.6	188.2	29.0	
Mg-6.5Li-4Zn		_	167.8	233.7	35.0	
Mg-5Li-3Zn		_	145.8	204.6	28.8	
Mg-8Li-3Zn		_	148.3	179.7	43.9	
Mg-11Li-3Zn	200.00 40.1	_	124.5	137.7	56.1	F20 61
Mg-5Li-3Zn-1Sn-0.4Mn	200 °C, 40:1	_	164.8	252.0	18.1	[286]
Mg-8Li-3Zn-1Sn-0.4Mn		_	157.8	201.1	30.9	
Mg-11Li-3Zn-1Sn-0.4Mn		_	156.6	148.7	49.3	
Mg-8Li-3Al-0.5Mn		_	222.4	193.6	15.6	
Ig-8Li-3Al-0.5Mn-0.25Sr		_	220.2	186.2	19.1	
Mg-8Li-3Al-0.5Mn-0.5Sr	300 °C, 25:1	_	242.2	206.9	22.4	[287]
Mg-8Li-3Al-0.5Mn-0.7Sr		_	265.5	174.5	17.1	
Mg-8Li-3Al-0.5Mn-1Sr		_	232.6	204.2	13.8	
Mg-1Zn		ED	151.2	207.6	10.1	
Mg-1Zn		TD	164.3	205.3	9.7	
Mg-1Zn-1Li		ED	112.1	211.6	15.6	
Mg-1Zn-1Li		TD	97.7	227.5	19.8	<b>50-</b> 03
Mg-1Zn-3Li	300 °C, 30:1	ED	91.4	201.3	18.2	[279]
Mg-1Zn-3Li		TD	85.6	225.4	23.8	
Mg-1Zn-5Li		ED	84.7	185.6	22.6	
Mg-1Zn-5Li		TD	73.3	228.4	30.3	

## 6.4 Mg-Bi based alloys

Mg-Bi-based alloys have attracted a lot of research attention in recent years [289–293]. The solid solubility of Bi in Mg is 1.12 at.% at 553 °C and decreases with decreasing temperature [294]. MENG et al [295] compared the mechanical properties of Mg-6Bi (wt.%) with pure Mg. It was found that the as-extruded Mg-6Bi alloys showed reasonable mechanical properties with the YS of 189 MPa, UTS of 228 MPa, and the EL of 19.9%. The finer grains and the abundant micro-/nano-sized Mg<sub>3</sub>Bi<sub>2</sub> precipitates were deemed to be responsible for the improvement of mechanical properties.

The effect of Ca on the mechanical properties of Mg-Bi alloys was studied by MENG et al [289]. It was found that the weakened texture with (2112) parallel to the extrusion direction was obtained by the simple single step extrusion in Mg-1.32Bi-0.72Ca alloy. In combination with the influence of grain refinement, the alloy exhibited the relatively high elongation of 43%. JIN et al [296] investigated the influence of Sn on microstructure and mechanical properties of the extruded Mg-Bi binary alloy. It was found that all the alloys showed partially recrystallized grain structure independent of Sn content. Nevertheless, Sn atoms inhibit the activity of dislocation slip and promote the DRX process, and finer grains were obtained by adding Sn. The combined influence of Sn in solid solution and grain refinement contributed to the improved mechanical properties in Mg-5Bi-4Sn alloys. Mechanical properties of typical Mg-Bi based alloys are compared in Table 15.

**Table 15** Mechanical properties of Mg–Bi based alloys

Alloy	Extrusion condition		UTS/ MPa	EL/ %	Ref.
Mg	300 °C, 36:1	120	208	12	[295]
Mg-2.5wt.%Bi	110 °C, 19:1		155	170 (110 °C)	)[294]
Mg-6wt.%Bi	300 °C, 36:1	189	228	19	[295]
Mg-5wt.%Bi- 1wt.%Si	RS, 19:1		240	40	[294]
Mg-5wt.%Bi- 1wt.%Ca	RS, 19:1		205	45	[294]
BAZ811	300 °C, 30:1	291	331	14.6	[290]
AZ31	300 °C, 30:1	200	284	24.5	[290]

#### 6.5 Mn-containing Mg alloys

Mn is one of the most effective clean elements that can remove impurities in Mg alloys [297,298]. However, the solid solubility of Mn in Mg is as low as 0.996 at.% at 650 °C, which decreases further with decreasing temperature [259,299]. Therefore, nano-sized  $\alpha$ -Mn particles exist in Mn-containing Mg alloys. These nano-sized  $\alpha$ -Mn particles could effectively refine the as-cast grain size and restrict the grain growth during deformation process [298,300–303].

Limited by the relatively low solubility in Mg, Mn is widely adopted as micro-alloying element in Mg alloys [259,297,299,304]. SHE et al [299] investigated the effect of Mn content on the mechanical properties of Mg-Zn alloys. With increasing Mn from 0 to 1.82 wt.%, the YS was found to accordingly increase from 173 to 290 MPa, mainly resulting from the fine grain size and  $\alpha$ -Mn precipitates. Similarly, the improved strengthductility balance by Mn addition was reported in the extruded Mg-Ca alloy [259]. The average size of dynamically recrystallized grains decreased from 10 to 1 μm with increasing Mn from 0 to 0.82 wt.%. Accordingly, the YS was increased from 181 to 305 MPa. PENG et al [304] reported a noticeable improvement of YS for the as-extruded Mg-Gd-Mn alloy with the addition of Mn. Specifically, for Mg-1.0Gd-1.5Mn alloy, the average grain size of dynamically recrystallized grains and the YS were determined to be  $\sim 1.2 \, \mu m$  and  $\sim 280 \, MPa$ , respectively. The YS was increased significantly compared with that of Mg-1.0Gd. Two major roles of Mn in the mechanical properties of wrought Mg alloys have been reported: (1) Refining the DRXed grain size via restricting the DRX grain growth during the hot mechanical process, which ultimately increases the strength of Mg alloys [259,305–308]; (2) Mn precipitates on the basal planes of Mg alloys. Since basal slip dominates the deformation of Mg alloys at room temperature, Mn precipitates on plane contribute noticeably precipitation strengthening [259,294,297,299,304]. Mechanical properties of Mn-containing Mg alloys are given in Table 16.

## 7 Summary and feature outlook

Mg alloys are very promising lightweight structural material. The wide application of Mg

**Table 16** Mechanical properties of Mn-containing Mg alloys

Alloy	Extrusion condition	YS/MPa	UTS/MPa	EL/%	Ref.
MA105	250 °C, 25:1	343	349	21.3	[297]
MA205	250 °C, 25:1	293	300	28.3	[297]
MA305	250 °C, 25:1	274	279	48.9	[297]
ZM20	280 °C, 25:1	173	255	16	[299]
ZM21	280 °C, 25:1	256	291	23	[299]
ZM22	280 °C, 25:1	290	315	24	[299]
Mg-0.3wt.%Al-0.2wt.%Ca-0.5wt.%Mn	350 °C, 20:1	206		29	[169]
Mg-0.3wt.%Al-0.3wt.%Ca-0.2wt.%Mn	400 °C, 20:1	136	203	29	[309]
Mg-0.3wt.%Al-0.3wt.%Ca-0.8wt.%Mn	400 °C, 20:1	190	229	24	[309]
Mg-0.6wt.%Al-0.3wt.%Ca-0.3wt.%Mn	450 °C, 25:1	165	232	14	[310]

alloys is deemed to contribute noticeably to the global issue of energy conservation and emission reduction. Nevertheless, current applications of wrought Mg alloys are very limited, despite the fact that many potential applications of Mg alloys are wrought products. The root cause is the relatively low ductility and strength of Mg. Alloying addition is one of the most efficient strategies to solve the problem. In particular, the micro-alloying design of Mg alloys is a very promising strategy to achieve the desired high mechanical properties at a low cost and facilitate significantly engineering applications of Mg alloys.

In the last two decades, significant progress in the alloying design of Mg alloys has been made from both theory and experiment. A series of new Mg alloys with improved mechanical properties have been developed. In the present review, we try to summarize recent advances in micro-alloying design of wrought Mg alloys from both theoretical and pragmatic perspectives, provide fundamental data required for establishing the relationship between chemical composition and mechanical properties of Mg alloys, and clarify to some extent the role of alloying elements in a series of promising Mg alloys. It is expected to provide helpful guidance for the development of novel wrought Mg alloys. Nevertheless, successive efforts from theory and experiment are required:

(1) First principle calculations based on density functional theory provide deep insight into the mechanisms of alloying influence and the fundamental data required for intelligent design of Mg alloys. However, available calculations are limited to binary systems for both intermetallic

compounds and solid solution phase. More theoretical efforts are thus needed to properly describe the intrinsic properties of Mg alloys containing multiple alloying elements and the influence mechanisms with complex interactions among different solute atoms. Moreover, while attempts have been made to calculate finite-temperature properties of intermetallic compounds, it remains very scarce for Mg alloys in solid solution state.

- (2) Attempts adopting theoretical simulations such as molecular dynamics, cellular automata, and crystal plasticity have been made to understand the deformation behavior and microstructure evolution in some representative Mg alloys. However, they remain in the preliminary stage and intensive efforts are required. More importantly, the integrated theoretical models combined with the merits of multi-scale simulations need to be developed.
- (3) Despite the numerous efforts made on the mechanical properties and microstructure of a great variety of Mg alloys, understanding of alloying influence on microstructure features including dislocation–precipitate interaction, plastic mechanisms, texture evolution, alloying segregation, and recrystallization behaviors is far from expectation. Universal criteria of alloying design are not established for Mg alloys, especially in the case of complex multicomponent and multiphase systems.
- (4) On the basis of the developed datasets from experiment and theory, machine learning methods can be adopted to establish the correlation between chemical composition and mechanical properties of Mg alloys. The algorithms applicable for multi-

objective optimization such as high strength and high ductility can significantly facilitate the intelligent design of novel wrought Mg alloys.

## **Acknowledgments**

authors The acknowledge the financial supports from the National Natural Science Foundation of China (Nos. U1764253, U2037601, 52001037, 51971044, 52101126), the National Defense Basic Scientific Research Program of China, China Postdoctoral Science Foundation (No. 2021M700566), the Natural Science Foundation of Chongqing, China (No. cstc2019jcyjmsxmX0234), Chongqing Science and Technology Commission, China (No. cstc2017zdcyzdzxX0006), Chongqing Scientific and Technological Talents Program, China (No. KJXX2017002), and Qinghai Technology Program, Science and (No. 2018-GX-A1).

## References

- [1] PRASAD S V S, PRASAD S B, VERMA K, MISHRA R K, KUMAR V, SINGH S. The role and significance of Magnesium in modern day research—A review [J]. Journal of Magnesium and Alloys, 2022, 10(1): 1–61.
- [2] SONG Jiang-feng, SHE Jia, CHEN Dao-lun, PAN Fu-sheng. Latest research advances on magnesium and magnesium alloys worldwide [J]. Journal of Magnesium and Alloys, 2020, 8(1): 1–41.
- [3] YANG Yan, XIONG Xiao-ming, CHEN Jing, PENG Xiao-dong, CHEN Dao-lun, PAN Fu-sheng. Research advances in magnesium and magnesium alloys worldwide in 2020 [J]. Journal of Magnesium and Alloys, 2021, 9(3): 705–747.
- [4] YOU Si-hang, HUANG Yuan-ding, KAINER K U, HORT N. Recent research and developments on wrought magnesium alloys [J]. Journal of Magnesium and Alloys, 2017, 5(3): 239–253.
- [5] ZHANG Zi-jian, YUAN Lin, SHAN De-bin, GUO Bin. The quantitative effects of temperature and cumulative strain on the mechanical properties of hot-extruded AZ80 Mg alloy during multi-directional forging [J]. Materials Science and Engineering A, 2021, 827: 142036.
- [6] LIU Ting-ting, YANG Qing-shan, GUO Ning, LU Yun, SONG Bo. Stability of twins in Mg alloys—A short review [J]. Journal of Magnesium and Alloys, 2020, 8(1): 66–77.
- [7] XU Yu-ling, WANG Shi-wei, WANG Yu-ye, CHEN Li, YANG Li-xiang, XIAO Lu, YANG Li, HORT N. Mechanical behaviors of extruded Mg alloys with high Gd and Nd content [J]. Progress in Natural Science: Materials International, 2021, 31(4): 591–598.
- [8] ZHAO Z Y, GUAN R G, SHEN Y F, BAI P K. Grain refinement mechanism of Mg-3Sn-1Mn-1La alloy during accumulative hot rolling [J]. Journal of Materials Science &

- Technology, 2021, 91: 251-261.
- [9] SU Chen, WANG Jing-feng, HU Hao, WEN You-lin, LIU Shi-jie, MA Kai. Enhanced strength and corrosion resistant of Mg-Gd-Y-Al alloys by LPSO phases with different Al content [J]. Journal of Alloys and Compounds, 2021, 885: 160557.
- [10] JANG H S, LEE J K, TAPIA A J S F, KIM N J, LEE B J. Activation of non-basal  $\langle c+a \rangle$  slip in multicomponent Mg alloys [J]. Journal of Magnesium and Alloys, 2021.
- [11] SUŁKOWSKI B, JANOSKA M, BOCZKAL G, CHULIST R, MROCZKOWSKI M, PAKA P. The effect of severe plastic deformation on the Mg properties after CEC deformation [J]. Journal of Magnesium and Alloys, 2020, 8(3): 761–768.
- [12] ZHONG Li-ping, WANG Yong-jian. Microstructure evolution and optimum parameters analysis for hot working of new type Mg-8Sn-2Zn-0.5Cu alloy [J]. Transactions of Nonferrous Metals Society of China, 2019, 29(11): 2290-2299.
- [13] ZHANG Wan-peng, MA Ming-long, YUAN Jia-wei, SHI Guo-liang, LI Yong-jun, LI Xing-gang, ZHANG Kui. Microstructure and thermophysical properties of Mg-2Zn-xCu alloys [J]. Transactions of Nonferrous Metals Society of China, 2020, 30(7): 1803-1815.
- [14] ZHANG Cheng, WU Liang, ZHAO Zi-long, XIE Zhi-hui, HUANG Guang-sheng, LIU Lei, JIANG Bin, ATRENS Andrej, PAN Fu-sheng. Effect of Li content on microstructure and mechanical property of Mg-xLi-3(Al-Si) alloys [J]. Transactions of Nonferrous Metals Society of China, 2019, 29(12): 2506–2513.
- [15] CHENG Xiong-ying, YUAN Yuan, CHEN Tao, ZHENG Ze-bang, MA Li-feng, JIANG Bin, TANG Ai-tao, PAN Fu-sheng. The effects of second-alloying-element on the formability of Mg-Sn alloys in respect of the stacking fault energies of slip systems [J]. Materials Today Communications, 2021: 102829.
- [16] ZHOU Tian-shui, ZHANG Quan-fa, LI Qian-qian, WANG Li-dong, LI Qing-lin, LIU De-xue. A simultaneous enhancement of both strength and ductility by a novel differential-thermal ECAP process in Mg-Sn-Zn-Zr alloy [J]. Journal of Alloys and Compounds, 2021, 889: 161653.
- [17] TSURU T, SOMEKAWA H, CHRZAN D C. Interfacial segregation and fracture in Mg-based binary alloys: Experimental and first-principles perspective [J]. Acta Materialia, 2018, 151: 78–86.
- [18] TONG L B, CHU J H, SUN W T, JIANG Z H, ZOU D N, LIU S F, KAMADO S, ZHENG M Y. Development of a high-strength Mg alloy with superior ductility through a unique texture modification from equal channel angular pressing [J]. Journal of Magnesium and Alloys, 2021, 9(3): 1007–1018.
- [19] BALASUBRAMANI N, WANG Gui, EASTON M A, STJOHN D H, DARGUSCH M S. A comparative study of the role of solute, potent particles and ultrasonic treatment during solidification of pure Mg, Mg–Zn and Mg–Zr alloys [J]. Journal of Magnesium and Alloys, 2021, 9(3): 829–839.
- [20] KAVYANI M, EBRAHIMI G R, EZATPOUR H R, JAHAZI M. Microstructure refinement, mechanical and biocorrosion properties of Mg–Zn–Ca–Mn alloy improved by a new

- severe plastic deformation process [J]. Journal of Magnesium and Alloys, 2021.
- [21] KUANG Jie, ZHANG Yu-qing, DU Xin-peng, ZHANG Jin-yu, LIU Gang, SUN Jun. On the strengthening and slip activity of Mg-3Al-1Zn alloy with pre-induced {1012} twins [J]. Journal of Magnesium and Alloys, 2021.
- [22] YAN H, SHAO X H, LI H P, CHEN R S, CUI H Z, HAN E H. Synergization of ductility and yield strength in a dilute quaternary Mg–Zn–Gd–Ca alloy through texture modification and Guinier–Preston zone [J]. Scripta Materialia, 2022, 207: 114257.
- [23] LUO J, YAN H, LU L W, CHEN R S, WU A R, YIN F C. Cold rollability improvement by twinning and twin-slip synergy in an Mg-Zn-Gd alloy with rare earth texture [J]. Journal of Alloys and Compounds, 2021, 883: 160813.
- [24] MINÁRIK P, ZEMKOVÁ M, VESELÝ J, BOHLEN J, KNAPEK M, KRÁL R. The effect of Zr on dynamic recrystallization during ECAP processing of Mg-Y-RE alloys [J]. Materials Characterization, 2021, 174: 111033.
- [25] OUYANG Si-jie, LIU Wen-cai, WU Guo-hua, JI Hao, GAO Zhan-kui, PENG Xiang, LI Zhong-quan, DING Wen-jiang. Microstructure and mechanical properties of as-cast Mg-8Li-xZn-yGd (x=1, 2, 3, 4; y=1, 2) alloys [J]. Transactions of Nonferrous Metals Society of China, 2019, 29(6): 1211–1222.
- [26] LIANG Xin-li, PENG Xiang, JI Hao, LIU Wen-cai, WU Guo-hua, DING Wen-jiang. Microstructure and mechanical properties of as-cast and solid solution treated Mg-8Li-xAl-yZn alloys [J]. Transactions of Nonferrous Metals Society of China, 2021, 31(4): 925–938.
- [27] HOU Cai-hong, HU Fan, QI Fu-gang, ZHAO Nie, ZHANG De-chuang, OUYANG Xiao-ping, ZHANG Ding-fei. Aging hardening and precipitate behavior of a solution-treated Mg-6Zn-4Sn-1Mn (wt.%) wrought Mg alloy [J]. Journal of Alloys and Compounds, 2021, 889: 161640.
- [28] JIN S C, CHA J W, LEE J H, LEE T, HAN S H, PARK S H. Improvement in tensile strength of extruded Mg-5Bi alloy through addition of Sn and its underlying strengthening mechanisms [J]. Journal of Magnesium and Alloys, 2021.
- [29] NIE J F. Precipitation and hardening in magnesium alloys [J]. Metallurgical and Materials Transactions A, 2012, 43(11): 3891-3939.
- [30] DING Zhi-bing, ZHAO Yu-hong, LU Ruo-peng, YUAN Mei-ni, WANG Zhi-jun, LI Hui-jun, HOU Hua. Effect of Zn addition on microstructure and mechanical properties of cast Mg-Gd-Y-Zr alloys [J]. Transactions of Nonferrous Metals Society of China, 2019, 29(4): 722-734.
- [31] DAI Shuai, WANG Feng, WANG Zhi, LIU Zheng, MAO Ping-li. Effect of Cu on microstructure, mechanical properties, and texture evolution of ZK60 alloy fabricated by hot extrusion-shearing process [J]. Transactions of Nonferrous Metals Society of China, 2020, 30(6): 1511-1523.
- [32] CHEN Xiao-yang, ZHANG Yang, CONG Meng-qi, LU Ya-lin, LI Xiao-ping. Effect of Sn content on microstructure and tensile properties of as-cast and as-extruded Mg-8Li-3Al-(1,2,3)Sn alloys [J]. Transactions of Nonferrous Metals Society of China, 2020, 30(8): 2079–2089.

- [33] CHANG Li-li, SHI Chun-chang, CUI Hong-wei. Enhancement of mechanical properties of duplex Mg-9Li-3Al alloy by Sn and Y addition [J]. Transactions of Nonferrous Metals Society of China, 2018, 28(1): 30–35.
- [34] BAGHANI A, KHALILPOUR H, MIRESMAEILI S M. Microstructural evolution and creep properties of Mg-4Sn alloys by addition of calcium up to 4 wt.% [J]. Transactions of Nonferrous Metals Society of China, 2020, 30(4): 896-904.
- [35] AMIRNEJAD M, RAJABI M, MOTAVALLI A. Effect of addition of Si on microstructure, mechanical properties, bio-corrosion and cytotoxicity of Mg-6Al-1Zn alloy [J]. Transactions of Nonferrous Metals Society of China, 2018, 28(9): 1755-1762.
- [36] WANG Chun-ming, ZENG Lu-ming, ZHANG Wen-long, TANG Fu-qian, DING Wu-cheng, XIAO Su-fen, LIANG Tong-xiang. Enhanced mechanical properties and corrosion resistance of rolled Mg-1.5Sn-0.5Ca alloy by Ce microalloying [J]. Materials Characterization, 2021, 179: 111325.
- [37] CHAI Yan-fu, SHAN Lei, JIANG Bin, YANG Hua-bao, HE Chao, HAO Wen-xing, HE Jun-jie, YANG Qing-shan, YUAN Ming, PAN Fu-sheng. Ameliorating mechanical properties and reducing anisotropy of as-extruded Mg-1.0Sn-0.5Ca alloy via Al addition [J]. Progress in Natural Science: Materials International, 2021, 31: 722-730.
- [38] XU Tian-cai, YANG Yan, PENG Xiao-dong, SONG Jiang-feng, PAN Fu-sheng. Overview of advancement and development trend on magnesium alloy [J]. Journal of Magnesium and Alloys, 2019, 7(3): 536-544.
- [39] LIU Yong, REN Hui, HU Wen-cheng, LI De-jiang, ZENG Xiao-qin, WANG Ke-gang, LU Jian. First-principles calculations of strengthening compounds in magnesium alloy: A general review [J]. Journal of Materials Science Technology, 2016, 32(12): 1222–1231.
- [40] YANG Kai-cheng, WANG Jiang, YAO Qing-rong, LU Zhao, RONG Mao-hua, ZHOU Huai-ying, RAO Guang-hui. Phase diagrams of permanent magnet alloys: Binary rare earth alloy systems [J]. Journal of Rare Earths, 2019, 37(10): 1040–1046.
- [41] CAI Y, SUN C Y, LI Y L, HU S Y, ZHU N Y, BARKER E I, QIAN L Y. Phase field modeling of discontinuous dynamic recrystallization in hot deformation of magnesium alloys [J]. International Journal of Plasticity, 2020, 133: 102773.
- [42] AHMAD R, WU Zhao-xuan, CURTIN W A. Analysis of double cross-slip of pyramidal I \( \langle c + a \rangle \) screw dislocations and implications for ductility in Mg alloys [J]. Acta Materialia, 2020, 183: 228–241.
- [43] LUO Qun, ZHAI Cong, SUN Dong-ke, CHEN Wei, LI Qian. Interpolation and extrapolation with the CALPHAD method [J]. Journal of Materials Science & Technology, 2019, 35(9): 2115–2120.
- [44] LUO Qun, GUO Yan-lin, LIU Bin, FENG Yu-jun, ZHANG Jie-yu, LI Qian, CHOU Kuo-chih. Thermodynamics and kinetics of phase transformation in rare earth-magnesium alloys: A critical review [J]. Journal of Materials Science & Technology, 2020, 44: 171–190.
- [45] LIU Cheng, LUO Qun, GU Qin-fen, LI Qian, CHOU Kuo-chih. Thermodynamic assessment of Mg-Ni-Y system

- focusing on long-period stacking ordered phases in the Mg-rich corner [J]. Journal of Magnesium and Alloys, 2021.
- [46] WANG Jin, MA Tang-peng, CHENG Kai-ming, ZHAN Cheng-wei, ZHOU Ji-xue, QIN Jing-yu, ZHAO Jing-rui, ZHANG Su-qing, ZHAO Guo-chen, WANG Xi-tao. The effect of additional element dissolving on the solid solubility of Zn in Mg alloy: A first-principles prediction strategy [J]. Journal of Alloys and Compounds, 2021, 877: 160312.
- [47] XIE Tian, ZHAO Peng-yu, CHEN Yu-yang, ZHANG Man-yu, WANG Yao-wei, YING Tao, ZHU Hong, ZENG Xiao-qin. Investigation on the corrosion behavior of single-phase and binary-phase Mg-Sc alloys: An experimental and first-principles study [J]. Materials Characterization, 2021, 179: 111294.
- [48] ZUO En-ci, DOU Xi-long, CHEN Ying-ying, ZHU Wen-jie, JIANG Gang, MAO Ai-jie, DU Ji-guang. Electronic work function, surface energy and electronic properties of binary Mg-Y and Mg-Al alloys: A DFT study [J]. Surface Science, 2021, 712: 121880.
- [49] ZHOU Dian-wu, LIU Jin-shui, XU Shao-hua, PENG Ping. Thermal stability and elastic properties of Mg<sub>2</sub>X (X=Si, Ge, Sn, Pb) phases from first-principle calculations [J]. Computational Materials Science, 2012, 51(1): 409–414.
- [50] HAN Wen-duo, LI Yao-hui, LI Xun-du, DAI Jia, LI Ke. Doping and adsorption mechanism of modifying the eutectic Mg<sub>2</sub>Si phase in magnesium alloys with rare earth elements: A first-principles study [J]. Applied Surface Science, 2020, 503: 144331.
- [51] XIA Xiang-sheng, ZHANG Kui, MA Ming-long, LI Ting. Constitutive modeling of flow behavior and processing maps of Mg-8.1Gd-4.5Y-0.3Zr alloy [J]. Journal of Magnesium and Alloys, 2020, 8(3): 917–928.
- [52] WANG Zhao-long, LUO Qun, CHEN Shuang-lin, CHOU Kuo-chih, LI Qian. Experimental investigation and thermodynamic calculation of the Mg-Ni-Y system (Y<50 at.%) at 400 and 500 °C [J]. Journal of Alloys and Compounds, 2015, 649: 1306–1314.
- [53] XIE Tian-ci, SHI Hui, WANG Hong-bin, LUO Qun, LI Qian, CHOU Kuo-chih. Thermodynamic prediction of thermal diffusivity and thermal conductivity in Mg-Zn-La/Ce system [J]. Journal of Materials Science & Technology, 2022, 97: 147-155.
- [54] SCHRÖDINGER E. An undulatory theory of the mechanics of atoms and molecules [J]. Physical Review, 1926, 28(6): 1049–1070.
- [55] BORN M, HUANG K. Dynamical theory of crystal lattices [M]. Oxford University, 1954.
- [56] HOHENBERG P, KOHN W. Inhomogeneous electron gas [J]. Physical Review B, 1964, 136(3): B864–B871.
- [57] KOHN W, SHAM L J. Self-consistent equations including exchange and correlation effects [J]. Physical Review A, 1965, 140(4): A1133-A1138.
- [58] SHI Zhang-zhi, CHEN Hong-ting, ZHANG Ke, DAI Fu-zhi, LIU Xue-feng. Crystallography of precipitates in Mg alloys [J]. Journal of Magnesium and Alloys, 2021, 9(2): 416–431.
- [59] RAMESHKUMAR S, JAIGANESH G, JAYALAKSHMI V. Structural, phonon, elastic, thermodynamic and electronic properties of Mg-X (X=La, Nd, Sm) intermetallics: The first principles study [J]. Journal of Magnesium and Alloys,

- 2019, 7(1): 166–185.
- [60] YANG Fang, WANG Ji-wei, KE Jiang-ling, PAN Zheng-gui, TANG Bi-yu. Elastic properties and electronic structures of Mg-Ce intermetallic compounds from first-principles calculations [J]. Physica Status Solidi (B): Basic Research, 2011, 248(9): 2097–2102.
- [61] CHEN Ying-ying, DOU Xi-long, ZHU Wen-jie, JIANG Gang, MAO Ai-jie. Structural, mechanical and thermodynamic properties study on Mg-Y alloys from first-principles calculations [J]. International Journal of Modern Physics B, 2020, 34(25): 2050220.
- [62] LIU Sha, ESTEBAN-MANZANARES G, LLORCA J. First-principles analysis of precipitation in Mg–Zn alloys [J]. Physical Review Materials, 2020, 4(9): 093609.
- [63] ZHU Wen-jie, CHEN Ying-ying, MAO Ai-jie, DU Ji-guang, JIANG Gang. First principles study of the elastic and thermodynamic properties of Mg-Al alloys [J]. Computational Materials Science, 2020, 177: 109587.
- [64] CHEN H L, LIN L, MAO P L, LIU Z. Phase stability, electronic, elastic and thermodynamic properties of Al–RE intermetallics in Mg–Al–RE alloy: A first principles study [J]. Journal of Magnesium and Alloys, 2015, 3(3): 197–202.
- [65] XU Kai, LIU Shu-hong, CHANG Ke-ke, LIANG Yong-peng, DU Yong, JIN Zhan-peng. A general thermodynamic model for the long-period stacking ordered phases in magnesium alloys [J]. Journal of Magnesium and Alloys, 2021, 9(1): 144–155.
- [66] GUO Yan-lin, LUO Qun, LIU Bin, LI Qian. Elastic properties of long-period stacking ordered phases in Mg-Zn-Y and Mg-Ni-Y alloys: A first-principles study [J]. Scripta Materialia, 2020, 178: 422-427.
- [67] GUO Yu-hao, WANG Wei-cheng, HUANG Han-qing, ZHAO Han-Han, JING Yu-hai, YI Guang-bin, LUO Lan, LIU Yong. Effect of doping Zn atom on the structural stability, mechanical and thermodynamic properties of AlLi phase in Mg-Li alloys from first-principles calculations [J]. Philosophical Magazine, 2020, 100(14): 1849–1867.
- [68] VITOS L. Computational quantum mechanics for materials engineers: The EMTO method and applications [M]. Springer London, 2007: 235–235.
- [69] LIU Xi-qin, LIU Zi-li, LIU Guo-dong, WANG Wen-jing, LI Jian. First-principles study of solid solution strengthening in Mg-X (X=Al, Er) alloys [J]. Bulletin of Materials Science, 2019, 42(1): 1–7.
- [70] HUANG Z W, ZHAO Y H, HOU H, HAN P D. Electronic structural, elastic properties and thermodynamics of Mg<sub>17</sub>Al<sub>12</sub>, Mg<sub>2</sub>Si and Al<sub>2</sub>Y phases from first-principles calculations [J]. Physica B: Condensed Matter, 2012, 407(7): 1075–1081.
- [71] YANG Li, YUAN Yuan, CHEN Tao, DAI Xu, ZHANG Ling, LI Da-jian, TANG Ai-tao, YI Wang, ZHANG Li-jun, PAN Fu-sheng. Diffusion behaviour and mechanical properties of binary Mg-Gd system [J]. Intermetallics, 2021, 133: 107171.
- [72] XU Wei-wei, WU Xiao-zhi, WANG Rui, LI Wei-guo, LIU Qing. Elastic properties of magnesium with virtual long-period stacking-ordered structure: First-principles study [J]. Computational Materials Science, 2015, 110: 191–197.
- [73] WANG Rui, WANG Shao-feng, YAO Yin, LIU Li-li, WU Xiao-zhi. The temperature-dependent elastic properties of

- B2-MgRE intermetallic compounds from first principles [J]. Physica B: Condensed Matter, 2012, 407(1): 96–102.
- [74] TAO Xiao-ma, OUYANG Yi-fang, LIU Hua-shan, FENG Yuan-ping, DU Yong, JIN Zhan-peng. Elastic constants of B2-MgRE (RE=Sc, Y, La-Lu) calculated with first-principles [J]. Solid State Communications, 2008, 148(7/8): 314–318.
- [75] CHEN Qiang, HUANG Zhi-wei, ZHAO Zu-de, SHU Da-yu. First principles study on elastic properties, thermodynamics and electronic structural of AB2 type phases in magnesium alloy [J]. Solid State Communications, 2013, 162: 1–7.
- [76] GANESHAN S, SHANG S L, ZHANG H, WANG Y, MANTINA M, LIU Z K. Elastic constants of binary Mg compounds from first-principles calculations [J]. Intermetallics, 2009, 17(5): 313–318.
- [77] MAO Ping-li, YU Bo, LIU Zheng, WANG Feng, JU Yang. First-principles calculations of structural, elastic and electronic properties of AB2 type intermetallics in Mg–Zn–Ca–Cu alloy [J]. Journal of Magnesium and Alloys, 2013, 1(3): 256–262.
- [78] FAN Tou-wen, KE Jiang-ling, FU Ling, TANG Bi-yu, PENG Li-ming, DING Wen-jiang. Ideal strength of Mg<sub>2</sub>X (X=Si, Ge, Sn and Pb) from first-principles [J]. Journal of Magnesium and Alloys, 2013, 1(2): 163–168.
- [79] GAO Yan, WU Chuang, FENG Wen-jiang, HE Yan, HE Hai-sheng, YANG Jing-yu, CHEN Xiu-yan. Effects of the rare earth Y on the structural and tensile properties of Mg-based alloy: A first-principles study [J]. Crystals, 2021, 11(8): 1003.
- [80] YANG Fang, FAN Tou-wen, WU Jian, TANG Bi-yu, PENG Li-ming, DING Wen-jiang. Effects of Y and Zn atoms on the elastic properties of Mg solid solution from first-principles calculations [J]. Physica Status Solidi (b), 2011, 248(12): 2809–2815.
- [81] YANG Xiao-min, ZHAO Yu-hong, HOU Hua, ZHENG Shu-hua, HAN Pei-de. First-principles calculations of electronic, elastic and thermal properties of magnesium doped with alloying elements [J]. Journal Wuhan University of Technology: Materials Science Edition, 2018, 33(1): 198–203.
- [82] GANESHAN S, SHANG S L, WANG Y, LIU Z K. Effect of alloying elements on the elastic properties of Mg from first-principles calculations [J]. Acta Materialia, 2009, 57(13): 3876–3884.
- [83] FANG Chao, ZHANG Jing, HUANG Ying, LIU Xue-jian, DONG Xiao-yu. Orientation dependence of elastic properties of Mg binary alloys: A first-principles study [J]. Computational Condensed Matter, 2020, 22: e00447.
- [84] YASI J A, NOGARET T, TRINKLE D R, QI Y, HECTOR L G, CURTIN W A. Basal and prism dislocation cores in magnesium: Comparison of first-principles and embeddedatom-potential methods predictions [J]. Modelling and Simulation in Materials Science and Engineering, 2009, 17(5): 055012.
- [85] VITEK V. Intrinsic stacking faults in body-centred cubic crystals [J]. Philosophical Magazine, 1968, 18: 773–786.
- [86] SHANG S L, WANG W Y, ZHOU B C, WANG Y, DARLING K A, KECSKES L J, MATHAUDHU S N, LIU Z K. Generalized stacking fault energy, ideal strength and

- twinnability of dilute Mg-based alloys: A first-principles study of shear deformation [J]. Acta Materialia, 2014, 67: 168–180.
- [87] WANG W Y, SHANG Shun-li, WANG Yi, MEI Zhi-gang, DARLING K A, KECSKES L J, MATHAUDHU S N, HUI Xi-dong, LIU Zi-kui. Effects of alloying elements on stacking fault energies and electronic structures of binary Mg alloys: A first-principles study [J]. Materials Research Letters, 2014, 2(1): 29–36.
- [88] WEN L, CHEN P, TONG Z F, TANG B Y, PENG L M, DING W J. A systematic investigation of stacking faults in magnesium via first-principles calculation [J]. European Physical Journal B, 2009, 72(3): 397–403.
- [89] HAN J, SU X M, JIN Z H, ZHU Y T. Basal-plane stacking-fault energies of Mg: A first-principles study of Liand Al-alloying effects [J]. Scripta Materialia, 2011, 64(8): 693–696.
- [90] TSURU T, UDAGAWA Y, YAMAGUCHI M, ITAKURA M, KABURAKI H, KAJI Y. Solution softening in magnesium alloys: The effect of solid solutions on the dislocation core structure and nonbasal slip [J]. Journal of Physics: Condensed Matter, 2013, 25(2): 022202.
- [91] PEI Zong-rui, ZHU Li-fang, FRIÁK M, SANDLÖBES S, von PEZOLD J, SHENG H W, RACE C P, ZAEFFERER S, SVENDSEN B, RAABE D, NEUGEBAUER J. Ab initio and atomistic study of generalized stacking fault energies in Mg and Mg-Y alloys [J]. New Journal of Physics, 2013, 15(4): 043020.
- [92] SANDLÖBES S, FRIÁK M, ZAEFFERER S, DICK A, YI Sang-bong, LETZIG D, PEI Zong-rui, ZHU Li-fang, NEUGEBAUER J, RAABE D. The relation between ductility and stacking fault energies in Mg and Mg—Y alloys [J]. Acta Materialia, 2012, 60(6/7): 3011–3021.
- [93] SANDLÖBES S, PEI Zong-rui, FRIÁK M, ZHU Li-fang, WANG F, ZAEFFERER S, RAABE D, NEUGEBAUER J. Ductility improvement of Mg alloys by solid solution: Ab initio modeling, synthesis and mechanical properties [J]. Acta Materialia, 2014, 70: 92–104.
- [94] MUZYK M, PAKIELA Z, KURZYDLOWSKI K J. Generalized stacking fault energy in magnesium alloys: Density functional theory calculations [J]. Scripta Materialia, 2012, 66(5): 219–222.
- [95] WANG Cheng, ZHANG Hua-yuan, WANG Hui-yuan, LIU Guo-jun, JIANG Qi-chuan. Effects of doping atoms on the generalized stacking-fault energies of Mg alloys from first-principles calculations [J]. Scripta Materialia, 2013, 69(6): 445–448.
- [96] ZHANG Jing, DOU Yu-chen, LIU Guo-bao, GUO Zheng-xiao. First-principles study of stacking fault energies in Mg-based binary alloys [J]. Computational Materials Science, 2013, 79: 564-569.
- [97] DONG Qing, LUO Zhe, ZHU Hong, WANG Le-yun, YING Tao, JIN Zhao-hui, LI De-jiang, DING Wen-jiang, ZENG Xiao-qin. Basal-plane stacking-fault energies of Mg alloys: A first-principles study of metallic alloying effects [J]. Journal of Materials Science & Technology, 2018, 34(10): 1773–1780.
- [98] NIE J F, SHIN K S, ZENG Z R. Microstructure, deformation, and property of wrought magnesium alloys [J]. Metallurgical

- and Materials Transactions A, 2020, 51: 6045-6109.
- [99] YASI J A, HECTOR L G, TRINKLE D R. Prediction of thermal cross-slip stress in magnesium alloys from direct first-principles data [J]. Acta Materialia, 2011, 59(14): 5652-5660.
- [100] ZENG Y, SHI O L, JIANG B, QUAN G F, PAN F S. Improved formability with theoretical critical shear strength transforming in Mg alloys with Sn addition [J]. Journal of Alloys and Compounds, 2018, 764: 555–564.
- [101] WU Zhao-xuan, CURTIN W A. The origins of high hardening and low ductility in magnesium [J]. Nature, 2015, 526(7571): 62–67.
- [102] WU Zhao-xuan, YIN Bing-lun, CURTIN W A. Energetics of dislocation transformations in hcp metals [J]. Acta Materialia, 2016, 119: 203–217.
- [103] WU Zhao-xuan, AHMAD R, YIN Bing-lun, SANDLÖBES S, CURTIN W A. Mechanistic origin and prediction of enhanced ductility in magnesium alloys [J]. Science, 2018, 359(6374): 447–452.
- [104] YIN Bing-lun, WU Zhao-xuan, CURTIN W A. First-principles calculations of stacking fault energies in Mg–Y, Mg–Al and Mg–Zn alloys and implications for  $\langle c+a \rangle$  activity [J]. Acta Materialia, 2017, 136: 249–261.
- [105] DING Zhi-gang, LIU Wei, SUN Hao, LI Shuang, ZHANG Da-long, ZHAO Yong-hao, LAVERNIA E J, ZHU Yun-tian. Origins and dissociation of pyramidal ⟨c+a⟩ dislocations in magnesium and its alloys [J]. Acta Materialia, 2018, 146: 265–272.
- [106] JANG H S, SEOL D, LEE B J. Modified embedded-atom method interatomic potentials for Mg-Al-Ca and Mg-Al-Zn ternary systems [J]. Journal of Magnesium and Alloys, 2021, 9(1): 317–335.
- [107] WU Y, HU W. Molecular dynamics simulations of thermodynamics, elastic constants and solid solution strengths for Mg-Gd alloys [J]. The European Physical Journal B, 2007, 57(3): 305–312.
- [108] GROH S, MARIN E B, HORSTEMEYER M F, BAMMANN D J. Dislocation motion in magnesium: A study by molecular statics and molecular dynamics [J]. Modelling and Simulation in Materials Science and Engineering, 2009, 17(7): 075009.
- [109] KIM D H, MANUEL M V, EBRAHIMI F, TULENKO J S, PHILLPOT S R. Deformation processes in [11\overline{120}]-textured nanocrystalline Mg by molecular dynamics simulation [J]. Acta Materialia, 2010, 58(19): 6217–6229.
- [110] SOMEKAWA H, MUKAI T. Molecular dynamics simulation of grain boundary plasticity in magnesium and solid-solution magnesium alloys [J]. Computational Materials Science, 2013, 77: 424–429.
- [111] HUANG Xiu-song, DONG Xi-xi, YANG Chun-ming, TIAN Feng, LIU Le-hua, CHEN Gao-qiang, LI Pei-jie. Investigation of atom distribution in Mg-9wt.%Al melt using small-angle X-ray scattering and molecular dynamics simulation [J]. Journal of Non-Crystalline Solids, 2017, 473: 47-53.
- [112] YANG Zhi-biao, LU Song, TIAN Yan-zhong, GU Zi-jian, MAO Hua-hai, SUN Jian, VITOS L. Assessing the magnetic order dependent γ-surface of Cr–Co–Ni alloys [J]. Journal of Materials Science & Technology, 2021, 80: 66–74.

- [113] YANG Qian-hua, XUE Chun, CHU Zhi-bing, LI Yu-gui, MA Li-feng. Molecular dynamics simulation of the effect of solute atoms on the compression of magnesium alloy [J]. Applied Physics A, 2021, 127(6): 1–10.
- [114] DING R, GUO Z X. Coupled quantitative simulation of microstructural evolution and plastic flow during dynamic recrystallization [J]. Acta Materialia, 2001, 49(16): 3163-3175.
- [115] SHU Da-yu, WANG Jing, JIANG Meng-hao, CHEN Gang, LU Li-wei, ZHANG Hong-ming. Modeling of dynamic recrystallization behavior of as-extruded AM50 magnesium alloy during hot compression by a cellular automaton method [J]. Metals, 2021, 11(1): 75.
- [116] HATAMI SADR M, JAFARZADEH H. Characterization of AZ91 magnesium alloy processed by cyclic contraction/expansion extrusion using the experimental and micromechanical cellular automaton finite element approach [J]. Proceedings of the Institution of Mechanical Engineers, Part L: Journal of Materials: Design and Applications, 2020, 234(11): 1417–1430.
- [117] WU He, XU Wen-chen, WANG Si-bing, YANG Zhong-ze, CHEN Yu, TENG Bu-gang, SHAN De-bin, GUO Bin. A cellular automaton coupled FEA model for hot deformation behavior of AZ61 magnesium alloys [J]. Journal of Alloys and Compounds, 2020, 816: 152562.
- [118] HE Yu-ying, BAI Sheng-wen, FANG Gang. Coupled CA-FE simulation for dynamic recrystallization of magnesium alloy during hot extrusion [J]. Journal of Magnesium and Alloys, 2022, 10(3): 769–785.
- [119] ASARO R J. Crystal plasticity [J]. Journal of Applied Mechanics, 1983, 50(4b): 921–934.
- [120] UCHIC M D, DIMIDUK D M, FLORANDO J N, NIX W D. Sample dimensions influence strength and crystal plasticity [J]. Science, 2004, 305(5686): 986–989.
- [121] ZHOU Guo-wei, JAIN M K, WU Pei-dong, SHAO Yi-chuan, LI Da-yong, PENG Ying-hong. Experiment and crystal plasticity analysis on plastic deformation of AZ31B Mg alloy sheet under intermediate temperatures: How deformation mechanisms evolve [J]. International Journal of Plasticity, 2016, 79: 19–47.
- [122] GITHENS A, GANESAN S, CHEN Z, ALLISON J, SUNDARARAGHAVAN V, DALY S. Characterizing microscale deformation mechanisms and macroscopic tensile properties of a high strength magnesium rare-earth alloy: A combined experimental and crystal plasticity approach [J]. Acta Materialia, 2020, 186: 77–94.
- [123] YAGHOOBI M, VOYIADJIS G Z, SUNDARARAGHAVAN V. Crystal plasticity simulation of magnesium and its alloys: A review of recent advances [J]. Crystals, 2021, 11(4): 435.
- [124] ABDOLVAND H, MAJKUT M, ODDERSHEDE J, SCHMIDT S, LIENERT U, DIAK B J, WITHERS P J, DAYMOND M R. On the deformation twinning of Mg AZ31B: A three-dimensional synchrotron X-ray diffraction experiment and crystal plasticity finite element model [J]. International journal of plasticity, 2015, 70: 77–97.
- [125] PARAMATMUNI C, KANJARLA A K. A crystal plasticity FFT based study of deformation twinning, anisotropy and micromechanics in HCP materials: Application to AZ31

- alloy [J]. International Journal of Plasticity, 2019, 113: 269–290.
- [126] MAYAMA T, NODA M, CHIBA R, KURODA M. Crystal plasticity analysis of texture development in magnesium alloy during extrusion [J]. International Journal of Plasticity, 2011, 27(12): 1916–1935.
- [127] FEATHER W G, GHORBANPOUR S, SAVAGE D J, ARDELJAN M, JAHEDI M, MCWILLIAMS B A, GUPTA N, XIANG Chong-chen, VOGEL S C, KNEZEVIC M. Mechanical response, twinning, and texture evolution of WE43 magnesium-rare earth alloy as a function of strain rate: experiments and multi-level crystal plasticity modeling [J]. International Journal of Plasticity, 2019, 120: 180–204.
- [128] LI Zi-han, ZHOU Guo-wei, LI Da-yong, WANG Hua-miao, TANG Wei-qin, PENG Ying-hong, ZUROB H S, WU Pei-dong. Crystal plasticity based modeling of grain boundary sliding in magnesium alloy AZ31B sheet [J]. Transactions of Nonferrous Metals Society of China, 2021, 31(1): 138–155.
- [129] SON H W, HYUN S K. Periodic formations of deformation twins and dislocation arrays via grain boundary sliding at serrated grain boundary in cold-shear- strained AZ31 alloy [J]. International Journal of Plasticity, 2020, 135: 102815.
- [130] ARDELJAN M, KNEZEVIC M. Explicit modeling of double twinning in AZ31 using crystal plasticity finite elements for predicting the mechanical fields for twin variant selection and fracture analyses [J]. Acta Materialia, 2018, 157: 339–354.
- [131] HABIB S A, LLOYD J T, MEREDITH C S, KHAN A S, SCHOENFELD S E. Fracture of an anisotropic rare-earth-containing magnesium alloy (ZEK100) at different stress states and strain rates: Experiments and modeling [J]. International Journal of Plasticity, 2019, 122: 285–318.
- [132] KUMAR M A, BEYERLEIN I J, LEBENSOHN R A, TOMÉ C N. Role of alloying elements on twin growth and twin transmission in magnesium alloys [J]. Materials Science and Engineering A, 2017, 706: 295–303.
- [133] HERRERA-SOLAZ V, HIDALGO-MANRIQUE P, PÉREZ-PRADO M T, LETZIG D, LLORCA J, SEGURADO J. Effect of rare earth additions on the critical resolved shear stresses of magnesium alloys [J]. Materials Letters, 2014, 128: 199–203.
- [134] RAEISINIA B, AGNEW S R. Using polycrystal plasticity modeling to determine the effects of grain size and solid solution additions on individual deformation mechanisms in cast Mg alloys [J]. Scripta Materialia, 2010, 63(7): 731–736.
- [135] LI Yong-kang, ZHA Min, JIA Hai-long, WANG Si-qing, ZHANG Hong-min, MA Xiao, TIAN Teng, MA Pin-kui, WANG Hui-yuan. Tailoring bimodal grain structure of Mg-9Al-1Zn alloy for strength-ductility synergy: Co-regulating effect from coarse Al<sub>2</sub>Y and submicron Mg<sub>17</sub>Al<sub>12</sub> particles [J]. Journal of Magnesium and Alloys, 2021, 9: 1556–1566.
- [136] ZHANG Yun, JIANG Hai-tao, KANG Qiang, WANG Yu-jiao, YANG Yong-gang, TIAN Shi-wei. Microstructure evolution and mechanical property of Mg-3Al alloys with addition of Ca and Gd during rolling and annealing process [J]. Journal of Magnesium and Alloys, 2020, 8(3): 769-779.

- [137] HWANG J H, ZARGARAN A, PARK G, LEE O, LEE B J, KIM N J. Effect of 1Al addition on deformation behavior of Mg [J]. Journal of Magnesium and Alloys, 2021, 9(2): 489–498.
- [138] KIM K H, HWANG J H, JANG H S, JEON J B, KIM N J, LEE B J. Dislocation binding as an origin for the improvement of room temperature ductility in Mg alloys [J]. Materials Science and Engineering A, 2018, 715: 266–275.
- [139] CHAUDRY U M, HAMAD K, KO Y G. Effect of calcium on the superplastic behavior of AZ31 magnesium alloy [J]. Materials Science and Engineering A, 2021, 815: 140874.
- [140] BAEK S M, LEE S Y, KIM J C, KWON J, JUNG H, LEE S, LEE K S, PARK S S. Role of trace additions of Mn and Y in improving the corrosion resistance of Mg-3Al-1Zn alloy [J]. Corrosion Science, 2021, 178: 108998.
- [141] CHELLIAH N M, PADAIKATHAN P, KUMAR R. Evaluation of electrochemical impedance and biocorrosion characteristics of as-cast and T4 heat treated AZ91 Mg-alloys in Ringer's solution [J]. Journal of Magnesium and Alloys, 2019, 7(1): 134–143.
- [142] LI Cheng-bo, YANG Shu-qing, DU Jun, LIAO Heng-bin, LUO Gan. Synergistic refining mechanism of Mg-3%Al alloy refining by carbon inoculation combining with Ca addition [J]. Journal of Magnesium and Alloys, 2020, 8(4): 1090-1101.
- [143] MA Chao-sheng, YU Wen-bo, PI Xu-feng, GUITTON A. Study of Mg-Al-Ca magnesium alloy ameliorated with designed Al<sub>8</sub>Mn<sub>4</sub>Gd phase [J]. Journal of Magnesium and Alloys, 2020, 8(4): 1084–1089.
- [144] QIU D, ZHANG M X, TAYLOR J A, FU H M, KELLY P M. A novel approach to the mechanism for the grain refining effect of melt superheating of Mg-Al alloys [J]. Acta Materialia, 2007, 55(6): 1863–1871.
- [145] SANI S A, EBRAHIMI G R, KIANI RASHID A R. Hot deformation behavior and dynamic recrystallization kinetics of AZ61 and AZ61 + Sr magnesium alloys [J]. Journal of Magnesium and Alloys, 2016, 4(2): 104–114.
- [146] XU Chen, WANG Jian-feng, CHEN Chen, WANG Chao, SUN Yu-feng, ZHU Shi-jie, GUAN Shao-kang. Initial micro-galvanic corrosion behavior between Mg<sub>2</sub>Ca and α-Mg via quasi-in situ SEM approach and first-principles calculation [J]. Journal of Magnesium and Alloys, doi: 10.1016/j.jma.2021.06.017.
- [147] BIAN M Z, SASAKI T T, NAKATA T, YOSHIDA Y, KAWABE N, KAMADO S, HONO K. Bake-hardenable Mg-Al-Zn-Mn-Ca sheet alloy processed by twin-roll casting [J]. Acta Materialia, 2018, 158: 278–288.
- [148] PENG Peng, HE Xiong-jiang-chuan, SHE Jia, TANG Ai-tao, RASHAD M, ZHOU Shi-bo, ZHANG Gen, MI Xiao-xi, PAN Fu-sheng. Novel low-cost magnesium alloys with high yield strength and plasticity [J]. Materials Science and Engineering A, 2019, 766: 138332.
- [149] SOMEKAWA H, SINGH A, MUKAI T, INOUE T. Effect of alloying elements on room temperature tensile ductility in magnesium alloys [J]. Philosophical Magazine, 2016, 96(25): 2671–2685.
- [150] YU Zheng-wen, TANG Ai-tao, WANG Qin, GAO Zheng-yuan, HE Jie-jun, SHE Jia, SONG Kai, PAN Fu-sheng. High strength and superior ductility of an ultra-fine grained

- magnesium-manganese alloy [J]. Materials Science and Engineering A, 2015, 648: 202–207.
- [151] ZHANG Shao-you, WANG Cheng, NING Hong, WANG Tong, ZHANG Cheng-cheng, YANG Zhi-zheng, WANG Hui-yuan. Relieving segregation in twin-roll cast Mg-8Al-2Sn-1Zn alloys via controlled rolling [J]. Journal of Magnesium and Alloys, 2021, 9(1): 254–265.
- [152] ZHANG Zhen-ya, YU Hua-shun, CHEN Gang, YU Hui, XU Chang-zheng. Correlation between microstructure and tensile properties in powder metallurgy AZ91 alloys [J]. Materials Letters, 2011, 65(17/18): 2686–2689.
- [153] JUNG J G, PARK S H, YU H, KIM Y M, LEE Y K, YOU B S. Improved mechanical properties of Mg-7.6Al-0.4Zn alloy through aging prior to extrusion [J]. Scripta Materialia, 2014, 93: 8-11.
- [154] LI Yong-bing, CHEN Yun-bo, CUI Hua, XIONG Bai-qing, ZHANG Ji-shan. Microstructure and mechanical properties of spray-formed AZ91 magnesium alloy [J]. Materials Characterization, 2009, 60(3): 240–245.
- [155] ZHA Min, ZHANG Hong-min, WANG Cheng, WANG Hui-yuan, ZHANG En-bo, JIANG Qi-chuan. Prominent role of a high volume fraction of Mg<sub>17</sub>Al<sub>12</sub> particles on tensile behaviors of rolled Mg-Al-Zn alloys [J]. Journal of Alloys and Compounds, 2017, 728: 682–693.
- [156] XU Qiong, MA Ai-bin, LI Yu-hua, SUN Jia-peng, YUAN Yu-chun, JIANG Jing-hua, NI Chao-ying. Microstructure evolution of AZ91 alloy processed by a combination method of equal channel angular pressing and rolling [J]. Journal of Magnesium and Alloys, 2020, 8(1): 192–198.
- [157] ZHANG Hang, ZHA Min, TIAN Teng, JIA Hai-long, GAO Dan, YANG Zhi-zheng, WANG Cheng, WANG Hui-yuan. Prominent role of high-volume fraction Mg<sub>17</sub>Al<sub>12</sub> dynamic precipitations on multimodal microstructure formation and strength-ductility synergy of Mg–Al–Zn alloys processed by hard-plate rolling (HPR) [J]. Materials Science and Engineering A, 2021, 808: 140920.
- [158] TRANG T T T, ZHANG J H, KIM J H, ZARGARAN A, HWANG J H, SUH B C, KIM N J. Designing a magnesium alloy with high strength and high formability [J]. Nature Communications, 2018, 9: 2522.
- [159] LIAO Heng-bin, ZHAN Mei-yan, LI Cheng-bo, MA Zhi-qiang, DU Jun. Grain refinement of Mg-Al alloys inoculated by MgAl<sub>2</sub>O<sub>4</sub> powder [J]. Journal of Magnesium and Alloys, 2021, 9(4): 1211–1219.
- [160] HU Fa-ping, ZHAO Shu-jie, GU Guang-lin, MA Zhen-duo, WEI Guo-bing, YANG Yan, PENG Xiao-dong, XIE Wei-dong. Strong and ductile Mg-0.4Al alloy with minor Mn addition achieved by conventional extrusion [J]. Materials Science and Engineering A, 2020, 795: 139926.
- [161] DOBROŇ P, DROZDENKO D, FEKETE K, KNAPEK M, BOHLEN J, CHMELÍK F. The slip activity during the transition from elastic to plastic tensile deformation of the Mg-Al-Mn sheet [J]. Journal of Magnesium and Alloys, 2021, 9(3): 1057–1067.
- [162] JING Bai, SUN Yang-shan, FENG Xue, SHAN Xue, JING Qiang, ZHU Tian-bai. Effect of Al contents on microstructures, tensile and creep properties of Mg-Al-Sr-Ca alloy [J]. Journal of Alloys and Compounds, 2007, 437(1/2): 247–253.

- [163] HAN Li-hong, HU H, NORTHWOOD D O. Effect of Ca additions on microstructure and microhardness of an as-cast Mg-5.0wt.%Al alloy [J]. Materials Letters, 2008, 62(3): 381-384.
- [164] HOMMA T, NAKAWAKI S, KAMADO S. Improvement in creep property of a cast Mg-6Al-3Ca alloy by Mn addition [J]. Scripta Materialia, 2010, 63(12): 1173–1176.
- [165] LASER T, HARTIG C, NÜERNBERG M R, LETZIG D, BORMANN R. The influence of calcium and cerium mischmetal on the microstructural evolution of Mg-3Al-1Zn during extrusion and resulting mechanical properties [J]. Acta Materialia, 2008, 56(12): 2791-2798.
- [166] JIANG Zhong-tao, JIANG Bin, YANG Hong, YANG Qing-shan, DAI Jia-hong, PAN Fu-sheng. Influence of the Al<sub>2</sub>Ca phase on microstructure and mechanical properties of Mg-Al-Ca alloys [J]. Journal of Alloys and Compounds, 2015, 647: 357–363.
- [167] BHATTACHARYYA J J, SASAKI T T, NAKATA T, HONO K, KAMADO S, AGNEW S R. Determining the strength of GP zones in Mg alloy AXM10304, both parallel and perpendicular to the zone [J]. Acta Materialia, 2019, 171: 231–239.
- [168] NAKATA T, MEZAKI T, AJIMA R, XU C, OH-ISHI K, SHIMIZU K, HANAKI S, SASAKI T T, HONO K, KAMADO S. High-speed extrusion of heat-treatable Mg-Al-Ca-Mn dilute alloy [J]. Scripta Materialia, 2015, 101: 28-31.
- [169] NAKATA T, MEZAKI T, XU C, OH-ISHI K, SHIMIZU K, HANAKI S, KAMADO S. Improving tensile properties of dilute Mg-0.27Al-0.13Ca-0.21Mn (at.%) alloy by low temperature high speed extrusion [J]. Journal of Alloys and Compounds, 2015, 648: 428-437.
- [170] LIU Huan, SUN Chao, WANG Ce, LI Yu-hua, BAI Jing, XUE Feng, MA Ai-bin, JIANG Jing-hua. Improving toughness of a Mg<sub>2</sub>Ca-containing Mg-Al-Ca-Mn alloy via refinement and uniform dispersion of Mg<sub>2</sub>Ca particles [J]. Journal of Materials Science & Technology, 2020, 59: 61-71.
- [171] NAKATA T, XU C, AJIMA R, SHIMIZU K, HANAKI S, SASAKI T T, MA L, HONO K, KAMADO S. Strong and ductile age-hardening Mg–Al–Ca–Mn alloy that can be extruded as fast as aluminum alloys [J]. Acta Materialia, 2017, 130: 261–270.
- [172] LIU Chun-quan, CHEN Xian-hua, CHEN Jiao, ATRENS A, PAN Fu-sheng. The effects of Ca and Mn on the microstructure, texture and mechanical properties of Mg-4Zn alloy [J]. Journal of Magnesium and Alloys, 2021, 9(3): 1084-1097.
- [173] LIU Peng, JIANG Hai-tao, CAI Zheng-xu, KANG Qiang, ZHANG Yun. The effect of Y, Ce and Gd on texture, recrystallization and mechanical property of Mg–Zn alloys [J]. Journal of Magnesium and Alloys, 2016, 4(3): 188–196.
- [174] DU Yu-zhou, ZHENG Ming-yi, JIANG Bai-ling. Comparison of microstructure and mechanical properties of Mg-Zn microalloyed with Ca or Ce [J]. Vacuum, 2018, 151: 221-225.
- [175] JIANG Wei-yan, WANG Jing-feng, ZHAO Wei-kang, LIU Qing-shan, JIANG Dian-ming, GUO Sheng-feng. Effect of Sn addition on the mechanical properties and bio-corrosion

- behavior of cytocompatible Mg-4Zn based alloys [J]. Journal of Magnesium and Alloys, 2019, 7(1): 15-26.
- [176] DU Yu-zhou, ZHENG Ming-yi, QIAO Xiao-guang, PENG Wen-qiang, JIANG Bai-ling. Effect of La addition on the microstructure and mechanical properties of Mg-6wt% Zn alloys [J]. Materials Science and Engineering A, 2016, 673: 47-54.
- [177] JIANG M G, XU C, NAKATA T, YAN H, CHEN R S, KAMADO S. High-speed extrusion of dilute Mg-Zn-Ca-Mn alloys and its effect on microstructure, texture and mechanical properties [J]. Materials Science and Engineering: A, 2016, 678: 329-338.
- [178] CHEN Jing-ai, SUN Yan, ZHANG Jin-shan, CHENG Wei-li, NIU Xiao-feng, XU Chun-xiang. Effects of Ti addition on the microstructure and mechanical properties of Mg-Zn-Zr-Ca alloys [J]. Journal of Magnesium and Alloys, 2015, 3(2): 121–126.
- [179] HORKY J, BRYŁA K, KRYSTIAN M, MOZDZEN G, MINGLER B, SAJTI L. Improving mechanical properties of lean Mg-Zn-Ca alloy for absorbable implants via Double Equal Channel Angular Pressing (D-ECAP) [J]. Materials Science and Engineering A, 2021, 826: 142002.
- [180] AL-SAMMAN T, LI X. Sheet texture modification in magnesium-based alloys by selective rare earth alloying [J]. Materials Science and Engineering A, 2011, 528(10/11): 3809–3822.
- [181] XIA Nan, WANG Cheng, GAO Yi-peng, HUA Zhen-ming, MA Chen-yi, DU Chun-feng, ZHANG Hang, ZHANG Hong-min, LI Mei-xuan, ZHA Min, WANG Hui-yuan. Enhanced ductility of Mg-1Zn-0.2Zr alloy with dilute Ca addition achieved by activation of non-basal slip and twinning [J]. Materials Science and Engineering A, 2021, 813: 141128.
- [182] HU Ke, LI Chun-yu, XU Guo-jun, GUO Rui-zhen, LE Qi-chi, LIAO Qi-yu. Effect of extrusion temperature on the microstructure and mechanical properties of low Zn containing wrought Mg alloy micro-alloying with Mn and La-rich misch metal [J]. Materials Science and Engineering: A, 2019, 742: 692-703.
- [183] LE Qi-chi, ZHANG Zhi-qiang, SHAO Zhi-wen, CUI Jian-zhong, XIE Yi. Microstructures and mechanical properties of Mg-2%Zn-0.4%RE alloys [J]. Transactions of Nonferrous Metals Society of China, 2010, 20: s352-s356.
- [184] ZAREIAN Z, EMAMY M, MALEKAN M, MIRZADEH H, KIM W J, BAHMANI A. Tailoring the mechanical properties of Mg–Zn magnesium alloy by calcium addition and hot extrusion process [J]. Materials Science and Engineering A, 2020, 774: 138929.
- [185] BAZHENOV V E, LI A V, KOMISSAROV A A, KOLTYGIN A V, TAVOLZHANSKII S A, BAUTIN V A, VOROPAEVA O O, MUKHAMETSHINA A M, TOKAR A A. Microstructure and mechanical and corrosion properties of hot-extruded Mg–Zn–Ca–(Mn) biodegradable alloys [J]. Journal of Magnesium and Alloys, 2021, 9(4): 1428–1442.
- [186] MIAO Hong-wei, HUANG Hua, SHI Yong-juan, ZHANG Hua, PEI Jia, YUAN Guang-yin. Effects of solution treatment before extrusion on the microstructure, mechanical properties and corrosion of Mg–Zn–Gd alloy *in vitro* [J]. Corrosion Science, 2017, 122: 90–99.

- [187] XU Yu-zhao, LI Jing-yuan, QI Ming-fan, LIAO Lu-hai, GAO Zhi-jun. Enhanced mechanical properties of Mg-Zn-Y-Zr alloy by low-speed indirect extrusion [J]. Journal of Materials Research and Technology, 2020, 9(5): 9856–9867.
- [188] WANG Xin, DU Yu-zhou, LIU Dong-jie, JIANG Bai-ling. Significant improvement in mechanical properties of Mg-Zn-La alloy by minor Ca addition [J]. Materials Characterization, 2020, 160: 110130.
- [189] FENG Su-qin, ZHANG Wen-ying, ZHANG Yan-hui, GUAN Jin-yu, XU Yong-chun. Microstructure, mechanical properties and damping capacity of heat-treated Mg–Zn–Y–Nd–Zr alloy [J]. Materials Science and Engineering A, 2014, 609: 283–292.
- [190] TONG L B, ZHANG Qing-xin, JIANG Z H, ZHANG J B, MENG Jian, CHENG L R, ZHANG Hong-jie. Microstructures, mechanical properties and corrosion resistances of extruded Mg–Zn–Ca–xCe/La alloys [J]. Journal of the Mechanical Behavior of Biomedical Materials, 2016, 62: 57–70.
- [191] SHI Hui, LI Qian, ZHANG Jie-yu, LUO Qun, CHOU K C. Re-assessment of the Mg-Zn-Ce system focusing on the phase equilibria in Mg-rich corner [J]. Calphad, 2020, 68: 101742.
- [192] DAS S K, KANG Y B, HA T K, JUNG I H. Thermodynamic modeling and diffusion kinetic experiments of binary Mg-Gd and Mg-Y systems [J]. Acta Materialia, 2014, 71: 164-175.
- [193] GAO L, CHEN R S, HAN E H. Effects of rare-earth elements Gd and Y on the solid solution strengthening of Mg alloys [J]. Journal of Alloys and Compounds, 2009, 481(1/2): 379–384
- [194] STANFORD N, ATWELL D, BARNETT M R. The effect of Gd on the recrystallisation, texture and deformation behaviour of magnesium-based alloys [J]. Acta Materialia, 2010, 58(20): 6773–6783.
- [195] STANFORD N, BARNETT M R. The origin of "rare earth" texture development in extruded Mg-based alloys and its effect on tensile ductility [J]. Materials Science and Engineering A, 2008, 496(1/2): 399–408.
- [196] WU W X, LI J, DONG J, DING W J. Deformation behavior and texture evolution in an extruded Mg-1Gd alloy during uniaxial compression [J]. Materials Science and Engineering A, 2014, 593: 48-54.
- [197] HU Yao-bo, DENG Juan, ZHAO Chong, PAN Fu-sheng, PENG Jian. Microstructure and mechanical properties of Mg-Gd-Zr alloys with low gadolinium contents [J]. Journal of Materials Science, 2011, 46(17): 5838-5846.
- [198] WU D, CHEN R S, HAN E H. Excellent room-temperature ductility and formability of rolled Mg-Gd-Zn alloy sheets [J]. Journal of Alloys and Compounds, 2011, 509(6): 2856-2863.
- [199] ZHAO Tian-shuo, HU Yao-bo, HE Bing, ZHANG Chao, ZHENG Tian-xu, PAN Fu-sheng. Effect of manganese on microstructure and properties of Mg-2Gd magnesium alloy [J]. Materials Science and Engineering A, 2019, 765: 138292.
- [200] HU Yao-bo, ZHANG Chao, ZHENG Tian-xu, PAN Fu-sheng, TANG Ai-tao. Strengthening effects of Zn addition on an

- ultrahigh ductility Mg-Gd-Zr magnesium alloy [J]. Materials, 2018, 11(10): 1942.
- [201] ZHAO Jun, JIANG Bin, YUAN Yuan, TANG Ai-tao, WANG Qing-hang, YANG Tian-hao, HUANG Guang-sheng, ZHANG Ding-fei, PAN Fu-sheng. Influence of Ca and Zn synergistic alloying on the microstructure, tensile properties and strain hardening of Mg-1Gd alloy [J]. Materials Science and Engineering A, 2020, 785: 139344.
- [202] LEI Bin, JIANG Bin, YANG Hua-bao, DONG Zhi-hua, WANG Qing-hang, YUAN Ming, HUANG Guang-sheng, SONG Jiang-feng, ZHANG Ding-fei, PAN Fu-sheng. Effect of Nd addition on the microstructure and mechanical properties of extruded Mg-Gd-Zr alloy [J]. Materials Science and Engineering A, 2021, 816: 141320.
- [203] SUN Jia-peng, LI Bang-jun, YUAN Jie, LI Xian-kai, XU Bing-qian, YANG Zhen-quan, HAN Jing, JIANG Jinghua, WU Guo-song, MA Ai-bin. Developing a high-performance Mg-5.7Gd-1.9Ag wrought alloy via hot rolling and aging [J]. Materials Science and Engineering A, 2021, 803: 140707.
- [204] ZHAO Jun, JIANG Bin, WANG Qing-hang, YANG Hua-bao, YUAN Ming, HUANG Guang-sheng, ZHANG Ding-fei, PAN Fu-sheng. Influence of Ce content on the microstructures and tensile properties of Mg-1Gd-0.5Zn alloys [J]. Materials Science and Engineering A, 2021, 823: 141675.
- [205] BASU I, AL-SAMMAN T. Triggering rare earth texture modification in magnesium alloys by addition of zinc and zirconium [J]. Acta Materialia, 2014, 67(2): 116–133.
- [206] AGNEW S R, YOO M H, TOMÉ C N. Application of texture simulation to understanding mechanical behavior of Mg and solid solution alloys containing Li or Y [J]. Acta Materialia, 2001, 49(20): 4277–4289.
- [207] COTTAM R, ROBSON J, LORIMER G, DAVIS B. Dynamic recrystallization of Mg and Mg-Y alloys: Crystallographic texture development [J]. Materials Science and Engineering A, 2008, 485(1/2): 375–382.
- [208] STANFORD N. Micro-alloying Mg with Y, Ce, Gd and La for texture modification-a comparative study [J]. Materials Science and Engineering A, 2010, 527(10/11): 2669–2677.
- [209] TEKUMALLA S, YANG C, SEETHARAMAN S, WONG W L E, GOH C S, SHABADI R, GUPTA M. Enhancing overall static/dynamic/damping/ignition response of magnesium through the addition of lower amounts (<2%) of yttrium [J]. Journal of Alloys and Compounds, 2016, 689: 350–358.
- [210] WU B L, ZHAO Y H, DU X H, ZHANG Y D, WAGNER F, ESLING C. Ductility enhancement of extruded magnesium via yttrium addition [J]. Materials Science and Engineering a-Structural Materials Properties Microstructure and Processing, 2010, 527(16/17): 4334–4340.
- [211] ZHOU Na, ZHANG Zhen-yan, JIN Li, DONG Jie, CHEN Bin, DING Wen-jiang. Ductility improvement by twinning and twin-slip interaction in a Mg-Y alloy [J]. Materials & Design, 2014, 56: 966–974.
- [212] ZHOU Na, ZHANG Zhen-yan, DONG Jie, LI Jin, DING Wen-jiang. High ductility of a Mg-Y-Ca alloy via extrusion [J]. Materials Science and Engineering A, 2013, 560: 103-110.

- [213] SUGAMATA M, HANAWA S, KANEKO J. Structures and mechanical properties of rapidly solidified Mg-Y based alloys [J]. Materials Science and Engineering A, 1997, 226/227/228: 861–866.
- [214] LI Qiang, WANG Qu-dong, LI Da-quan, DING Wen-jiang. Effect of Nd and Y addition on microstructure and mechanical properties of extruded Mg-Zn-Zr alloy [J]. Materials Science Forum, 2007, 546/547/548/549: 413-416.
- [215] ZHANG Tian-xiang, ZHAO Xue-ting, LIU Jia-hao, ZHANG Rui-jie, WANG Xian-fei, YUAN Yong, LI Zhong-quan, HAN Zhi-qiang. The microstructure, fracture mechanism and their correlation with the mechanical properties of as-cast Mg-Nd-Zn-Zr alloy under the effect of cooling rate [J]. Materials Science and Engineering A, 2021, 801(1): 140382.
- [216] ZHENG Xing-wei, DONG Jie, WANG Shi-ming. Microstructure and mechanical properties of Mg-Nd-Zn-Zr billet prepared by direct chill casting [J]. Journal of Magnesium and Alloys, 2018, 6(1): 95-99.
- [217] RAMESHKUMAR S, JAIGANESH G, JAYALAKSHMI V. Structural, phonon, elastic, thermodynamic and electronic properties of Mg–X (X=La, Nd, Sm) intermetallics: The first principles study [J]. Journal of Magnesium and Alloys, 2019, 7(1): 166–185.
- [218] OKAMOTO H. Mg-Nd [J]. Journal of Phase Equilibria and Diffusion, 2007, 28(4): 405.
- [219] NIE Jian-feng. Precipitation and hardening in magnesium alloys [J]. Metallurgical and Materials Transactions A, 2012, 43(11): 3891–3939.
- [220] ZHANG Ya-ping, HUANG Yuan-ding, FEYERABEND F, BLAWERT C, GAN Wei-min, MAAWAD E, YOU Si-hang, GAVRAS S, SCHARNAGL N, BODE J, VOGT C, ZANDER D, WILLUMEIT-RÖMER R, KAINER K U, HORT N. Influence of the amount of intermetallics on the degradation of Mg–Nd alloys under physiological conditions [J]. Acta Biomaterialia, 2021, 121: 695–712.
- [221] JIANG Quan-tong, LU Dong-zhu, WANG Ning, WANG Xiu-tong, ZHANG Jie, DUAN Ji-zhou, HOU Bao-rong. The corrosion behavior of Mg-Nd binary alloys in the harsh marine environment [J]. Journal of Magnesium and Alloys, 2021, 9(1): 292–304.
- [222] ZHAI Cong, LUO Qun, CAI Qi, GUAN Ren-guo, LI Qian. Thermodynamically analyzing the formation of Mg<sub>12</sub>Nd and Mg<sub>41</sub>Nd<sub>5</sub> in Mg–Nd system under a static magnetic field [J]. Journal of Alloys and Compounds, 2019, 773: 202–209.
- [223] HADORN J P, AGNEW S R. A new metastable phase in dilute, hot-rolled Mg-Nd alloys [J]. Materials Science and Engineering A, 2012, 533: 9-16.
- [224] ZHANG Hui, WANG Shao-qing. First-principles study on the phase stability of Mg-La and Mg-Nd binary alloys [J]. Acta Metallurgica Sinica, 2013, 48(7): 889–894.
- [225] MENG F G, LIU H S, LIU L B, JIN Z P. Thermodynamic optimization of Mg-Nd system [J]. Transactions of Nonferrous Metals Society of China, 2007, 17(1): 77–81.
- [226] SUN B Z, TAN J, ZHANG H X, SUN Y H. Atomic scale investigation of a novel metastable structure in aged Mg-Nd alloys [J]. Scripta Materialia, 2019, 161: 6-12.
- [227] CHOUDHURI D, DENDGE N, NAG S, MEHER S, ALAM T, GIBSON M A, BANERJEE R. Homogeneous and heterogeneous precipitation mechanisms in a binary Mg-Nd

- alloy [J]. Journal of Materials Science, 2014, 49(20): 6986-7003.
- [228] HUANG Zhi-hua, YANG Chao-ming, ALLISON J E, QI Liang, MISRA A. Dislocation cross-slip in precipitation hardened Mg-Nd alloys [J]. Journal of Alloys and Compounds, 2021, 859: 157858.
- [229] LIU Shuang, ZHANG Jing, XI Guo-qiang, WAN Xin, ZHANG Da-hao, ZHONG Ming-hong, YANG Cheng-bo, PAN Fu-sheng. Effects of intermediate annealing on twin evolution in twin-structured Mg-Nd alloys [J]. Journal of Alloys and Compounds, 2018, 763: 11–17.
- [230] HADORN J P, HANTZSCHE K, YI S, BOHLEN J, LETZIG D, AGNEW S R. Effects of solute and second-phase particles on the texture of Nd-containing Mg alloys [J]. Metallurgical & Materials Transactions A, 2012, 43(4): 1363–1375.
- [231] ALI Y, QIU Dong, JIANG Bin, PAN Fu-sheng, ZHANG Ming-xing. Current research progress in grain refinement of cast magnesium alloys: A review article [J]. Journal of Alloys and Compounds, 2015, 619: 639–651.
- [232] WU D, CHEN R S, KE W Y. Microstructure and mechanical properties of a sand-cast Mg-Nd-Zn alloy [J]. Materials & Design, 2014, 58: 324-331.
- [233] WANG W Z, WU D, CHEN R S, QI Y, YE H Q, YANG Z Q. Revisiting the role of Zr micro-alloying in a Mg-Nd-Zn alloy [J]. Journal of Alloys and Compounds, 2020, 832: 155016.
- [234] HA Chang-wan, BOHLEN J, ZHOU Xiao-hua, BROKMEIER H G, KAINER K U, SCHELL N, LETZIG D, YI Sang-bong. Texture development and dislocation activities in Mg Nd and Mg Ca alloy sheets [J]. Materials Characterization, 2021, 175: 111044.
- [235] LIU Xuan, ZHANG Zhi-qiang, LE Qi-chi, BAO Lei. Effects of Nd/Gd value on the microstructures and mechanical properties of Mg-Gd-Y-Nd-Zr alloys [J]. Journal of Magnesium and Alloys, 2016, 4(3): 214-219.
- [236] LV Bin-Jiang, WANG Sen, XU Tie-Wei, GUO Feng. Effects of minor Nd and Er additions on the precipitation evolution and dynamic recrystallization behavior of Mg-6.0Zn-0.5Mn alloy [J]. Journal of Magnesium and Alloys, 2021, 9(3): 840-852.
- [237] SHENG L Y, DU B N, HU Z Y, QIAO Y X, XIAO Z P, WANG B J, XU D K, ZHENG Y F, XI T F. Effects of annealing treatment on microstructure and tensile behavior of the Mg–Zn–Y–Nd alloy [J]. Journal of Magnesium and Alloys, 2020, 8(3): 601–613.
- [238] OMORI G, MATSUO S, ASADA H. Precipitation process in a Mg-Ce alloy [J]. Transactions of the Japan Institute of Metals, 1975, 16(5): 247-255.
- [239] ZHANG Xin, KEVORKOV D G, PEKGULERYUZ M O. Study on the binary intermetallic compounds in the Mg–Ce system [J]. Intermetallics, 2009, 17(7): 496–503.
- [240] SUN B Z, ZHANG H X, DONG Y, REN J X, TIAN Y, XIE G M, TAN J, SUN Y H, XIAO N. Rotational and translational domains of beta precipitate in aged binary Mg-Ce alloys [J]. Journal of Magnesium and Alloys, 2021, 9(3): 1039–1056.
- [241] SAITO K, KANEKI H. TEM study of real precipitation behavior of an Mg-0.5at.%Ce age-hardened alloy [J]. Journal of Alloys and Compounds, 2013, 574: 283-289.

- [242] HADORN J P, MULAY R P, HANTZSCHE K, YI S, BOHLEN J, LETZIG D, AGNEW S R. Texture weakening effects in Ce-containing Mg alloys [J]. Metallurgical and Materials Transactions A, 2013, 44(3): 1566–1576.
- [243] MISHRA R K, BRAHME A, SABAT R K, LI Jin, INAL K. Twinning and texture randomization in Mg and Mg-Ce alloys [J]. International Journal of Plasticity, 2019, 117: 157-172.
- [244] JIANG Lan, JONAS J J, MISHRA R K. Dynamic strain aging behavior of a Mg-Ce alloy and its implications for extrusion [J]. Materials Science Forum, 2012, 706/707/708/709: 1193-1198.
- [245] PAN Hu-cheng, XIE Dong-sheng, LI Jing-ren, XIE Hong-bo, HUANG Qiu-yan, YANG Qing-shan, QIN Gao-wu. Development of novel lightweight and cost-effective Mg-Ce-Al wrought alloy with high strength [J]. Materials Research Letters, 2021, 9(8): 329–335.
- [246] HU Ling-fei, GU Qin-fen, LI Qian, ZHANG Jie-yu, WU Guang-xin. Effect of extrusion temperature on microstructure, thermal conductivity and mechanical properties of a Mg-Ce-Zn-Zr alloy [J]. Journal of Alloys and Compounds, 2018, 741: 1222–1228.
- [247] YU Kun, LI Wen-xian, ZHAO Jun, MA Zheng-qing, WANG Ri-chu. Plastic deformation behaviors of a Mg-Ce-Zn-Zr alloy [J]. Scripta Materialia, 2003, 48(9): 1319–1323.
- [248] LV Bin-jiang, PENG Jian, PENG Yi, TANG Ai-tao. The effect of addition of Nd and Ce on the microstructure and mechanical properties of ZM21 Mg alloy [J]. Journal of Magnesium and Alloys, 2013, 1(1): 94–100.
- [249] TAMURA Y, KAWAMOTO S, SODA H, MCLEAN A. Effects of lanthanum and zirconium on cast structure and room temperature mechanical properties of Mg-La-Zr Alloys [J]. Materials Transactions, 2011, 52(9): 1777–1786.
- [250] LUO Qun, ZHAI Cong, GU Qin-fen, ZHU Wen-fei, LI Qian. Experimental study and thermodynamic evaluation of Mg-La-Zn system [J]. Journal of Alloys and Compounds, 2020, 814: 152297.
- [251] DU Yu-zhou, QIAO Xiao-guang, ZHENG Ming-yi, WU Kiddy, XU S W. Development of high-strength, low-cost wrought Mg-2.5mass%Zn alloy through micro-alloying with Ca and La [J]. Materials & Design, 2015, 85: 549-557.
- [252] ZENGIN H, TUREN Y. Effect of La content and extrusion temperature on microstructure, texture and mechanical properties of Mg–Zn–Zr magnesium alloy [J]. Materials Chemistry and Physics, 2018, 214: 421–430.
- [253] LI Rui-hong, JIANG Bin, CHEN Zhi-jun, PAN Fu-sheng, GAO Zhan-yong. Microstructure and mechanical properties of Mg<sub>14</sub>Li<sub>1</sub>Al<sub>0.3</sub>La alloys produced by two-pass extrusion [J]. Journal of Rare Earths, 2017, 35(12): 1268–1272.
- [254] BU Fan-qiang, YANG Qiang, GUAN Kai, QIU Xin, ZHANG De-ping, SUN Wei, ZHENG Tian, CUI Xiao-peng, SUN Shi-cheng, TANG Zong-min, LIU Xiao-juan, MENG Jian. Study on the mutual effect of La and Gd on microstructure and mechanical properties of Mg-Al-Zn extruded alloy [J]. Journal of Alloys and Compounds, 2016, 688: 1241–1250.
- [255] MA Rui, LV Shu-hui, XIE Ze-feng, YANG Qiang, YAN Zi-xiang, MENG Fan-zhi, QIU Xin. Achieving high strength-ductility in a wrought Mg-9Gd-3Y-0.5Zr alloy by

- modifying with minor La addition [J]. Journal of Alloys and Compounds, 2021, 884: 161062.
- [256] ZHANG J B, TONG L B, XU C, JIANG Z H, CHENG L R, KAMADO S, ZHANG H J. Influence of Ca-Ce/La synergistic alloying on the microstructure and mechanical properties of extruded Mg–Zn alloy [J]. Materials Science and Engineering A, 2017, 708: 11–20.
- [257] LI Jing-ren, ZHANG Ai-yue, PAN Hu-cheng, REN Yu-ping, ZENG Zhuo-ran, HUANG Qiu-yan, YANG Chang-lin, MA Li-feng, QIN Gao-wu. Effect of extrusion speed on microstructure and mechanical properties of the Mg-Ca binary alloy [J]. Journal of Magnesium and Alloys, 2021, 9(4): 1297–1303.
- [258] JEONG Y S, KIM W J. Enhancement of mechanical properties and corrosion resistance of Mg-Ca alloys through microstructural refinement by indirect extrusion [J]. Corrosion Science, 2014, 82: 392-403.
- [259] SHE Jia, ZHOU Shi-bo, PENG Peng, TANG Ai-tao, WANG Y, PAN Hu-cheng, YANG C L, PAN Fu-sheng. Improvement of strength-ductility balance by Mn addition in Mg-Ca extruded alloy [J]. Materials Science and Engineering A, 2020, 772: 138796.
- [260] XIE Dong-sheng, PAN Hu-cheng, LI Man, LI Jing-ren, REN Yu-ping, HUANG Qiu-yan, YANG Chang-lin, MA Li-feng, QIN Gao-wu. Role of Al addition in modifying microstructure and mechanical properties of Mg-1.0wt.%Ca based alloys [J]. Materials Characterization, 2020, 169: 110608.
- [261] HENDERSON H B, RAMASWAMY V, WILSON-HEID A E, KESLER M S, ALLEN J B, MANUEL M V. Mechanical and degradation property improvement in a biocompatible Mg-Ca-Sr alloy by thermomechanical processing [J]. Journal of the Mechanical Behavior of Biomedical Materials, 2018, 80: 285-292.
- [262] GENG J, NIE J F. Microstructure and mechanical properties of extruded Mg-1Ca-1Zn-0.6Zr alloy [J]. Materials Science and Engineering A, 2016, 653: 27-34.
- [263] LIU Yan-hui, CHENG Wei-li, ZHANG Yao, NIU Xiao-feng, WANG Hong-xia, WANG Li-fei. Microstructure, tensile properties, and corrosion resistance of extruded Mg-1Bi-1Zn alloy: The influence of minor Ca addition [J]. Journal of Alloys and Compounds, 2020, 815: 152414.
- [264] LIU X Q, QIAO X G, PEI R S, CHI Y Q, YUAN L, ZHENG M Y. Role of extrusion rate on the microstructure and tensile properties evolution of ultrahigh-strength low-alloy Mg-1.0Al-1.0Ca-0.4Mn (wt.%) alloy [J]. Journal of Magnesium and Alloys, 2021.
- [265] ZHAO Chao-yong, PAN Fu-sheng, ZHAO Shuang, PAN Hu-cheng, SONG Kai, TANG Ai-tao. Preparation and characterization of as-extruded Mg-Sn alloys for orthopedic applications [J]. Materials & Design, 2015, 70: 60-67.
- [266] CHAI Yan-fu, JIANG Bin, SONG Jiang-feng, LIU Bo, HUANG Guang-sheng, ZHANG Ding-fei, PAN Fu-sheng. Effects of Zn and Ca addition on microstructure and mechanical properties of as-extruded Mg-1.0Sn alloy sheet [J]. Materials Science and Engineering A, 2019, 746: 82-93.
- [267] PAN Hu-cheng, QIN Gao-wu, XU Ming, FU He, REN Yu-ping, PAN Fu-sheng, GAO Zheng-yuan, ZHAO Chao-yong, YANG Qing-shan, SHE Jia, SONG Bo.

- Enhancing mechanical properties of Mg-Sn alloys by combining addition of Ca and Zn [J]. Materials & Design, 2015, 83: 736-744.
- [268] SHE J, PAN F S, PENG P, TANG A T, YU Z, WU L, PAN H C, ZHAO C, GAO Z Y, LUO S, RASHAD M. Microstructure and mechanical properties of as-extruded Mg-xAl-5Sn-0·3Mn alloys (x=1, 3, 6 and 9) [J]. Materials Science and Technology, 2015, 31(3): 344–348.
- [269] WANG Qing-hang, SHEN Ya-qun, JIANG Bin, TANG Ai-tao, SONG Jiang-feng, JIANG Zhong-tao, YANG Tian-hao, HUANG Guang-sheng, PAN Fu-sheng. A micro-alloyed Mg-Sn-Y alloy with high ductility at room temperature [J]. Materials Science and Engineering: A, 2018, 735: 131-144.
- [270] QIAN Xiao-ying, ZENG Ying, JIANG Bin, YANG Q R, WAN Yang-jie, QUAN Gao-feng, PAN Fu-sheng. Grain refinement mechanism and improved mechanical properties in Mg-Sn alloy with trace Y addition [J]. Journal of Alloys and Compounds, 2020, 820: 153122.
- [271] WANG Qing-hang, JIANG Bin, TANG Ai-tao, HE Chao, ZHANG Ding-fei, SONG Jiang-feng, YANG Tian-hao, HUANG Guang-sheng, PAN Fu-sheng. Formation of the elliptical texture and its effect on the mechanical properties and stretch formability of dilute Mg-Sn-Y sheet by Zn addition [J]. Materials Science and Engineering A, 2019, 746: 259-275.
- [272] CHAI Yan-fu, JIANG Bin, SONG Jiang-feng, WANG Qing-hang, GAO Hang, LIU Bo, HUANG Guang-sheng, ZHANG Ding-fei, PAN Fu-sheng. Improvement of mechanical properties and reduction of yield asymmetry of extruded Mg—Sn—Zn alloy through Ca addition [J]. Journal of Alloys and Compounds, 2019, 782: 1076–1086.
- [273] PAN Hu-cheng, QIN Gao-wu, HUANG Yun-miao, REN Yu-ping, SHA Xue-chao, HAN Xiao-dong, LIU Zhi-quan, LI Cai-fu, WU Xiao-lei, CHEN Hou-wen, HE Cong, CHAI Lin-jiang, WANG Yun-zhi, NIE Jian-feng. Development of low-alloyed and rare-earth-free magnesium alloys having ultra-high strength [J]. Acta Materialia, 2018, 149: 350–363.
- [274] ZHANG Ai-yue, KANG Rui, WU Lu, PAN Hu-cheng, XIE Hong-bo, HUANG Qiu-yan, LIU Yu-jie, AI Zheng-rong, MA Li-feng, REN Yu-ping, QIN Gao-wu. A new rare-earth-free Mg-Sn-Ca-Mn wrought alloy with ultra-high strength and good ductility [J]. Materials Science and Engineering A, 2019, 754: 269–274.
- [275] CHAI Yan-fu, HE Chao, JIANG Bin, FU Jie, JIANG Zhong-tao, YANG Qing-shan, SHENG Hao-ran, HUANG Guang-sheng, ZHANG Ding-fei, PAN Fu-sheng. Influence of minor Ce additions on the microstructure and mechanical properties of Mg-1.0Sn-0.6Ca alloy [J]. Journal of Materials Science & Technology, 2020, 37: 26-37.
- [276] ELSAYED F R, SASAKI T T, OHKUBO T, TAKAHASHI H, XU S W, KAMADO S, HONO K. Effect of extrusion conditions on microstructure and mechanical properties of microalloyed Mg-Sn-Al-Zn alloys [J]. Materials Science and Engineering A, 2013, 588: 318-328.
- [277] HUANG Qiu-yan, LIU Yang, ZHANG Ai-yue, JIANG Hao-xin, PAN Hu-cheng, FENG Xiao-hui, YANG Chang-lin, LUO Tian-jiao, LI Ying-ju, YANG Yuan-sheng. Age hardening responses of as-extruded Mg-2.5Sn-1.5Ca alloys

- with a wide range of Al concentration [J]. Journal of Materials Science & Technology, 2020, 38: 39-46.
- [278] LI Xiao-qiang, REN Liang, LE Qi-chi, BAO Lei, JIN Pei-peng, WANG Ping, CHENG Chun-long, ZHOU Xiong, HU Cheng-lu. Reducing the yield asymmetry in Mg-5Li-3Al-2Zn alloy by hot-extrusion and multi-pass rolling [J]. Journal of Magnesium and Alloys, 2021, 9(3): 937-949.
- [279] MASOUMI M, HOSEINI M, PEKGULERYUZ M. The influence of Ce on the microstructure and rolling texture of Mg-1% Mn alloy [J]. Materials Science and Engineering: A, 2011, 528(7/8): 3122-3129.
- [280] OHUCHI K, IWASAWA S, KAMADO S, KOJIMA Y, NINOMIYA R. Effects of Nd and Ag additions on the microstructures and mechanical properties of Mg-8mass%Li alloy [J]. Journal of Japan Institute of Light Metals, 1992, 42(8): 446-452.
- [281] DONG Han-wu, WANG Li-dong, WU Yao-ming, WANG Li-min. Effect of Y on microstructure and mechanical properties of duplex Mg-7Li alloys [J]. Journal of Alloys and Compounds, 2010, 506(1): 468-474.
- [282] GUO Xu-ying, WU Rui-zhi, ZHANG Jing-huai, LIU Bin, ZHANG Mi-lin. Influences of solid solution parameters on the microstrucuture and hardness of Mg-9Li-6Al and Mg-9Li-6Al-2Y [J]. Materials & Design, 2014, 53: 528-533.
- [283] HAO Mei-juan, CHENG Wei-li, WANG Li-fei, MOSTAED E, BIAN Li-ping, WANG Hong-xia, NIU Xiao-feng. Texture evolution in Mg-8Sn-1Zn-1Al alloy during hot compression via competition between twinning and dynamic precipitation [J]. Materials Science and Engineering A, 2019, 748: 418-427.
- [284] LI Chuan-qiang, HE Yi-bin, HUANG Huai-pei. Effect of lithium content on the mechanical and corrosion behaviors of HCP binary Mg-Li alloys [J]. Journal of Magnesium and Alloys, 2021, 9(2): 569–580.
- [285] LIU Yang, WU Yuan-hao, BIAN Dong, GAO Shuang, LEEFLANG S, GUO Hui, ZHENG Yu-feng, ZHOU Jie. Study on the Mg-Li-Zn ternary alloy system with improved mechanical properties, good degradation performance and different responses to cells [J]. Acta Biomaterialia, 2017, 62: 418-433.
- [286] SON H T, KIM Y H, KIM D, KIM J H, YU H S. Effects of Li addition on the microstructure and mechanical properties of Mg-3Zn-1Sn-0.4Mn based alloys [J]. Journal of Alloys and Compounds, 2013, 564: 130-137.
- [287] XU Tian-cai, PENG Xiao-dong, JIANG Jun-wei, XIE Wei-dong, CHEN Yuan-fang, WEI Guo-bing. Effect of Sr content on microstructure and mechanical properties of Mg-Li-Al-Mn alloy [J]. Transactions of Nonferrous Metals Society of China, 2014, 24(9): 2752–2760.
- [288] ZHAO Jun, FU Jie, JIANG Bin, TANG Ai-tao, SHENG Hao-ran, YANG Tian-hao, HUANG Guang-sheng, ZHANG Ding-fei, PAN Fu-sheng. Influence of Li addition on the microstructures and mechanical properties of Mg-Li alloys [J]. Metals and Materials International, 2021, 27(6): 1403-1415.
- [289] MENG S J, YU H, FAN S D, KIM Y M, PARK S H, ZHAO W M, YOU B S, SHIN K S. A high-ductility extruded

- Mg-Bi-Ca alloy [J]. Materials Letters, 2020, 261: 127066.
- [290] TANG Ying, LI Yong-sheng, ZHAO Wei-min, ROSLYAKOVA I, ZHANG Li-jun. Thermodynamic descriptions of quaternary Mg-Al-Zn-Bi system supported by experiments and their application in descriptions of solidification behavior in Bi-additional AZ casting alloys [J]. Journal of Magnesium and Alloys, 2020, 8(4): 1238-1252.
- [291] MENG F, SUN S, MA J, CHRONISTER C, HE J, LI W. Anisotropic thermoelectric figure-of-merit in Mg<sub>3</sub>Sb<sub>2</sub> [J]. Materials Today Physics, 2020, 13: 100217.
- [292] LIU Yang, CHENG Wei-li, LIU Yan-hui, NIU Xiao-feng, WANG Hong-xia, WANG Li-fei, CUI Ze-qin. Effect of alloyed Ca on the microstructure and corrosion behavior of extruded Mg-Bi-Al-based alloys [J]. Materials Characterization, 2020, 163: 110292.
- [293] YU Hui, FAN Shao-da, MENG Shuai-ju, CHOI J O, LI Zhong-jie, GO Y, KIM Y M, ZHAO Wei-min, YOU Bong-sun, SHIN K S. Microstructural evolution and mechanical properties of binary Mg–xBi (x=2, 5, and 8 wt.%) alloys [J]. Journal of Magnesium and Alloys, 2021, 9(3): 983–994.
- [294] MENG Shuai-ju, YU Hui, FAN Shao-da, LI Qi-zhi, PARK S H, SUH J S, KIM Y M, NAN Xiao-Long, BIAN Ming-zhe, YIN Fu-xing, ZHAO Wei-min, YOU Bong-sun, SHIN K S. Recent progress and development in extrusion of rare earth free Mg alloys: A review [J]. Acta Metallurgica Sinica (English Letters), 2019, 32(2): 145–168.
- [295] MENG Shuai-ju, YU Hui, LI Li-chao, QIN Jia-nan, WOO S K, GO Y, KIM Y M, PARK S H, ZHAO Wei-min, YIN Fu-xing, YOU Bong-sun, SHIN K S. Effects of Ca addition on the microstructures and mechanical properties of as-extruded Mg-Bi alloys [J]. Journal of Alloys and Compounds, 2020, 834: 155216.
- [296] JIN S C, LEE J U, GO J, YU H, PARK S H. Effects of Sn addition on the microstructure and mechanical properties of extruded Mg-Bi binary alloy [J]. Journal of Magnesium and Alloys, 2022, 10(3): 850–861.
- [297] PENG Peng, TANG Ai-tao, WANG Bo, ZHOU Shi-bo, SHE Jia, ZHANG Jian-yue, PAN Fu-sheng. Achieving superior combination of yield strength and ductility in Mg-Mn-Al alloys via ultrafine grain structure [J]. Journal of Materials Research and Technology, 2021, 15: 1252–1265.
- [298] FANG X Y, YI D Q, NIE J F, ZHANG X J, WANG B R, XIAO L R. Effect of Zr, Mn and Sc additions on the grain size of Mg-Gd alloy [J]. Journal of Alloys and Compounds, 2009, 470(1/2): 311–316.
- [299] SHE Jia, PENG Peng, XIAO L, TANG Ai-tao, WANG Y, PAN Fu-sheng. Development of high strength and ductility in Mg-2Zn extruded alloy by high content Mn-alloying [J]. Materials Science and Engineering A, 2019, 765: 138203.
- [300] TONG L B, CHU J H, SUN W T, JIANG Z H, ZOU D N, WANG K S, KAMADO S, ZHENG M Y. Development of high-performance Mg-Zn-Ca-Mn alloy via an extrusion process at relatively low temperature [J]. Journal of Alloys and Compounds, 2020, 825: 153942.
- [301] HOU Cai-hong, QI Fu-gang, YE Zhi-song, ZHAO Nie, ZHANG Ding-fei, OUYANG Xiao-ping. Effects of Mn addition on the microstructure and mechanical properties of

- Mg-Zn-Sn alloys [J]. Materials Science and Engineering A, 2020, 774: 138933.
- [302] NAKATA T, XU C, SUZAWA K, YOSHIDA K, KAWABE N, KAMADO S. Enhancing mechanical properties of rolled Mg-Al-Ca-Mn alloy sheet by Zn addition [J]. Materials Science and Engineering A, 2018, 737: 223-229.
- [303] WANG Qing-hang, JIANG Bin, TANG Ai-tao, FU Jie, JIANG Zhong-tao, SHENG Hao-ran, ZHANG Ding-fei, HUANG Guang-sheng, PAN Fu-sheng. Unveiling annealing texture formation and static recrystallization kinetics of hot-rolled Mg-Al-Zn-Mn-Ca alloy [J]. Journal of Materials Science & Technology, 2020, 43: 104-118.
- [304] PENG Peng, TANG Ai-tao, SHE Jia, ZHANG Jian-yue, ZHOU Shi-bo, SONG Kai, PAN Fu-sheng. Significant improvement in yield stress of Mg-Gd-Mn alloy by forming bimodal grain structure [J]. Materials Science and Engineering A, 2021, 803: 140569.
- [305] WANG Kui, WANG Jing-feng, HUANG Song, GAO Shi-qing, GUO Sheng-feng, LIU Shi-jie, CHEN Xian-hua, PAN Fu-sheng. Enhanced mechanical properties of Mg-Gd-Y-Zn-Mn alloy by tailoring the morphology of long period stacking ordered phase [J]. Materials Science and Engineering A, 2018, 733: 267-275.
- [306] WANG Kui, WANG Jing-feng, DOU Xiao-xu, HUANG Yuan-ding, HORT N, GAVRAS S, LIU Shi-jie, CAI Yan-wu,

- WANG Jin-xing, PAN Fu-sheng. Microstructure and mechanical properties of large-scale Mg-Gd-Y-Zn-Mn alloys prepared through semi-continuous casting [J]. Journal of Materials Science & Technology, 2020, 52: 72–82.
- [307] WANG Qing-hang, JIANG Bin, LIU Lin-tao, YANG Qing-shan, XIA Da-biao, ZHANG Ding-fei, HUANG Guang-sheng, PAN Fu-sheng. Reduction per pass effect on texture traits and mechanical anisotropy of Mg-Al-Zn-Mn-Ca alloy subjected to unidirectional and cross rolling [J]. Journal of Materials Research and Technology, 2020, 9(5): 9607–9619.
- [308] SU Ning, WU Yu-juan, CHANG Zhi-yu, DENG Qing-chen, PENG Li-ming, YANG Kun, CHEN Qiang. Selective variant growth of precipitates in an as-extruded Mg-Gd-Zn-Mn alloy [J]. Materials Letters, 2020, 272: 127853.
- [309] NAKATA T, XU C, MATSUMOTO Y, SHIMIZU K, SASAKI T T, HONO K, KAMADO S. Optimization of Mn content for high strengths in high-speed extruded Mg-0.3Al-0.3Ca (wt.%) dilute alloy [J]. Materials Science and Engineering A, 2016, 673: 443-449.
- [310] CIHOVA M, SCHÄUBLIN R, HAUSER L B, GERSTL S S A, SIMSON C, UGGOWITZER P J, LÖFFLER J F. Rational design of a lean magnesium-based alloy with high age-hardening response [J]. Acta Materialia, 2018, 158: 214–229.

## 变形镁合金微合金化研究进展: 理论与设计

蒋斌1,2,董志华2,张昂2,宋江凤1,2,潘复生1,2

- 1. 重庆大学 国家镁合金材料工程技术研究中心, 重庆 400044;
- 2. 重庆大学 材料科学与工程学院 机械传动国家重点实验室, 重庆 400044

摘 要:变形镁合金微合金化是发展低成本、高性能镁合金的重要方向。近二十年来,变形镁合金在理论研究及 微合金化设计领域取得了重要研究进展。本文中作者重点从理论计算及合金设计两方面总结变形镁合金最新研究 进展,为建立镁合金成分一性能关系奠定基础。首先,概述第一性原理计算、分子动力学、元胞自动机和晶体塑性有限元等不同尺度下镁合金性能的研究进展,继而分析 Mg-Al、Mg-Zn、Mg-RE、Mg-Sn 和 Mg-Ca 等重要变形镁合金体系中合金元素的作用,最后,展望微合金化变形镁合金的发展方向,为新型变形镁合金的高效设计提供指导。

关键词: 镁合金; 合金化设计; 力学性能; 理论计算; 实验表征

(Edited by Bing YANG)